

AD-A088 283

TENNESSEE UNIV KNOXVILLE DEPT OF CHEMISTRY F/G 7/3
LOW TEMPERATURE FLUORINE CHEMISTRY OF ELECTRONEGATIVE ELEMENTS.(U)
JUL 80 G MAMANTOV, R A CROCOMBE AFOSR-77-3165

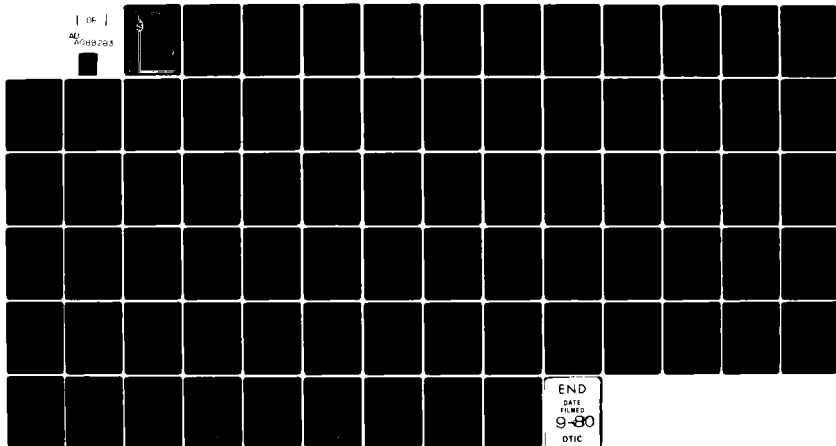
UNCLASSIFIED

AFOSR-TR-80-0600

NL

[OF]

AD-A088283



END
DATE
FILMED
9-80
DTIC



MICROCOPY RESOLUTION TEST CHART
NATIONAL BUREAU OF STANDARDS-1963-A

AD A088283

80-0600

LEVEL

20 JUL 1980

(12)

LOW TEMPERATURE FLUORINE CHEMISTRY
OF ELECTRONEGATIVE ELEMENTS

Final Report

Prepared by:

Gleb Mamantov, Principal Investigator
Richard A. Crocombe, Research Associate

July 15, 1980

Air Force Office of Scientific Research

AFOSR 77-3165

12/1/76 - 2/29/80

DTIC
ELECTE
AUG 28 1980
D
D(fe)

DEPARTMENT of CHEMISTRY

The University of Tennessee • Knoxville
APPROVED FOR PUBLIC RELEASE
DISTRIBUTION UNLIMITED

Approved for public release;
distribution unlimited.

FILE COPY

Unclassified

SECURITY CLASSIFICATION OF THIS PAGE (When Data Entered)

12 REPORT DOCUMENTATION PAGE		READ INSTRUCTIONS BEFORE COMPLETING FORM	
1. REPORT NUMBER AFOSR-TR-80-0600	2. GOVT ACCESSION NO. AD-A088 283	3. RECIPIENT'S CATALOG NUMBER	
4. TITLE (and Subtitle) LOW TEMPERATURE FLUORINE CHEMISTRY OF ELECTRONEGATIVE ELEMENTS.		5. TYPE OF REPORT & PERIOD COVERED Final Report, 12/1/76-2/29/80	
6. AUTHOR(s) Gleb Mamantov Richard A. Crocombe		7. PERFORMING ORG. REPORT NUMBER AFOSR-76-01 F.1	
8. PERFORMING ORGANIZATION NAME AND ADDRESS Department of Chemistry University of Tennessee Knoxville, Tennessee.		9. CONTRACT OR GRANT NUMBER(s) AFOSR-77-3165	
10. CONTROLLING OFFICE NAME AND ADDRESS Air Force Office of Scientific Research/NC Bolling Air Force Base, DC 20332		11. PROGRAM ELEMENT, PROJECT, TASK AREA & WORK UNIT NUMBERS 61102 F 2303/B2	
12. MONITORING AGENCY NAME & ADDRESS (if different from Controlling Office)		13. REPORT DATE 15 Jul 15, 1980	
14. SECURITY CLASS. (of this report) Unclassified		15. NUMBER OF PAGES 76	
16. DISTRIBUTION STATEMENT (of this Report) Approved for public release; distribution unlimited.		17. SECURITY CLASS. (of this report)	
17. DISTRIBUTION STATEMENT (of the abstract entered in Block 20, if different from Report)		18. DECLASSIFICATION/DOWNGRADING SCHEDULE	
18. SUPPLEMENTARY NOTES			
19. KEY WORDS (Continue on reverse side if necessary and identify by block number) Fluorine, interhalogens, infrared laser, matrix isolation.			
20. ABSTRACT (Continue on reverse side if necessary and identify by block number) This program was concerned with the synthesis and characterization of fluorine-containing compounds by novel methods. A detailed study of the systems $X_2 + F_2$ where $X = Cl, Br, \text{ or } I$ was carried out, producing evidence for the new species XF_2, X_2F and X_2F_2 as well as some of the normally unfavored members of the series XF_n ($n=1,3,5$). High resolution infrared spectra of the interhalogen compounds ClF and $BrCl$ were measured for the first time. The uses of an infrared laser to produce new species in matrices via multiphoton dissociation and to open new synthetic routes in			

Unclassified

SECURITY CLASSIFICATION OF THIS PAGE (When Data Entered)

REPORT DOCUMENTATION PAGE	
1. REPORT NUMBER	2. GOVT ACCESSION NO.
3. TYPE OF REPORT & PERIOD COVERED	4. TITLE AND SUBTITLE
the gas phase have been examined. A new technique of obtaining infrared spectra of short-lived species has been studied and its potential evaluated.	
5. AUTHOR(s)	6. AUTHORING ORGANIZATION NAME AND ADDRESS
7. AUTHORING ORGANIZATION REPORT NUMBER	8. PERFORMING ORGANIZATION NAME AND ADDRESS
9. PERFORMING ORGANIZATION REPORT NUMBER	10. PROGRAM ELEMENT, PROJECT, TASK, AND WORK UNIT NUMBERS
11. DISTRIBUTION STATEMENT (For Public Release Only)	12. DISTRIBUTION STATEMENT (For Public Release Only)
13. DISTRIBUTION STATEMENT (For Public Release Only)	14. DISTRIBUTION STATEMENT (For Public Release Only)
15. DISTRIBUTION STATEMENT (For Public Release Only)	16. DISTRIBUTION STATEMENT (For Public Release Only)
17. DISTRIBUTION STATEMENT (For Public Release Only)	18. DISTRIBUTION STATEMENT (For Public Release Only)
19. DISTRIBUTION STATEMENT (For Public Release Only)	20. DISTRIBUTION STATEMENT (For Public Release Only)
21. DISTRIBUTION STATEMENT (For Public Release Only)	22. DISTRIBUTION STATEMENT (For Public Release Only)
23. DISTRIBUTION STATEMENT (For Public Release Only)	24. DISTRIBUTION STATEMENT (For Public Release Only)
25. DISTRIBUTION STATEMENT (For Public Release Only)	26. DISTRIBUTION STATEMENT (For Public Release Only)
27. DISTRIBUTION STATEMENT (For Public Release Only)	28. DISTRIBUTION STATEMENT (For Public Release Only)
29. DISTRIBUTION STATEMENT (For Public Release Only)	30. DISTRIBUTION STATEMENT (For Public Release Only)
31. DISTRIBUTION STATEMENT (For Public Release Only)	32. DISTRIBUTION STATEMENT (For Public Release Only)
33. DISTRIBUTION STATEMENT (For Public Release Only)	34. DISTRIBUTION STATEMENT (For Public Release Only)
35. DISTRIBUTION STATEMENT (For Public Release Only)	36. DISTRIBUTION STATEMENT (For Public Release Only)
37. DISTRIBUTION STATEMENT (For Public Release Only)	38. DISTRIBUTION STATEMENT (For Public Release Only)
39. DISTRIBUTION STATEMENT (For Public Release Only)	40. DISTRIBUTION STATEMENT (For Public Release Only)
41. DISTRIBUTION STATEMENT (For Public Release Only)	42. DISTRIBUTION STATEMENT (For Public Release Only)
43. DISTRIBUTION STATEMENT (For Public Release Only)	44. DISTRIBUTION STATEMENT (For Public Release Only)
45. DISTRIBUTION STATEMENT (For Public Release Only)	46. DISTRIBUTION STATEMENT (For Public Release Only)
47. DISTRIBUTION STATEMENT (For Public Release Only)	48. DISTRIBUTION STATEMENT (For Public Release Only)
49. DISTRIBUTION STATEMENT (For Public Release Only)	50. DISTRIBUTION STATEMENT (For Public Release Only)
51. DISTRIBUTION STATEMENT (For Public Release Only)	52. DISTRIBUTION STATEMENT (For Public Release Only)
53. DISTRIBUTION STATEMENT (For Public Release Only)	54. DISTRIBUTION STATEMENT (For Public Release Only)
55. DISTRIBUTION STATEMENT (For Public Release Only)	56. DISTRIBUTION STATEMENT (For Public Release Only)
57. DISTRIBUTION STATEMENT (For Public Release Only)	58. DISTRIBUTION STATEMENT (For Public Release Only)
59. DISTRIBUTION STATEMENT (For Public Release Only)	60. DISTRIBUTION STATEMENT (For Public Release Only)
61. DISTRIBUTION STATEMENT (For Public Release Only)	62. DISTRIBUTION STATEMENT (For Public Release Only)
63. DISTRIBUTION STATEMENT (For Public Release Only)	64. DISTRIBUTION STATEMENT (For Public Release Only)
65. DISTRIBUTION STATEMENT (For Public Release Only)	66. DISTRIBUTION STATEMENT (For Public Release Only)
67. DISTRIBUTION STATEMENT (For Public Release Only)	68. DISTRIBUTION STATEMENT (For Public Release Only)
69. DISTRIBUTION STATEMENT (For Public Release Only)	70. DISTRIBUTION STATEMENT (For Public Release Only)
71. DISTRIBUTION STATEMENT (For Public Release Only)	72. DISTRIBUTION STATEMENT (For Public Release Only)
73. DISTRIBUTION STATEMENT (For Public Release Only)	74. DISTRIBUTION STATEMENT (For Public Release Only)
75. DISTRIBUTION STATEMENT (For Public Release Only)	76. DISTRIBUTION STATEMENT (For Public Release Only)
77. DISTRIBUTION STATEMENT (For Public Release Only)	78. DISTRIBUTION STATEMENT (For Public Release Only)
79. DISTRIBUTION STATEMENT (For Public Release Only)	80. DISTRIBUTION STATEMENT (For Public Release Only)
81. DISTRIBUTION STATEMENT (For Public Release Only)	82. DISTRIBUTION STATEMENT (For Public Release Only)
83. DISTRIBUTION STATEMENT (For Public Release Only)	84. DISTRIBUTION STATEMENT (For Public Release Only)
85. DISTRIBUTION STATEMENT (For Public Release Only)	86. DISTRIBUTION STATEMENT (For Public Release Only)
87. DISTRIBUTION STATEMENT (For Public Release Only)	88. DISTRIBUTION STATEMENT (For Public Release Only)
89. DISTRIBUTION STATEMENT (For Public Release Only)	90. DISTRIBUTION STATEMENT (For Public Release Only)
91. DISTRIBUTION STATEMENT (For Public Release Only)	92. DISTRIBUTION STATEMENT (For Public Release Only)
93. DISTRIBUTION STATEMENT (For Public Release Only)	94. DISTRIBUTION STATEMENT (For Public Release Only)
95. DISTRIBUTION STATEMENT (For Public Release Only)	96. DISTRIBUTION STATEMENT (For Public Release Only)
97. DISTRIBUTION STATEMENT (For Public Release Only)	98. DISTRIBUTION STATEMENT (For Public Release Only)
99. DISTRIBUTION STATEMENT (For Public Release Only)	100. DISTRIBUTION STATEMENT (For Public Release Only)

Unclassified

CONTENTS

	<u>PAGE</u>
Abstract	1
1. Interhalogen Compounds	2
(A) Introduction	2
(B) Matrix-Isolation Studies	3
(C) Diatomic Interhalogens	8
(D) References for Section 1	10
2. Infrared Laser Photochemistry	12
(A) Matrix-Isolation Studies	12
(B) Gas-Phase Studies	17
(C) References for Section 2	22
3. Low Temperature Synthesis	24
(A) References for Section 3	41
4. Time Resolved Spectroscopy	42
(A) References for Section 4	44
5. Appendix 1: Inorg. Chem., <u>17</u> , 970 (1978)	45
6. Appendix 2: Diatomic Interhalogens	53
(A) Introduction	53
(B) Chlorine Monofluoride Spectra	53
(C) Spectral Interpretation	53
(D) Experimental	57
(E) Bromine Monochloride Spectra	62
(F) Experimental	62
(G) References for Appendix 2	65
7. Appendix 3: J. Amer. Chem. Soc., <u>100</u> , 6526 (1979)	66
8. Appendix 4: Appl. Spectrosc., <u>34</u> , 399 (1980)	67

Abstract

This program was concerned with the synthesis and characterization of fluorine-containing compounds by novel methods. A detailed study of the systems $X_2 + F_2$ where $X = Cl, Br, \text{ or } I$ was carried out, producing evidence for the new species XF_2 , X_2F and X_2F_2 as well as some of the normally unfavored members of the series XF_n ($n=1,3,5$). High resolution infrared spectra of the interhalogen compounds ClF and $BrCl$ were measured for the first time. The uses of an infrared laser to produce new species in matrices via multiphoton dissociation and to open up new synthetic routes in the gas phase have been examined. A new technique of obtaining infrared spectra of short-lived species has been studied and its potential evaluated.

Accu-son for	
NTIS G-0-1	
DDC TAB	
Unannounced	
Justification	
By	
Distribution/	
Availability codes	
Dist	
Avail and/or special	

AIR FORCE OFFICE OF SCIENTIFIC RESEARCH (AFSC)
 NOTICE OF TRANSMITTAL TO DDC
 This technical report has been reviewed and is
 approved for public release IAW AFR 190-18 (7b).
 Distribution is unlimited.
 A. D. BLOOM
 Technical Information Officer

1. INTERHALOGEN COMPOUNDS,

(A) INTRODUCTION

This part of the program was concerned with the preparation, detection and characterization of unusual interhalogen species. The physical and chemical properties of the interhalogens were comprehensively reviewed in 1973¹ and the literature published up to 1976 has been surveyed². The quality of information available for these compounds falls into three broad classes. In the first group are compounds which are stable, monomeric and whose properties are reasonably defined (IF_7 , IF_5 , ClF_5 , BrF_5 , ClF , ICl and IBr), and whose structural parameters have been determined by precise (e.g. microwave spectroscopy, electron diffraction or X-ray diffraction) methods. There is a second group of stable compounds whose properties are complicated by molecular association (I_2Cl_6 , BrF_3 , ClF_3) and for which data for the monomeric species have been obtained by less precise methods. The third group comprises those compounds which tend to dissociate or disproportionate at room temperature (IF_3 , IF , BrF and BrCl), for which only a few data are available. The known properties of transient or radical species are naturally few.

The major methods for the study of interhalogen radicals have been infrared, Raman and E.S.R. spectroscopy of the matrix-isolated molecules. Nelson and Pimentel presented evidence of a T-shaped BrBrCl_2 species and suggested that BrCl_3 and Br_3Cl may also be formed³. Mamantov et al.^{4a} reported infrared evidence for ClF_2^\cdot which implied that this radical was obtusely bent, despite other work proposing that the isoelectronic radicals Cl_3^\cdot ⁵ and Br_3^\cdot ⁶ are linear. Infrared spectroscopic evidence consistent with $\text{Cl}_2\text{F}^\cdot$, Cl_2F_2 and $\text{Cl}_2\text{F}_3^\cdot$ was also given by Mamantov et al.^{4b}. and the application of Raman and UV-visible spectroscopy confirmed the existence of ClF_2^\cdot and lent support to the non-linear hypothesis⁷. However no asymmetry or splitting of ν_1 was found, which would be attributable to a Cl-isotope shift, but large unspecified slitwidths were employed. A second study⁸ of the Cl_3^\cdot radical indicated that the evidence for its linearity was mistaken; the bands assigned to it in fact arose from the linear Cl_3^- ion. E.S.R. matrix studies have detected and characterized ClF_4^\cdot ⁹, ClF_6^\cdot ^{10,11}, BrF_6^\cdot ^{11,12} and IF_6^\cdot ¹¹.

(B) MATRIX ISOLATION STUDIES

This work deals with the detection of XF_2^\cdot , X_2F_2 and XF_2^\cdot interhalogens. The experimental details, the spectra obtained and their interpretation are contained in Appendix 1 (Inorg. Chem., 17, 970 (1978)). It is appropriate to discuss the data and conclusions in slightly more detail. The spectra of both the diatomic interhalogens¹ and main group fluorides¹³ have recently been reviewed, and the trends in their vibrational frequencies and force constants have been noted. It is clear that, for the lower oxidation state interhalogens, the force constant for an X-F bond decreases on descending the group, and that in molecules with two types of X-F bond the shorter bond has the greater force constant. However, it is noteworthy that in the series ClF_5 , BrF_5 and IF_5 both the force constants for the apical and basal X-F bonds increase on descending the group.

The most complete data for radical interhalogens are available for the XF_2^\cdot species (Table 1). The trends from ClF_2^+ through ClF_2^\cdot to ClF_2^- are clearly visible. It is appropriate to note that for ClF_2^\cdot ν_2 and ν_3 have only been detected in infrared spectra and ν_1 only in Raman spectra. A naive application of "selection rules" implies that the molecule is linear. However the intensity of ν_1 in infrared spectra and ν_3 in Raman spectra for an XY_2 molecule having an interbond angle α more than 140° may be negligible²⁰. In such case a lower limit for α may be calculated using anharmonic frequencies for ν_3 obtained by isotopic substitution of the central atom, albeit with a large possible error as α approaches 180° ²¹. Application of this treatment to ClF_2^\cdot leads to $\alpha = 136 \pm 4^\circ$. Confirmation of a bent geometry could come from the observation of a central atom isotope shift for ν_1 in the Raman effect. In the case of BrF_2^\cdot observation of ν_3 at 569 cm^{-1} with isotope splitting leads to an interbond angle of $152 \pm 8^\circ$, the larger uncertainty reflecting the smaller shift derived from $^{79}\text{Br} - ^{81}\text{Br}$ substitution. The deformation mode, ν_2 , is expected to lie considerably below that of ClF_2^\cdot (242 cm^{-1}) since the comparable deformation in BrF_3 (ν_5, b_1) is smaller by 80 cm^{-1} than that of ClF_3 . It would therefore be beyond the spectral range of the experiments carried out. The Raman data obtained for both were disappointing and no band attributable to ν_1 was detected.

Reasonably complete data were obtained for the X_2F^\cdot systems (Table 2). The vibrational modes are listed merely in order of wavenumber, and the potential

TABLE 1

Data for XF_2 Species

Species	Symmetry	Observed Frequencies (cm^{-1})			Bond Angle (degrees)	f_r ($\text{mdyn } \text{\AA}^{-1}$)
		ν_1	ν_2	ν_3		
ClF_2^+ ^{7,14,15}	C_{2v}	807	387	830	100	4.74
ClF_2^\cdot ^{4,7}	C_{2v}	500	242	578	136 ± 4	2.48
ClF_2^- ¹⁶	$\text{D}_{\infty h}$	476		635	180	2.35
BrF_2^\cdot	C_{2v}			569	152 ± 8	
BrCl_2^\cdot	C_{2v}			325		
$^{35}\text{ClF}^a$		773.5				4.562
$^{79}\text{BrF}^{17}$		663.6				4.071
$\text{BrCl}^{18,19}$		439.5				2.832

(a) See section 3(c)

TABLE 2Data for X_2F Species

Compound	Observed Frequencies (cm^{-1}) ^c		
	ν_1^a	ν_2^b	ν_3
$^{35}\text{Cl}_2\text{F}$	559	464	270
$^{79}\text{Br}_2\text{F}$	507		
I_2F	499		
$^{35}\text{ClF}^d$	773.5		
$^{79}\text{BrF}^{17}$	663.6		
IF^{22}	618		
$^{35}\text{Cl}_2^{22}$		556.9	
$^{79}\text{Br}_2^{22}$		323.2	
I_2^{22}		213.4	

a. Largely X-F stretching character.

b. Largely X-X stretching character.

c. Uncorrected for anharmonicity.

d. See Section 3c.

energy distribution (Appendix 1) indicates that ν_1 of Cl_2F has largely Cl-F stretching character, ν_2 largely Cl-Cl stretching character and ν_3 is almost entirely the bending mode. As expected ν_2 is much weaker in intensity than ν_1 . In the heavier species ν_2 will have more X-X stretching character and thus become less intense and lower in frequency. ν_3 for these species is very likely to appear at less than 200 cm^{-1} . Thus the failure to observe ν_2 and ν_3 for Br_2F and I_2F is not unexpected. The force constants and bonding for these compounds are discussed in detail in Appendix 1.

Data for the X_2Y_2 systems are shown in Table 3. In a T-shaped X_2Y_2 molecule there are three modes of largely stretching character - $\nu_1(a_1)$; $\nu_2(a_1)$; and $\nu_4(b_1)$. Of these ν_1 is essentially the symmetric stretch of the Y-X-Y unit and since the YXY angle is expected to be close to 180° this will be a low intensity I.R. band. Similarly ν_2 will have largely X-X stretching character and will be weak. Therefore the only stretching mode anticipated to be detected will be ν_4 , an antisymmetric stretching mode of a close-to linear Y-X-Y unit. The closest approximation to a well-characterized mode of a stable molecule will therefore be $\nu_4(b_1)$ of ClF_3 ²³, BrF_3 ²³ and IF_5 ²⁵. IF_3 is a poorly characterized polymeric solid²⁴ and data obtained from it are not strictly comparable. The spectra for these X_2Y_2 species have been assigned based on the $\text{Cl}-\overset{\text{F}}{\underset{\text{F}}{\text{Cl}}}$ type structure rather than the alternative $\text{Cl}-\overset{\text{F}}{\text{Cl}}-\text{F}$ model. In the first place the bands observed fit close-to-linear rather than almost-right-angle F-Cl-F units. In the latter case the symmetric and antisymmetric stretching modes would be expected to have similar intensities and different isotope shifts would be expected. Secondly these are the shapes predicted by VSEPR theory when the central atom is three coordinate with two lone pairs.²⁶ In such a case the basic coordination unit is a trigonal bipyramid with the lone pairs in equatorial sites, and the more electronegative ligands in axial sites. These rules have found general application in p-block elements, and for instance all the mixed pentahalides of phosphorus and antimony conform to this model²⁶. The other possible type of X_2Y_2 unit is a loosely associated dimer. Species of this type may be responsible for the breadth of some of the bands assigned to the interhalogen diatomic molecules. The shapes that these adopt are not known beyond the fact that these dimers are polar.²⁷

One last point of significance in this work is that no charged species were produced in these experiments. The energy of the photolytic sources used was insufficient to ionize the halogens or interhalogens employed¹.

TABLE 3

Data for X_2Y_2 Species
Observed Frequency (cm^{-1})

Compound	$\nu_4(b_1)$
$^{35}\text{Cl}_2\text{F}_2$	627
$^{79}\text{Br}_2\text{F}_2$	554
I_2F_2	526
$^{79}\text{Br}_2\text{Cl}_2$	325
ClF_3^{23}	677
BrF_3^{23}	597
IF_3 (solid) ²⁴	480*
IF_5^{25}	593
$\text{BrCl}^{18,19}$	439.5

* This frequency is probably abnormally low due to F-bridging.

(C) DIATOMIC INTERHALOGENS

In the above discussion of interhalogen radicals, many of the spectra obtained are related to the vibrational spectra of the halogens and diatomic interhalogens. However it is surprising to find that some of the spectra available for these species were obtained at low resolution, and therefore the vibrational and rotational constants are not precisely determined. Three interhalogen compounds, related to those studied in section B, illustrate this point.

The best infrared data available for chlorine monofluoride date from 1951²⁸, in which work the values of ω_e and $\omega_e x_e$ calculated for ^{35}ClF were 786.34 and 6.23 cm^{-1} , respectively, compared with 783.543 and 5.2046 in this work. The resolution claimed for this earlier work is 0.4 cm^{-1} , a high figure for that time, and this represents some of the best infrared data available for an interhalogen. The rotational constants have been redetermined from older microwave data more recently²⁹. ClF is, however, a stable compound, albeit very reactive, so that these spectra are relatively easy to measure.

Bromine monochloride is an example of an interhalogen that exists in equilibrium with its elements; the equilibrium constant for the reaction is 0.15¹⁸. The latest reports of the infrared spectrum of BrCl vapor date from 1954¹⁸ and 1955¹⁹. These spectra were recorded at low resolution and since there are, in natural abundance BrCl, four isotopic variants present, only estimates of ω_e and $\omega_e x_e$ were given. There have been several low resolution Raman investigations of both the vapor and liquid phases³⁰⁻³², and more recently UV-visible absorption³³ and emission studies³⁴ have been reported.

Bromine monofluoride presents more difficult problems. It exists only in equilibrium with Br_2 , BrF_3 and BrF_5 ³⁵ and, since this system contains fluorides, it is especially corrosive and reactive. All Br-F stretching modes occur between 600-750 cm^{-1} and consequently measurement of the BrF vapor-phase infrared spectrum is difficult because of bands from interfering compounds even at low resolution. At higher resolutions, when long scanning times are necessary, the sample composition can vary significantly. The only report of the gas-phase spectrum, published in 1959³⁶, employed large unspecified slitwidths. BrF has been observed in matrices but appears to be subject to a large matrix shift³⁷. The best data arise from a flame emission study (1955)¹⁷ that gives values of 672.6 and 4.5 cm^{-1} for ω_e and $\omega_e x_e$. There is a large scatter in all the reported vibrational data for this molecule.

It may be misleading to employ existing infrared spectral data in detailed comparisons, or to attempt any more sophisticated analyses above those in (B) above and Appendix 1 without better data, and therefore the infrared vapor-phase spectra of these molecules were remeasured. This work was performed in conjunction with the Department of Physics, University of Tennessee, and is presented in Appendix 2.

(D) REFERENCES FOR SECTION 1.

1. A. J. Downs and C. J. Adams, in 'Comprehensive Inorganic Chemistry', J.C.Bailar et al. eds., Pergamon, Oxford, 1973, Vol. 2, p 1107.
2. Inorganic Chemistry of the Main Group Elements, Vol. 1-6, The Chemical Society, London.
3. L. Y. Nelson and G. C. Pimentel, Inorg. Chem., 7, 1695 (1968).
- 4a. G. Mamantov, E. J. Vasini, M. C. Moulton, D. G. Vickroy, and T. Maekawa J. Chem. Phys., 54, 3419 (1971).
- 4b. M. R. Clarke, W. H. Fletcher, G. Mamantov, E. J. Vasini and D. G. Vickroy, Inorg. Nucl. Chem. Lett., 8, 611 (1972).
5. L. Y. Nelson and G. C. Pimentel, J. Chem. Phys., 47, 3761 (1967).
6. D. H. Boal and G. A. Ozin, J. Chem. Phys., 55, 3598 (1971).
7. E. S. Prochaska and L. Andrews, Inorg. Chem., 16, 339 (1977).
8. B. S. Ault and L. Andrews, J. Chem. Phys., 64, 4853 (1976).
9. J. R. Morton and K. F. Preston, J. Chem. Phys., 58, 3112 (1973).
10. K. Nishikida, F. Williams, G. Mamantov and N. R. Smyrl, J. Amer. Chem. Soc., 97, 3526 (1975).
11. A. R. Boale, J. R. Morton and K. F. Preston, Inorg. Chem., 14, 3127 (1975); J. Phys. Chem., 80, 2954 (1976).
12. K. Nishikida, F. Williams, G. Mamantov and N. R. Smyrl, J. Chem. Phys., 63, 1693 (1975).
13. N. R. Smyrl and G. Mamantov, Adv. Inorg. Chem. Radiochem., 21, 231 (1978).
14. R. J. Gillespie and M. J. Morton, Inorg. Chem. 9, 616 (1970).
15. K. O. Christe and C. J. Schack, Inorg. Chem., 9, 2296 (1970).
16. K. O. Christe, W. Sawodny and J. P. Guertin, Inorg. Chem., 6, 1159 (1967).
17. P. H. Brodersen and J. E. Sicre, Z. Phys., 141, 515 (1955).
18. H. C. Mattraw, C. F. Pachucki and N. J. Hawkins, J. Chem. Phys., 22, 1117 (1954).
19. W. V. F. Brooks and B. Crawford, J. Chem. Phys., 23, 363 (1955).
20. I. R. Beattie and M. J. Gall, J. Chem. Soc. (A), 1971, 3569.
21. J. K. Burdett, M. Poliakoff, J. J. Turner and H. Dubost, Adv. Infrared Raman Spectrosc., 2, 1 (1976).
22. K. P. Huber and G. Herzberg, Molecular Spectra and Molecular Structure. Vol. IV: Constants of Diatomic Molecules. (Van Nostrand Reinhold, New York, 1979).
23. R. A. Frey, R. L. Redington and A. L. K. Aljibury, J. Chem. Phys., 54, 344 (1971).

24. M. Schmeisser, D. Naumann and E. Lehmann, J. Fluorine Chem., 3, 441 (1973).
25. L. E. Alexander and I. R. Beattie, J. Chem. Soc. (A), 1971, 3091.
26. See e.g. R. J. Gillespie, 'Molecular Geometry', Van Nostrand-Reinhold, New York, 1972.
27. K. V. Chance, K. H. Bowen, J. S. Winn and W. Klemperer, J. Chem. Phys., 72, 791 (1980).
28. A. H. Nielsen and E. A. Jones, J. Chem. Phys., 19, 1117 (1951).
29. F. J. Lovas and E. Tiemann, J. Chem. Phys. Ref. Data, 3, 609 (1974).
30. H. Stammreich, R. Fournieris and Y. Tavares, Spectrochim. Acta, 17, 1173 (1961).
31. W. Holzer, W. F. Murphy and H. J. Bernstein, J. Chem. Phys., 52, 399 (1970).
32. F. Wallart, Can. J. Spectros. 17, 128 (1972).
33. J. A. Coxon, J. Mol. Spectros., 50, 142 (1974).
34. S. G. Hadley, M. J. Bina and G. D. Brabson, J. Phys. Chem., 78, 1833 (1974).
35. L. Stein, J. Amer. Chem. Soc., 81, 1269 (1959).
36. L. Stein, J. Amer. Chem. Soc., 81, 1273 (1959).
37. R. R. Smardzewski and W. B. Fox, J. Fluorine Chem., 7, 453 (1976).

2. INFRARED LASER PHOTOCHEMISTRY

(A) MATRIX-ISOLATION STUDIES

It is well established that polyatomic molecules in the gas phase at low pressures may be dissociated by high power infrared laser irradiation, and that this may proceed with isotopic selectivity¹. There have been several reports of I.R. laser photolysis of molecules isolated in matrices^{2-8,11,12}, and, if this was a generally applicable technique, it would lead to the possibilities of discovering more information about modes of dissociation, and, via trapping, the investigation of novel intermediate species.

Three approaches to this have been reported. The first involved irradiation of the unsaturated complex $\text{Fe}(\text{CO})_4$, labelled with ^{13}CO , with a low power CO laser. In a series of papers²⁻⁶ it was demonstrated that this molecule was very labile and interconversion of the various conformers, as well as their selective reaction, were achieved. A key point is that it is thought that these processes require only the energy of a single I.R. photon.

The second study dealt with irradiation of matrix-isolated SF_6 with a high power CO_2 laser^{7,8}. SF_6 may be dissociated in the gas phase by irradiating its ν_3 band at ca. 940 cm^{-1} , and this process requires 40-60 photons^{9,10}. This can be isotopically selective - i.e. $^{32}\text{SF}_6$ is dissociated but $^{34}\text{SF}_6$ is affected to a proportionately far lesser extent. It was claimed that isotopically selective multiphoton dissociation of SF_6 , isolated in CO and Ar matrices, had been detected and monitored by the relative intensities of the $^{32}\text{SF}_6$ and $^{34}\text{SF}_6$ bands at ca. 940 cm^{-1} .

The third study was entitled 'SPARCCS'^{11,12} - single-photon-absorption reaction chemistry in the solid state. It was claimed that a reaction between UF_6 and SiH_4 , and a number of other reactant pairs, was stimulated by irradiation with a low power diode laser operating in the 16μ region where ν_3 of UF_6 occurs. The effects observed were small and required irradiation times of up to 10 hours.

The claim for observation of multiphoton effects in matrices appeared important and therefore a detailed study of several systems was undertaken. The results obtained are summarized in Appendix 3 (J. Amer. Chem. Soc., 100, 6526 (1979)). The published paper contains only brief details of this work and it will be discussed in more detail here.

Of immediate interest to this project is the claim by Ambartzumian *et al*^{7,8} to have observed selective dissociation of $^{32}\text{SF}_6$ in argon and carbon monoxide matrices using a carbon dioxide laser operating in the 940 cm^{-1} region. They estimated that each molecule absorbs energy corresponding to about 150 quanta of CO_2 laser radiation. We were surprised that no dissociation products were detected using infrared spectroscopy since vibrational data are available for the likely products (SF_4 ¹³, S_2F_{10} ¹⁴, SF_5 ¹⁵). A reported decrease in absorption due to $^{32}\text{SF}_6$ from about 95% to about 55% would be expected to yield photo-products having substantial absorbances.

A systematic series of experiments was, therefore, carried out involving CO_2 laser irradiation of SF_6 in both argon and nitrogen matrices. Spectra similar to those published by Ambartzumian *et al*^{7,8} were obtained but we do not believe that they represent convincing evidence for dissociation. Furthermore, analogous experiments were performed with other matrix-isolated species, in both inert and reactive matrices, and similar negative results were obtained. The systems studied are listed in the table of Appendix 3.

Figure 2.1 shows the infrared spectrum of SF_6 suspended in a nitrogen matrix in the region of $\nu_3(t_{1u})$, the infrared active sulfur-fluorine stretching mode. The absorption at 938 cm^{-1} arises from $^{32}\text{SF}_6$ and that at 921 cm^{-1} from $^{34}\text{SF}_6$. Natural abundance sulfur has an isotopic composition of ^{32}S 95.0%, ^{33}S 0.76% and ^{34}S 4.22%. The matrix sample ratio employed here was 42,000/1, the most dilute used in this study, and under these conditions no bands attributable to aggregate species are detected. After subjecting this sample to photolysis (100 pulses, 1 J per pulse unfocussed, P(26) of $00^\circ 1-10^\circ 0 \equiv 938.7\text{ cm}^{-1}$) the absorption due to both $^{32}\text{SF}_6$ and $^{34}\text{SF}_6$ decreased uniformly and no bands arising from new species were seen in the range $2800-200\text{ cm}^{-1}$. The matrix, which was "glassy" after deposition, had a "frosty" appearance after photolysis. Ambartzumian *et al*^{7,8} note that the absorption peak of $^{32}\text{SF}_6$ exhibited a red shift of about 2 cm^{-1} . We did not observe this effect but note that the half-width of the band is smaller after irradiation. We also noted that the contour of this band in both argon and nitrogen matrices changed on annealing; the band contours are complex because of (a) low site symmetries leading to a partial lifting of the degeneracy of the t_{1u} mode (b) possible multiple site effects. Our observations suggested that these results are simply a reflection of evaporation of the matrix (plus solute), perhaps with a slight isotope selection effect.

In more concentrated matrices (SF_6/N_2 1/1000-1/2000) the spectra obtained are complicated by aggregation effects. Small absorbances are seen at 949 and

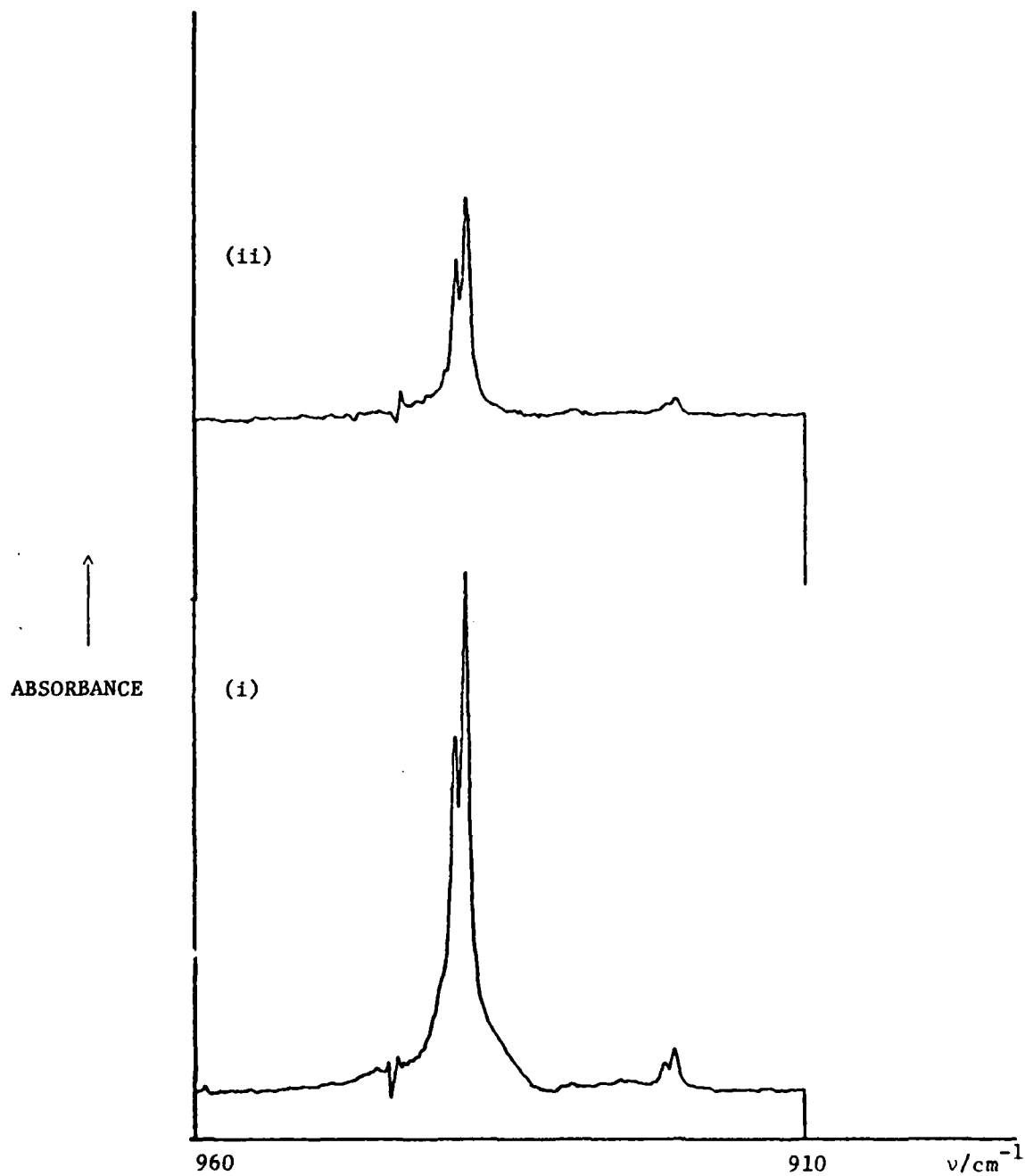


Fig. 2.1

 $\text{SF}_6:\text{N}_2$ 1:42,000

(i) Before photolysis

(ii) After photolysis

Note: Vertical scale is the same for both spectra.

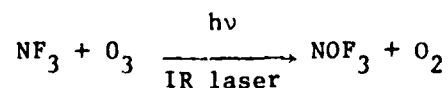
944 cm^{-1} on the high wavenumber side and 929 and 926 cm^{-1} on the lower side of the main band. After annealing these matrices at 26 K the high wavenumber bands merge into the shoulder of the 938 cm^{-1} peak and the 929 cm^{-1} band grows at the expense of the feature at 926 cm^{-1} . $^{33}\text{SF}_6$ (0.76% abundant) makes a small contribution to the intensity of the band at 929 cm^{-1} . These more concentrated matrices are more susceptible to damage during photolysis so that for comparable initial absorbances greater evaporation is observed per pulse the more concentrated the matrix. When pure SF_6 was used a few pulses caused almost complete evaporation, despite the high sublimation point (-64°C) of the pure substance. When the laser beam was focussed to a 'line' about 1 mm x 5 mm one pulse is sufficient to vaporize totally the illuminated portion of the matrix in both dilute matrices and those with low total optical densities. Prolonged photolyses caused the cesium iodide substrate to fracture. In all of the above cases no absorbances attributable to photoproducts were observed.

Possible reasons for this failure are:

1. Recombination of fragments produced if these products are held in a tight matrix 'cage'.
2. Photofragments are produced but are vaporized along with the matrix.
3. SF_6 molecules do not absorb sufficient photons to be dissociated because of (a) low laser power and/or (b) anharmonic effects.
4. Vibrational relaxation to the matrix occurs rapidly, also causing thereby local heating and vaporization.

Of these possibilities, (3) may be discounted on the evidence presented by Ambartzumian *et al*^{7,8}. No quantitative data are available to sustain (4) but in this connection we found that pure solid transmits even a focussed laser beam with no damage, as does any matrix if the frequency of irradiation is $> 10 \text{ cm}^{-1}$ removed from absorption band. It would be difficult to test (2) but a series of experiments was performed to investigate (1).

Nitric oxide was used to trap possible radicals produced by photolysis of NF_3 and N_2F_4 , and the possible reaction



was also investigated. No evidence was found for production of photoproducts,

(the matrix isolation infrared spectra of these compounds are well known¹⁶⁻¹⁹). Furthermore, when irradiating N_2F_4 at a frequency corresponding to ν_8 absorption of the gauche isomer, no change in trans:gauche conformer ratio was found.

We tentatively concluded that although we could not duplicate the results of Ambartzumian et. al.^{7,8}, they may be due to the differential evaporation of $^{32}SF_6$ and $^{34}SF_6$ from the matrix under special circumstances. Two papers published almost simultaneously with ours^{20,21} and further studies that appeared soon after have contributed to the understanding of these effects.

Davies et. al.²⁰ demonstrated that the apparent isotope enrichment is caused by deviations from Beer's Law arising from partial ablation of the matrix. Irradiation of only part of the matrix, or of the whole with a non-uniform beam (characteristic of the output of TEA lasers under usual conditions), causes a non-uniform sample to be produced. These workers also observed no dissociation products, and presented the hypothesis that efficient vibrational relaxation by the matrix host would prevent efficient ladder climbing by the guest.

Jones et. al.²¹ subsequently demonstrated that I.R. laser irradiation at moderate powers does cause evaporation of guest SF_6 molecules from the matrix, but that $^{34}SF_6$ molecules evaporate at the same rate as $^{32}SF_6$ when only the latter are irradiated. They suggest that $^{32}SF_6$ molecules distribute their energy (i.e. vibrationally relax) to other guest molecules which can then migrate to the surface and leave the matrix. The same group demonstrated in another paper²² that in the case of the UF_6-SiH_4 'SPARCCS' experiment the induced reaction is caused by near-I.R. radiation from the spectrometer's Nernst glower and not from 16 μ I.R. laser radiation. The most recent contribution to this field has shown that in two specific cases I.R. laser photolysis does not induce cis-trans isomerization in stable molecules²³.

At this point it appeared that the only bona fide I.R. laser matrix photolysis results were those of Turner et. al.²⁻⁶ on the labile and reactive $Fe(CO)_4$ systems where it is entirely plausible that absorption of only one I.R. photon could cause isomerization. At this point our work in the photolysis of molecules already in matrices came to an end.

Some experiments were performed to investigate the effect of photolysis of the gas sample during deposition. The matrix/sample mixture (N_2/SF_6 1/2000) was passed down a 70 cm long copper tube, 3.5 cm in diameter, connected by 1.25 cm tubing through a ball valve to the cryostat shroud. In a typical experiment the mixture was deposited over 30 min., during which time laser radiation

at 944.2 cm^{-1} , 2 J per pulse, was directed down the tube. This failed to produce any compounds other than SF_6 in the matrix deposit although there was a slight enhancement of $^{34}\text{SF}_6$. This is attributed to the low duty cycle of the laser (max. rep. rate $\sim 1\text{ Hz}$, pulse length up to $2\text{ }\mu\text{s}$), and the possibility that reactive radical species produced could be absorbed onto the walls of the tube and valve.

In order for an experiment of this type to be successful several modifications would be required. An approach would be to employ pulsed deposition using automatically controlled valves synchronized to the laser pulse so that deposition occurred only when the laser was 'on'. The laser beam could be directed across the substrate used, inside the high vacuum chamber, so that radicals produced could not diffuse to the walls. A system of this type is described in the literature²⁴ for use with U.V.-visible flash photolysis apparatus.

EXPERIMENTAL

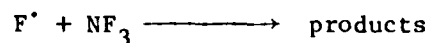
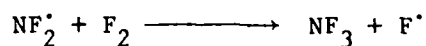
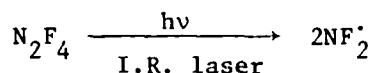
A closed-cycle Cryodyne 350 refrigerator was used, whose temperature was monitored and controlled to within $\pm 1\text{ K}$ using a Cryogenic Technology Inc. digital electronic temperature controller in conjunction with a gold-chromel thermocouple and resistance heater. Matrix mixtures were prepared in a stainless steel vacuum line well-passivated with chlorine trifluoride (Matheson 98%). In most cases gas mixtures were prepared and deposited from a single manifold. In the case of the NF_3/O_3 experiments the Ar/NF_3 and Ar/O_2 mixtures were prepared separately and only the Ar/O_2 mixture was passed through the microwave discharge. A Raytheon Microtherm Model CMD10 microwave generator supplied a maximum of 125 W at 2450 MHz. The energy was directed through an Evenson-type cavity, to generate a discharge in a 0.5 inch Pyrex tube. Between the discharge zone and the cold plate was a 1mm diameter orifice. Infrared spectra were recorded on a Digilab Model FTS 20 Fourier transform spectrometer. A Lumonics TEA 103-2 CO_2 laser was operated in the $10.6\text{ }\mu$ region with an energy of 1-3 J per pulse. Output modes were monitored using an Optical Engineering Model 10 R spectrum analyser.

(B) GAS PHASE STUDIES

The object of this phase of the work was to investigate the possibility of synthesizing NF_4BF_4 using an infrared laser. I.R. laser irradiation of the reactants isolated in matrices had been planned but the work reported in section 2(A) above indicated that this was unlikely to lead to any reaction.

NF_3 has two gas phase bands that fall in the operating range of the CO_2 laser. ν_1 (a_1) has PQR structure and is centered at 1032 cm^{-1} , while the stronger ν_3 (e) has a perturbed PR structure and is centered at 908 cm^{-1} . NF_3 was irradiated using the CO_2 laser tuned to P(34), P(36) and P(38) of the $00^{\circ}1-02^{\circ}0$ band, corresponding to 1033.48 , 1031.46 and 1029.43 cm^{-1} and also with several lines around 925 cm^{-1} . The laser operates at only very low power below 925 cm^{-1} , and therefore irradiation of the more favorable P branch side of ν_3 was not possible and most experiments were concerned with the irradiation of the ν_1 band. Irradiation of NF_3 alone, $\text{NF}_3 + \text{H}_2$ and $\text{NF}_3 + \text{BF}_3 + \text{F}_2$ produced no spectroscopically detectable changes. Neither F_2 nor BF_3 have any infrared absorbing bands in the CO_2 laser region (approx. $1080 - 920 \text{ cm}^{-1}$) so that initiation of the $\text{NF}_3 + \text{BF}_3 + \text{F}_2$ reaction in a direct manner with CO_2 laser photolysis appeared to be impossible.

N_2F_4 is known to suffer dissociation when irradiated with CO_2 laser radiation at 944 cm^{-1} in the gas phase at low pressures, producing $\text{NF}_2^{\cdot 25}$. This suggests a second approach to laser synthesis of NF_4BF_4 . Because the first step in the production of this compound by conventional U.V. photolysis is the generation of F^{\cdot} , the following sequence should be possible:



The I.R. photolysis of a N_2F_4 mixture produced almost complete conversion to NF_3 in a few flashes. Therefore the I.R. laser photolysis of a $\text{NF}_3 + \text{BF}_3 + 2\text{F}_2$ mixture was examined, and the progress of the reaction monitored spectroscopically, and via the pressure drop. Whereas conversion of $\text{N}_2\text{F}_4 + \text{F}_2$ to NF_3 proceeds with no decrease in pressure the formation of NF_4BF_4 will cause a decrease. In a few flashes the N_2F_4 concentration decreased and that of NF_3 became substantial, and then a slow pressure drop and parallel loss of BF_3 occurred. It is probable that the photolysis of the residual N_2F_4 was producing F^{\cdot} (as above) which then initiated the formation of NF_4BF_4 . The initial rate of conversion per flash of reactants into NF_4BF_4 was only 0.2%. After extended photolysis (e.g. about 4000 flashes) traces of a white powder could be detected in the cell.

This technique is clearly severely limited. Assuming a gas cell of conventional size (2.5 cm diameter, 10 cm long) an initial pressure of 100 torr (i.e. 25 torr NF_3 , 25 torr BF_3 and 50 torr F_2) and a 100% conversion then 7.2×10^{-5} moles of product would result, corresponding to 12.7 mg. However even these are optimistic figures because 100 torr is a high pressure for N_2F_4 multiphoton dissociation (it is more likely that thermal processes were mostly responsible), and in no case was more than a 10% loss of BF_3 observed. Nevertheless after many cycles of photolysis, cell evacuation and refilling, a small quantity of greyish powder was removed from the cell under inert atmosphere conditions, and sealed in a glass tube for Raman spectroscopic examination. It was anticipated that the sample would be contaminated by nickel and copper fluorides from the cell walls so that an X-ray powder investigation would be troublesome.

The weight of the sample was estimated visually to be about 1 mg. Recording a Raman spectrum of this sample was difficult owing not only to its small size, but also its contamination with dark particles presumed to be copper and nickel fluorides. No spectrum corresponding to that of NF_4BF_4 could be obtained. The same sample was subsequently examined as an AgCl mini-pellet but again no features assignable to NF_4BF_4 were observed.

The claim that NF_4BF_4 was produced therefore rests upon the circumstantial evidence of pressure drop and decrease in amount of BF_3 . Whether it was or was not produced it can be concluded that this procedure is slow and inefficient compared to U.V. Photolysis (see Section 3) and that further investigation of a method involving IR laser photolysis is not profitable at this time.

The case of NF_4BF_4 production is not entirely typical, because of the low yield in the system, so that it is misleading to draw conclusions for the prospects of I.R. laser photochemical synthesis from this one case. In others the yield (conversion per flash) may be large and a pressure of about a torr of product can be made per flash. However the restriction of working at low pressure remains. To investigate this a qualitative study of the I.R. laser photolysis of hexafluoroacetone (HFA) was undertaken. At low pressures (1 torr or less) photolysis of HFA at 970.56 cm^{-1} with about 1J per pulse unfocussed produced only C_2F_6 and CO . At higher pressures products (C_2F_4 and CF_3CFO) that are formed in thermal decomposition appear. Addition of a foreign gas (e.g. H_2) at low pressures can give rise to new products (e.g. CF_3H) but as the total pressure rises, the conversion per flash falls until, at a total pressure of more than 200 torr, the reaction is completely quenched. The absorbing mole-

cules suffer collisional deactivation before enough photons can be absorbed for dissociation.

Thus these limitations may preclude the application of I.R. laser photolysis in bulk systems unless one particular compound, isomer or isotopic variant is inaccessible by usual syntheses. It may be of application where selective reaction of a small quantity is required - e.g. in removing trace quantities of contaminants or in doping processes.

An example of the preparation of a small amount of an isotopically substituted compound is the synthesis of $^{13}\text{CF}_2 = ^{13}\text{CF}_2$. It was of interest to Dr. T. F. Williams of this Department to obtain a small quantity of this material in order to extend ESR studies of C_2F_4 ²⁶⁻²⁸, and all attempts to prepare the isotopically enriched substance by conventional thermolysis had failed. The infrared laser photolysis of gaseous CHClF_2 has, however, been shown²⁹ to produce C_2F_4 and HCl cleanly.

The study of the laser photolysis of CHClF_2 ²⁹ showed that the reaction proceeded at pressures up to 100 torr, rendering its use in small-quantity synthesis feasible. The CO_2 laser frequency used was 1088 cm^{-1} , on the low frequency side of a band centered at 1114 cm^{-1} , which has a complex contour. This band was originally assigned³⁰ as the antisymmetric (a'') CF_2 stretching mode, but as a result of later Raman^{31,32} and matrix-isolation infrared studies³³, Milligan et al.³³ reassigned this band as a coincidence between the symmetric (a') and antisymmetric carbon-fluorine stretching modes.

Natural abundance CHClF_2 was prepared from CHCl_3 by reaction with an $\text{SbF}_3/\text{SbCl}_5$ mixture at 60°C for 40 minutes³⁴. The resulting gas was condensed upon NaOH and CaCl_2 in order to remove acidic gases and for drying. The infrared spectrum of this gas indicated that the major product was CHClF_2 , with small quantities of CHF_3 ³⁰, CO_2 , COClF ³⁵ and SiF_4 also present. Treatment of $^{13}\text{CHCl}_3$ (Merck) in a similar fashion produced largely $^{13}\text{CHClF}_2$, and small quantities of $^{13}\text{CHF}_3$, $^{13}\text{CO}_2$, $^{13}\text{COClF}$ and SiF_4 .

The conditions used for the photolysis of $^{13}\text{CHClF}_2$ were not optimal, but represented the results of several compromises, since it was not possible, given the small quantity of material available, to perform a series of experiments to determine the best procedure. Because the infrared spectrum of $^{13}\text{CHClF}_2$ is different from that of the ^{12}C isotopomer, and the performance of the IR laser changes from line to line, the conditions used for photolysis of the ^{12}C compound will not be necessarily suitable for the ^{13}C compound. In particular, the laser power and energy density were maintained at lower values than could have been used,

to ensure that there was a low possibility of damage to the infrared cell windows, which could result in the loss of the precursor or product. It was also desirable to use a comparatively high pressure (50 torr) of gas in the cell to eliminate the need for its frequent emptying and refilling. The use of such a pressure implies that the process is essentially thermal rather than collision-free unimolecular decomposition.

Typically 50 torr of $^{13}\text{CHClF}_2$ were placed in a Pyrex IR cell equipped with greaseless valves (Kontes) and aluminum end pieces, to which KBr windows were sealed via Viton o-rings. The cell was 2.5 cm in diameter and 10 cm long. The infrared spectrum of the gas was taken, and the sample was then irradiated with up to 1000 IR laser flashes at 1078.58 cm^{-1} (R20 of 00°1-02°0) with an energy of 0.7 to 1.0 J per pulse, most of which was contained in a 100 ns wide FWHM pulse. The approximately parallel beam, 1.2 cm in diameter, was arranged so that it passed through the center portions of both KBr windows to minimize wall reactions. After photolysis the IR spectrum of the cell contents was recorded, and then the products were pumped out, and the cell was refilled.

The extent of the reaction was monitored by appearance of C_2F_4 . The spectrum of $^{12}\text{CF}_2 = ^{12}\text{CF}_2$ was recorded at differing pressures in the photolysis cell, and the pressure was correlated with the height of the Q-branch of $\nu_{12}(\text{b}_{3u})^{36}$ at 555.5 cm^{-1} . The sample of C_2F_4 was obtained from PCR, and pressures were measured using MKS Baratron (0.1 to 10 torr) and Heise (10 to 50 torr) gauges. This bend shifts to 552.0 cm^{-1} in $^{13}\text{CF}_2$ $^{13}\text{CF}_2$ and it was assumed that the absorption coefficients for the two isotopomers were identical. After 5 fills of the cell it was estimated, using this method, that approximately 50 torr of $^{13}\text{CF}_2$ $^{13}\text{CF}_2$ had been produced, representing a 40% conversion. This is not as great as could have been achieved under optimized conditions. (It is worth noting that the starting material was only 90% enriched in ^{13}C , but unlike other procedures it is expected that this will increase the enrichment, because the absorption of $^{12}\text{CHClF}_2$ at the frequency used is very small compared to that of $^{13}\text{CHClF}_2$. Because this is a thermal process this 'extra' enrichment factor may not be large. The products were not examined mass-spectroscopically to test this thesis.) One improvement implemented in a subsequent experiment was to absorb chemically the HCl produced during photolysis, since it competes for the CF_2 produced, ultimately limiting the extent of reaction²⁹. Sufficient $^{13}\text{CF}_2 = ^{13}\text{CF}_2$ was produced for several ESR experiments³⁷, and to record infrared spectra of its stronger IR bands.

(C) REFERENCES FOR SECTION 2

1. See e.g. P. A. Schultz, Aa. S. Sudbø, D. J. Krojnovich, H. S. Kwok, Y. R. Shen and Y. T. Lee, *Ann. Rev. Phys. Chem.*, 30, 379 (1979).
2. A. McNeish, M. Poliakoff, K.P. Smith and J. J. Turner, *J. C. S. Chem. Comm.*, 1976, 859
3. B. Davies, A. McNeish, M. Poliakoff, M. Tranquille and J. J. Turner, *Chem. Phys. Lett.*, 52, 477 (1977).
4. B. Davies, A. McNeish, M. Poliakoff and J. J. Turner, *J. Amer. Chem. Soc.*, 99, 7573 (1977).
5. B. Davies, A. McNeish, M. Poliakoff, M. Tranquille and J. J. Turner, *J. C. S. Chem. Comm.*, 1978, 36.
6. M. Poliakoff, B. Davies, A. McNeish, M. Tranquille and J. J. Turner, *Ber. Bunsenges. Phys. Chem.*, 82, 121 (1978).
7. R. V. Ambartzumian, Yu. A. Gorokhov, G. N. Makarov, A. A. Poretzky and N. P. Furzikov, *JETP Lett.*, 24, 287 (1976).
8. R. V. Ambartzumian, Yu. A. Gorokhov, G. N. Makarov, A. A. Poretzky and N. P. Furzikov, in 'Laser Spectroscopy', Vol. 3, J. C. Hall and J. L. Carlsten eds., Springer Verlag, New York, 1977, p. 439.
9. J. L. Lyman, S. D. Rockwood and S. M. Freund, *J. Chem. Phys.*, 67, 4545 (1977).
10. R. V. Ambartzumian, Yu. A. Gorokhov, V. S. Letokhov and G. N. Makarov, *JEPT Lett.*, 21, 171 (1975).
11. E. Catalano and R. E. Barletta, *J. Chem. Phys.*, 66, 4706 (1977).
12. E. Catalano, R. E. Barletta and R. K. Pearson, *J. Chem. Phys.*, 70, 3291 (1979).
13. K. O. Christe, E. C. Curtis, C. J. Schack, S. J. Cyvin, J. Brunvoll and W. Sawodny, *Spectrochim. Acta*, 32A, 1141 (1976).
14. R. R. Smardzewski, R. E. Nofhle and W. B. Fox, *J. Mol. Spectrosc.*, 62, 449 (1976).
15. R. R. Smardzewski and W. B. Fox, *J. Chem. Phys.*, 67, 2309 (1977).
16. R. J. L. Popplewell, F. N. Masri and H. W. Thompson, *Spectrochim. Acta*, 23A, 2797 (1967).
17. L. Brewer and J. L. F. Wang, *J. Chem. Phys.*, 56, 759 (1972).
18. R. R. Smardzewski and W. B. Fox, *J. Chem. Phys.*, 60, 2193 (1974).
19. M. D. Harmony and R. J. Myers, *J. Chem. Phys.*, 37, 636 (1962).
20. B. Davies, M. Poliakoff, K. P. Smith and J. J. Turner, *Chem. Phys. Lett.*, 58, 28 (1978).
21. L. H. Jones, S. Ekberg and L. B. Asprey, *J. Chem. Phys.*, 70, 1566 (1979).

22. L. H. Jones and S. A. Ekberg, J. Chem. Phys., 71, 4764 (1979).
23. M. Tasumi, H. Takeuchi and H. Nakano, Chem. Phys. Lett., 68, 44 (1979).
24. L. J. Allamandola, D. Lucas and G. C. Pimentel, Rev. Sci. Instrum., 49, 913 (1978).
25. J. L. Lyman and R. J. Jensen, Chem. Phys. Lett., 13, 421 (1972).
26. R. I. McNeil, M. Shiotani, F. Williams and M. B. Yin, Chem. Phys. Lett., 51, 433 (1977).
27. R. I. McNeil, M. Shiotani, F. Williams and M. B. Yin, Chem. Phys. Lett., 51, 438 (1977).
28. J. R. Morton, K. P. Preston, J. T. Wang and F. Williams, Chem. Phys. Lett., 64, 71 (1979).
29. E. Grunwald, K. J. Olszyna, D. F. Dever and B. Knishkowsky, J. Amer. Chem. Soc., 99, 6515 (1977).
30. E. K. Plyler and W. S. Benedict, J. Res. Nat. Bur. Stand., 47, 212 (1951).
31. W. Holzer and H. Moser, J. Mol. Spectrosc., 20, 188 (1966).
32. W. Holzer, J. Mol. Spectrosc., 25, 123 (1968)
33. D. E. Milligan, M. E. Jacox, J. H. McAuley and C. E. Smith, J. Mol. Spectrosc., 45, 377 (1973).
34. L. Andrews, H. Willner and F. T. Prochaska, J. Fluorine Chem., 13, 273 (1979).
35. A. H. Nielsen, T. G. Burke, P. J. H. Woltz and D. C. Smith, J. Chem. Phys., 20, 596 (1952).
36. J. R. Nielsen, H. H. Claassen and D. C. Smith, J. Chem. Phys., 18, 812 (1950).
37. J. T. Wang and F. Williams, unpublished work.

3. LOW TEMPERATURE SYNTHESIS

The object of this phase of the work was to investigate low temperature syntheses of NF_4BF_4 and the mechanism of the formation of that compound by photolytic methods. There have been several descriptions of preparative methods of NF_4^+ salts including use of high pressure and temperature^{1,2}, low temperature - irradiation³, low temperature glow discharge^{4,5}, metathesis^{6,7} and low temperature UV photolysis^{8,9}. The most successful method appears to be low temperature UV photolysis⁹, in which NF_3 and BF_3 were condensed at 77K into a pan-shaped quartz reactor, and F_2 added. Photolysis was achieved using a GE BH-6 lamp filtered merely through a quartz plate. However such a static system suffers from a low quantum yield (0.015), initially ascribed⁶ to the build up of product on the reactor walls blocking the UV radiation, but subsequently⁹ to the low thermal stability of some of the intermediates.

It was felt that UV photolysis using the rotating cryostat at 77K would eliminate the problem of product build-up, since fresh reactants are deposited on top of the product using this system, and that solid and matrix-isolation studies at 15K could enable intermediates to be trapped and studied, even if they did have low thermal stability. There has also been considerable discussion of the mechanism of the formation of NF_4BF_4 ^{8,10-12} and characterization of any intermediates by vibrational spectroscopy would aid in its elucidation. The nature of the studies was determined by the physical properties of the precursors at 77 and 15K, respectively. At 15K NF_3 , BF_3 , and F_2 are all solids with very low vapor pressures, but at 77K although BF_3 is still solid, NF_3 is a liquid with a vapor pressure of about 10^{-2} torr and fluorine is a liquid with a pressure of over 400 torr. Both of these are higher than the normal operating pressure of the rotating cryostat - (10^{-6} torr).

Figs. 3.1 and 3.2 show the effect of UV -visible photolysis upon a 1:1:1 mixture of NF_3 , BF_3 and F_2 condensed onto a CsI plate at 15K in a conventional closed-cycle cryostat. Trace (a) is a spectrum of the solid mixture, (b) that obtained after 15 mins. photolysis, (c) that after 15 mins. further photolysis and (d) that of the solid material remaining after the cryostat had warmed to room temperature and the volatile materials had been pumped away. The photolysis source was a GE BH-6 high pressure mercury lamp and no filtering, other than that of the quartz plate on the cryostat shroud, was used. Trace (d) corresponds to the previously reported IR spectra of NF_4BF_4 ^{3,9,13} (taken as powder between AgCl plates) with the exception of small bands at ca. 1090 and 610 cm^{-1} which arise from atmospheric attack upon the outer (shroud) CsI windows, and which

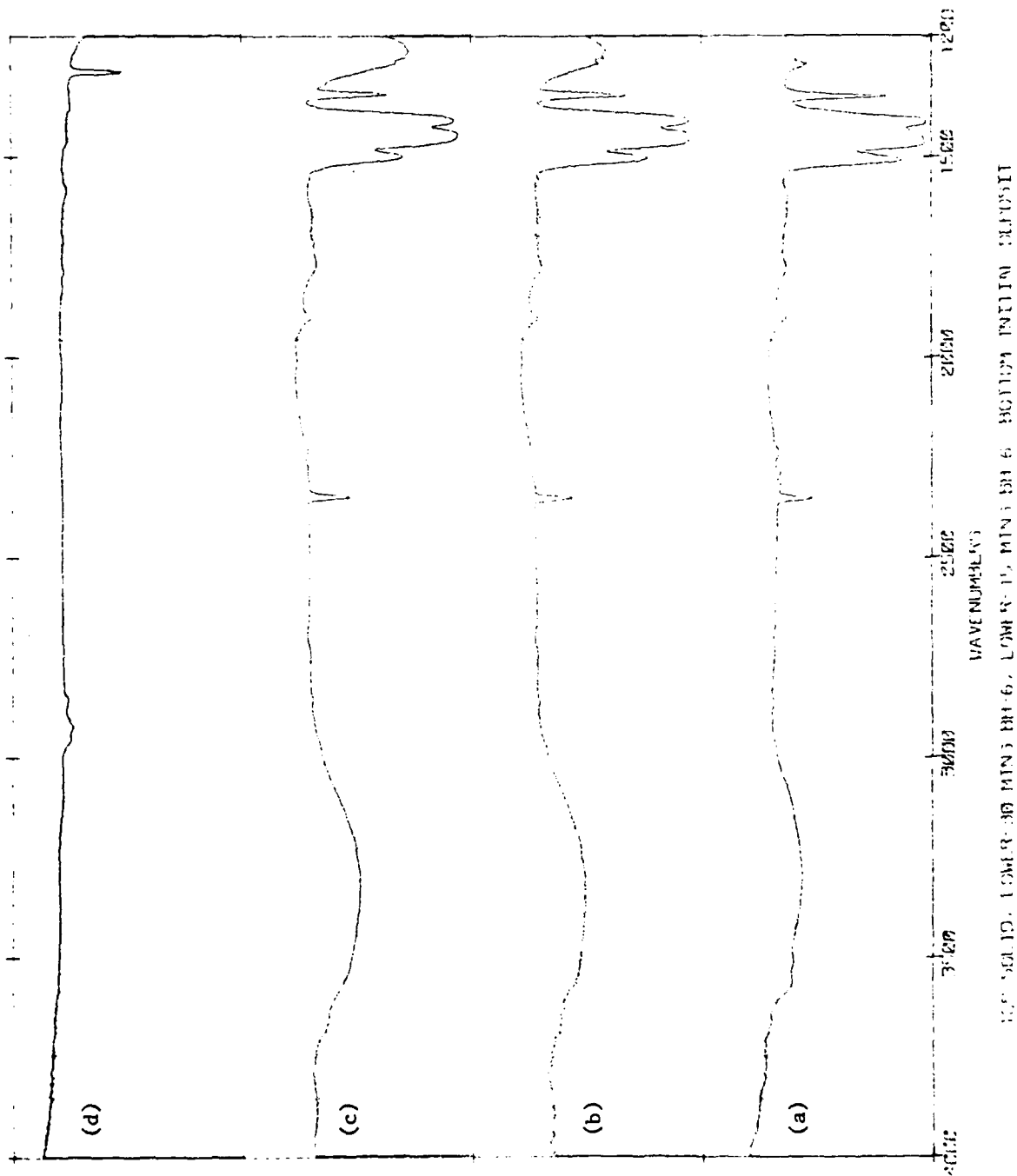


Fig. 3.1 FT-IR spectra of NF_3 , BF_3 and F_2 mixture.

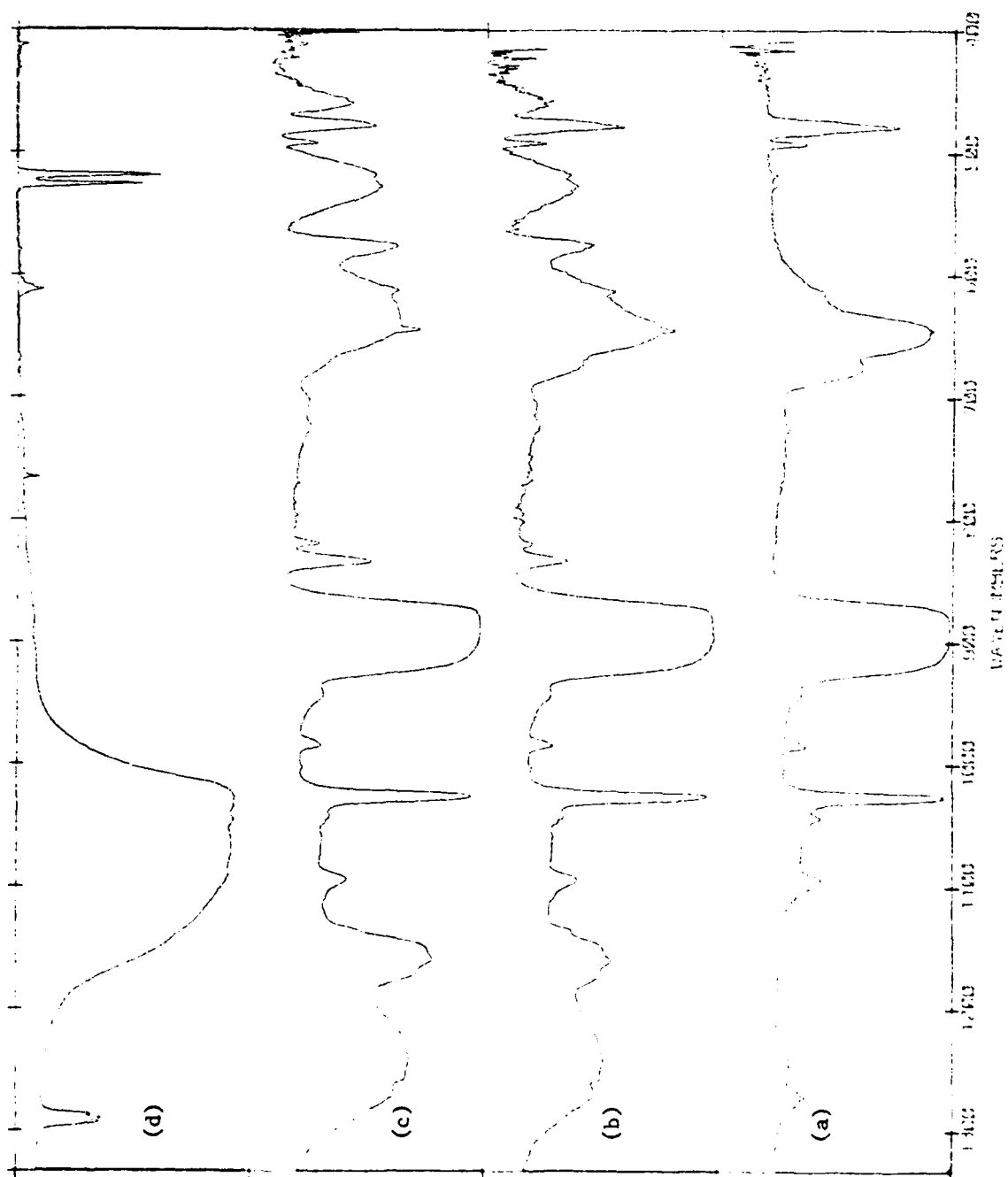


Fig. 3.2 FT-IR spectra of NF_3 , BF_3 and F_2 mixture.

may be seen in all the spectra reproduced in this section. Fig. 3.3 shows the spectrum of a thinner deposit in the $1200\text{--}1000\text{ cm}^{-1}$ region, in which more detail is evident.

Some spectral changes can be seen in traces (b) and (c). The bands produced have not been given definite assignments, but possibly arise from intermediates produced in the course of the reaction. The data are summarized in Table 5.1. Assignment of the bands is difficult because of their breadth and possible complications arising from perturbation by their neighbors and aggregation effects. In order to obtain better data, in which for instance, ^{10}B – ^{11}B and ^{14}N – ^{15}N isotope shifts might be resolved, enabling bands to be assigned, this reaction was studied in the matrix-isolated state. In a typical experiment a mixture of 1:1:3:400 of $\text{NF}_3\text{:BF}_3\text{:F}_2\text{:Ar}$ was deposited at 15K. Figs. 3.4 and 3.5 compare the spectrum of this mixture to that of the pure solid mixture previously obtained. This sample was subjected to uv-visible radiation from the BH-6 lamp at both 15K and 30K, the higher temperature being used to facilitate migration of F^{\bullet} within the matrix. In none of these experiments was any significant change observed. Figs. 3.6 and 3.7 show spectra of this deposit before and after extensive photolysis, including 15 mins. at 30K. The slight changes in band shapes and intensities result from annealing.

The second approach to the synthesis utilized 77K, a temperature readily attained in the rotating cryostat using liquid nitrogen as the coolant. Because of the high vapor pressure of F_2 at 77K, ClF , a nonvolatile solid at this temperature, was used as the fluorine atom source. Initial studies were made using 1:1:2 mixtures of NF_3 , BF_3 and ClF , but the liquid nature of NF_3 and its considerable vapor pressure demanded the use of a mixture more concentrated in NF_3 so that losses of it could be tolerated. (The cryostat was not pumped on during deposition or photolysis in this set of experiments, and the pressure in the chamber rose from 10^{-7} before deposition to ca. 5×10^{-3} torr afterwards.) A typical experiment entailed deposition of the mixture while the drum rotated at ca. 100 r.p.m. with simultaneous unfiltered BH-6 photolysis. A sequence of spectra obtained in this manner are shown in Figs. 3.8 – 3.11. Figs. 3.8 and 3.9 show spectra taken after deposition / photolysis and after some of the volatile material had been pumped off, and Figs. 3.10 and 3.11 show spectra taken after the cryostat had warmed up and all materials volatile at room temperature had been pumped away. A band can be seen at 1040 cm^{-1} , distorted by a window feature at 1090 cm^{-1} , but assignment of this to NF_4BF_4 is uncertain. The other major feature in the spectra

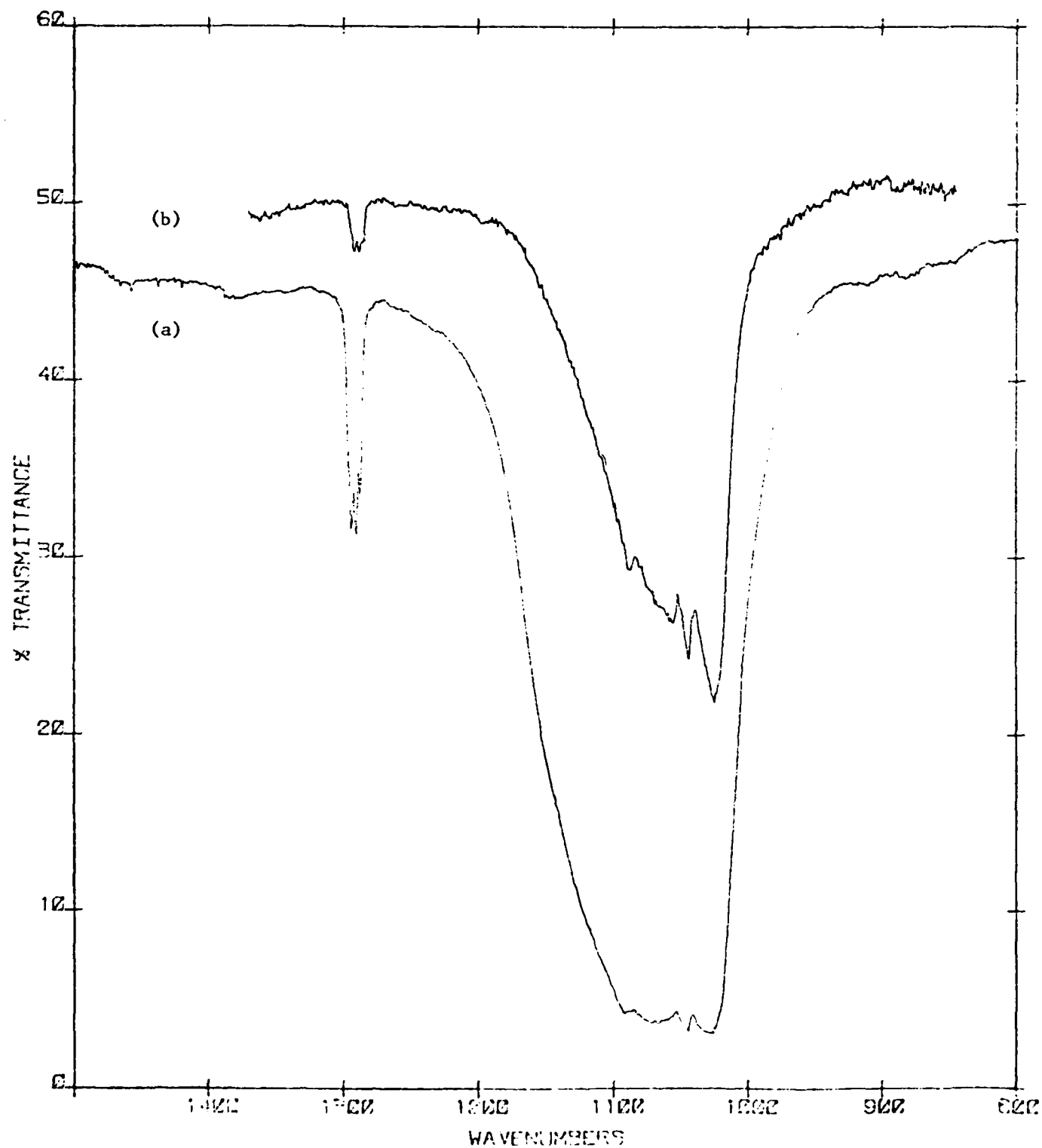


Fig. 3.3 FT-IR spectra of solid remaining on window
(a) Thick deposit
(b) Thin deposit

TABLE 5.1

SUMMARY OF OBSERVED BANDS IN LOW TEMPERATURE STUDIES

All frequencies given in cm^{-1}

NF_3 solid	BF_3 solid	New bands produced by	Non volatile solid	$\text{NF}_4^+ \text{a}$	$\text{BF}_4^- \text{a}$	Rotating Cryostat ^b	CsI Window impurities	$\text{NF}_4^+ \text{a}$	$3\text{F}_4^- \text{a}$
1272 CF_4	1320 $\nu_3^{10\text{B}}$	1290 m, br	1294		1302 (1310) $\nu_1^{+}\nu_4$		1378 m		1298 $\nu_1^{+}\nu_4$
1257 CF_4	1445 $\nu_3^{11\text{B}}$		1290				1344 m		
1134 $\nu_2^{+}\nu_4$	1405 agg. ^c		1287	1225 (1230) $2\nu_4$		1250 w	1336 m		
1024 ν_1	1348 agg.	1160 s	1092 vs, vbr ^d	1165 (1162) ν_3		1150 sh	1090 vs	1180, 1162 ν_3	
984 $2\nu_4$	1335 agg.		1072 vs, vbr		(1063) $2\nu_4$		835 w		
880 ν_3	675 $\nu_2^{10\text{B}}$		1044 vs, vbr	(1063) $\nu_2^{+}\nu_4$		1040 m	612 m		1120, 1057 ν_3
644 ν_2	636 $\nu_2^{11\text{B}}$		1025 vs, vbr		1025 ν_3		610 m		
491 ν_4	474 ν_4	835, 820 m	777		775 (775) ν_1	770 w			722 ν_1
		575 m	612 ^e			725 w			
			610 ^e sh	611 (613) ν_4				609 ν_4	
		528, 518 m	526, 519		527 (529) ν_4				525, 522 ν_4
		460 m	460	448 ν_2					

a. Two sets of data and assignments are given in Ref. 3, see also Ref. 9.

b. Excluding bands due to oil and CsI windows.

c. BF_3 aggregates in condensed phases; R. G. Steinhardt et al., J. Chem. Phys., 43, 4528 (1965)d. In thick samples this band extends from ca. 1200-1000 cm^{-1} and is poorly resolved.

e. CsI impurity bands observed in this region.

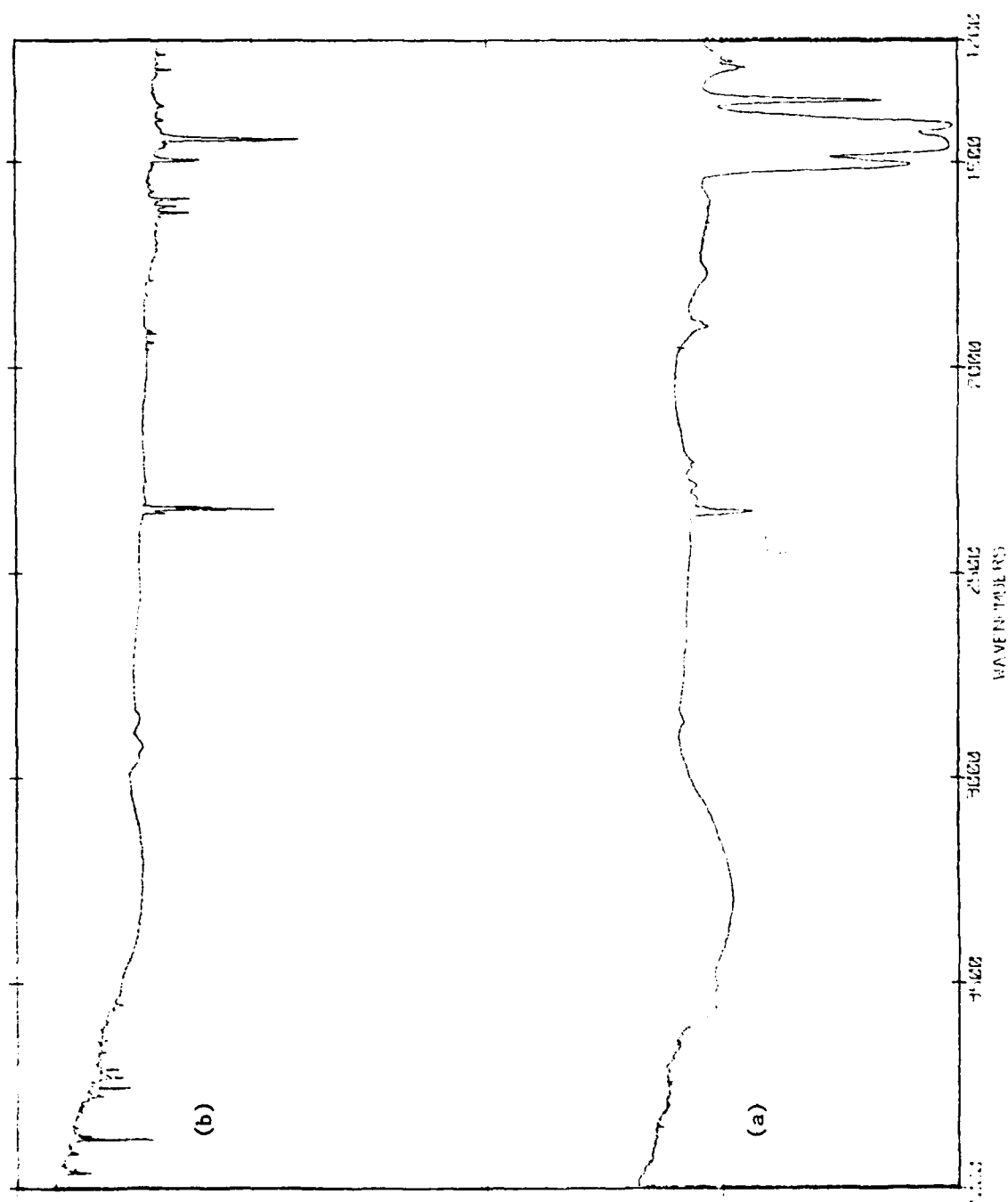


Fig. 3.4 FT-IR spectra of NF_3 , BF_3 and F_2 mixtures.

(a) Solid

(b) Matrix isolated in Ar

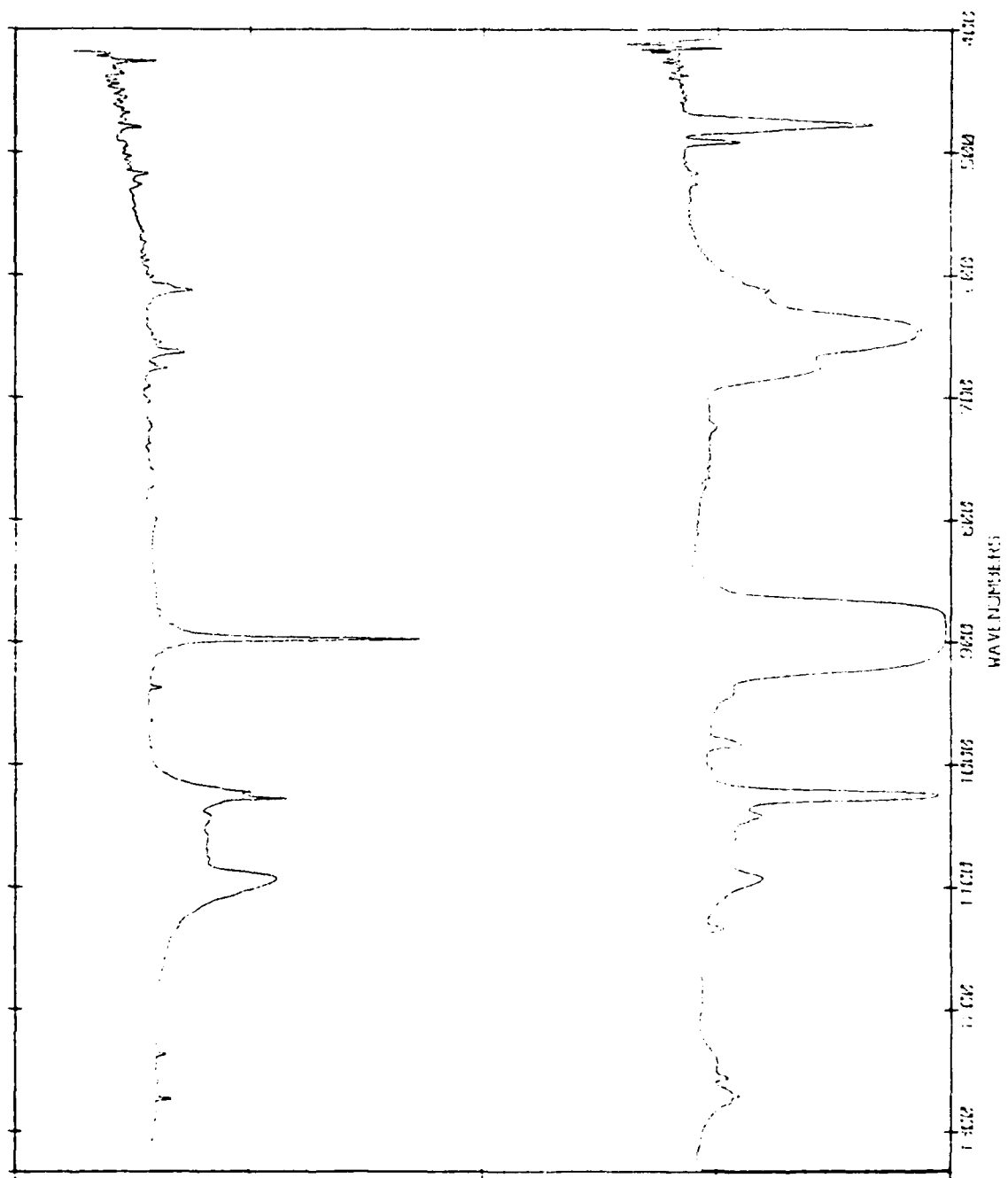


Fig. 3.5 FT-IR spectra of NF_3 , BF_3 and F_2 mixtures

(a) Solid

(b) Matrix isolated in Ar

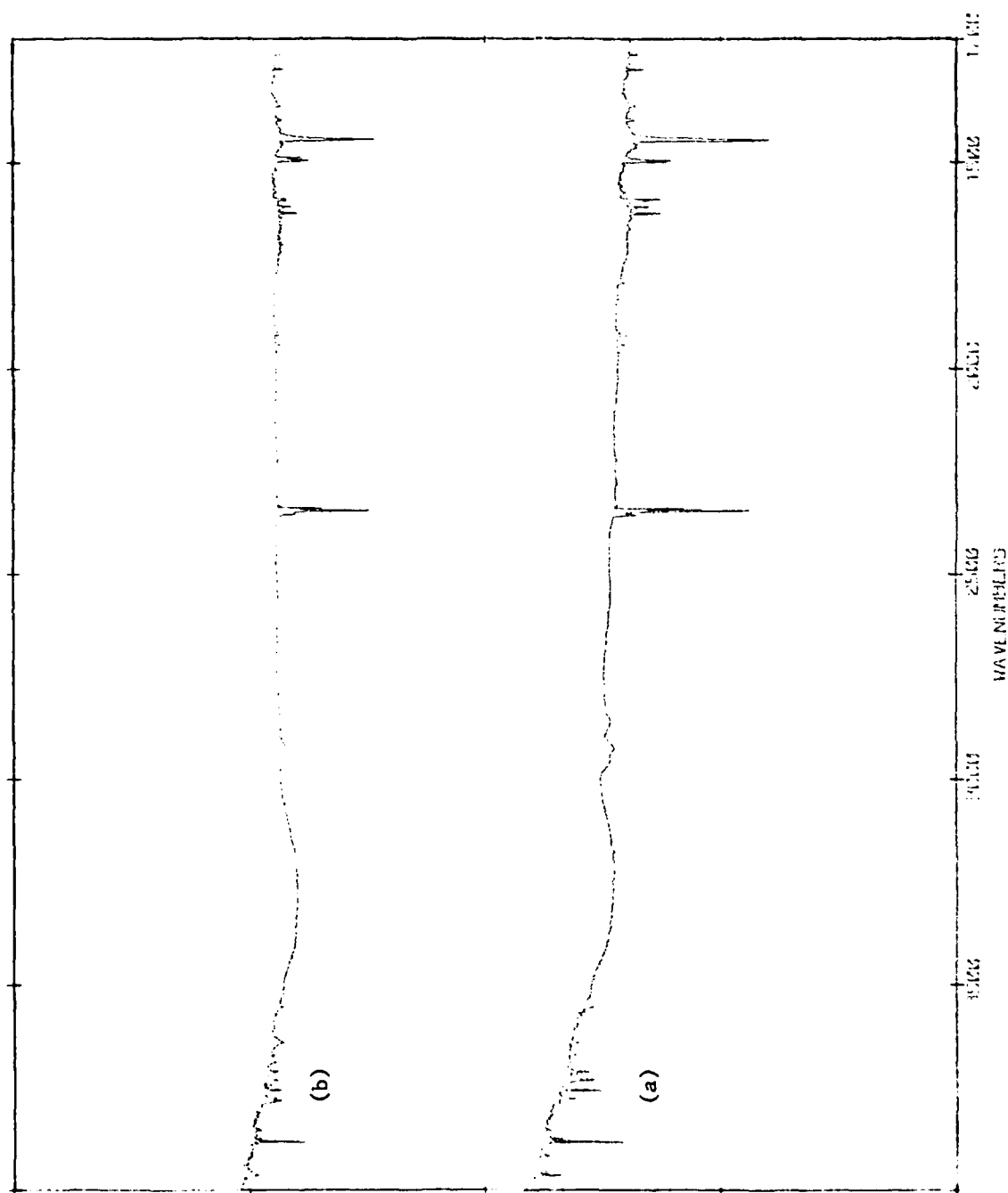


Fig. 3.6 FT-IR spectra of matrix-isolated NF_3 , BF_3 and F_2 mixture
(a) Before photolysis
(c) After photolysis.

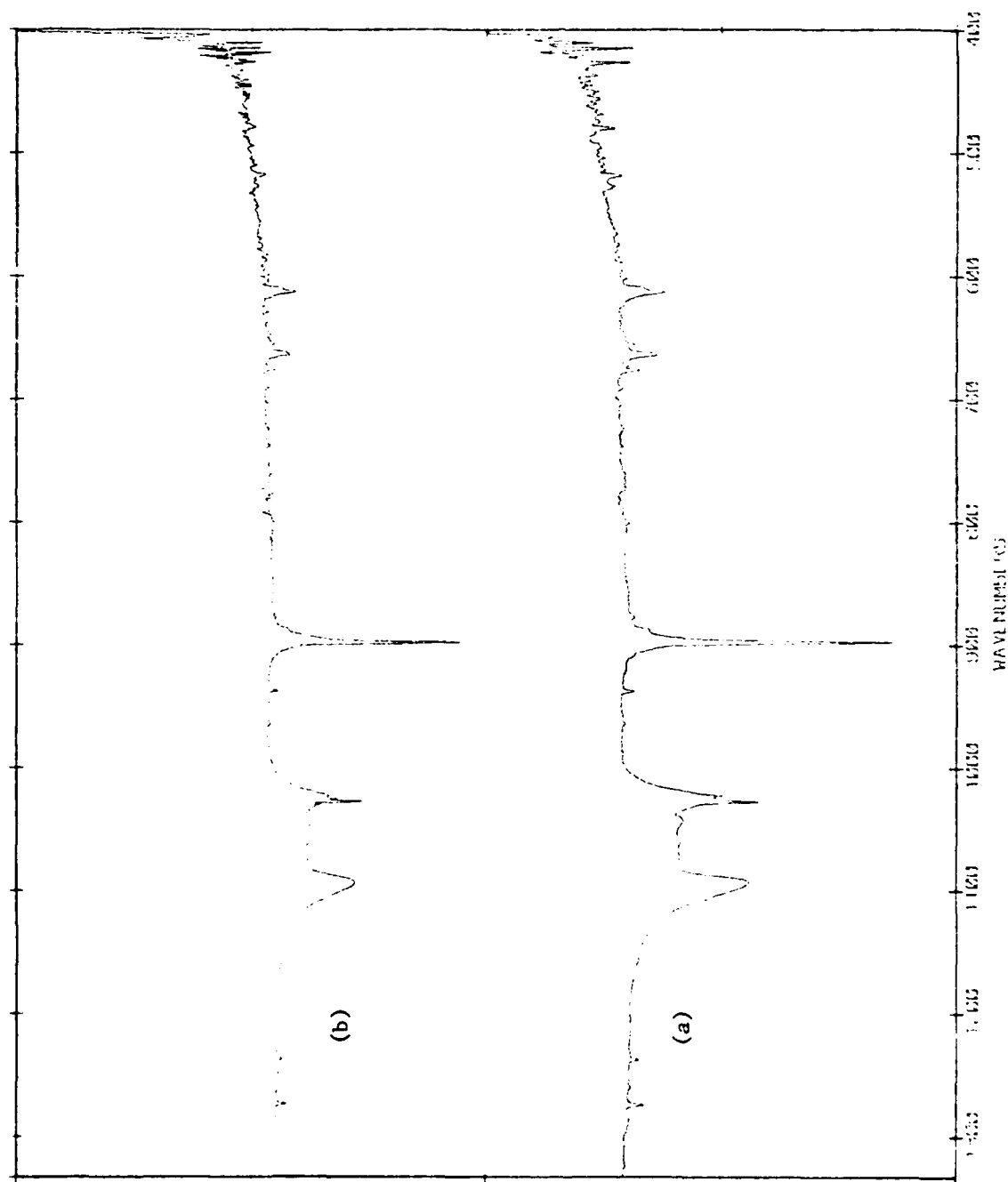


Fig. 3.7 FT-IR spectra of matrix-isolated NF_3 , BF_3 and F_2 mixture.

(a) Before photolysis

(b) After photolysis.

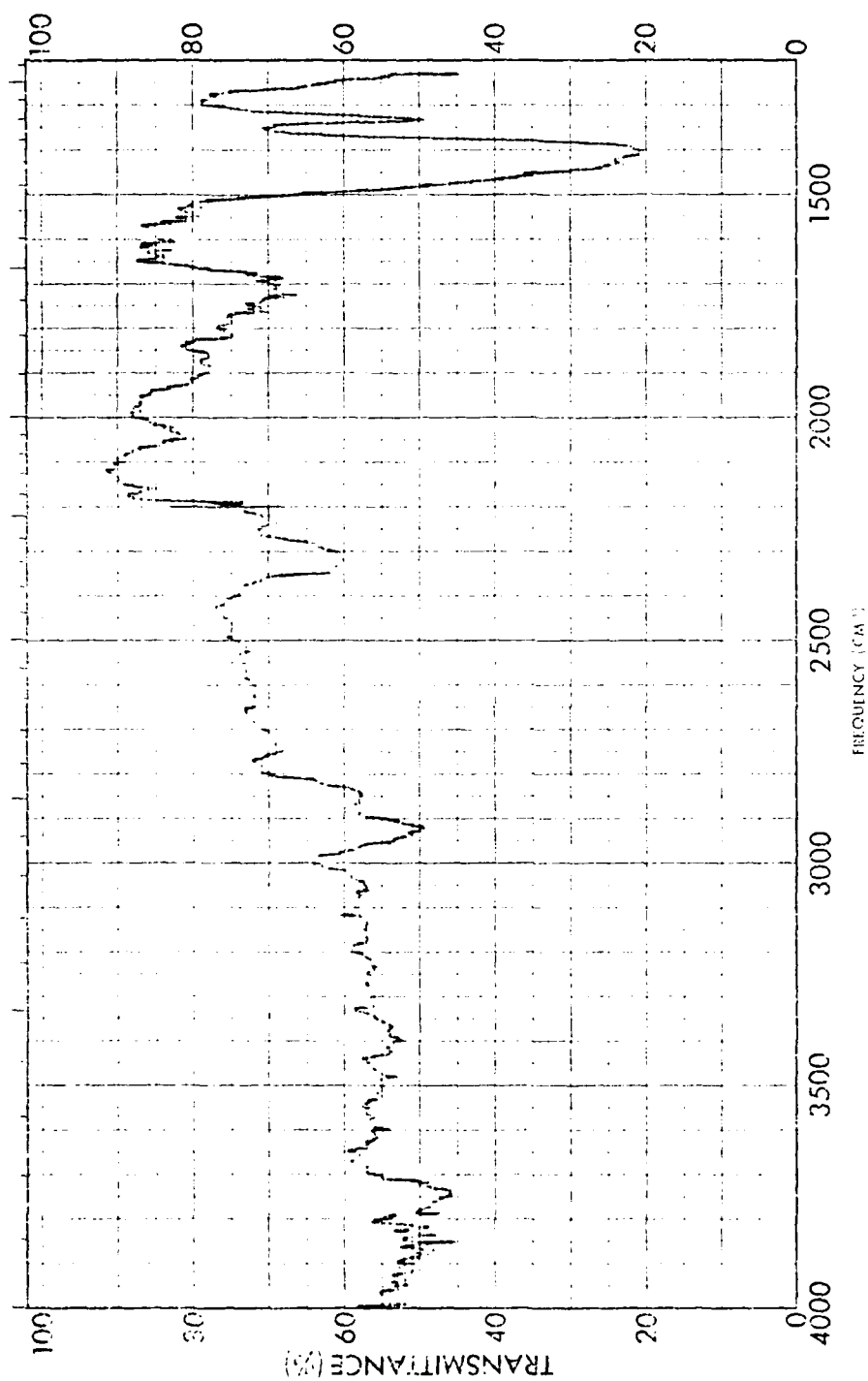


Fig. 3.8 IR spectrum of NF_3 , BF_3 and ClF mixture at 77K after photolysis.

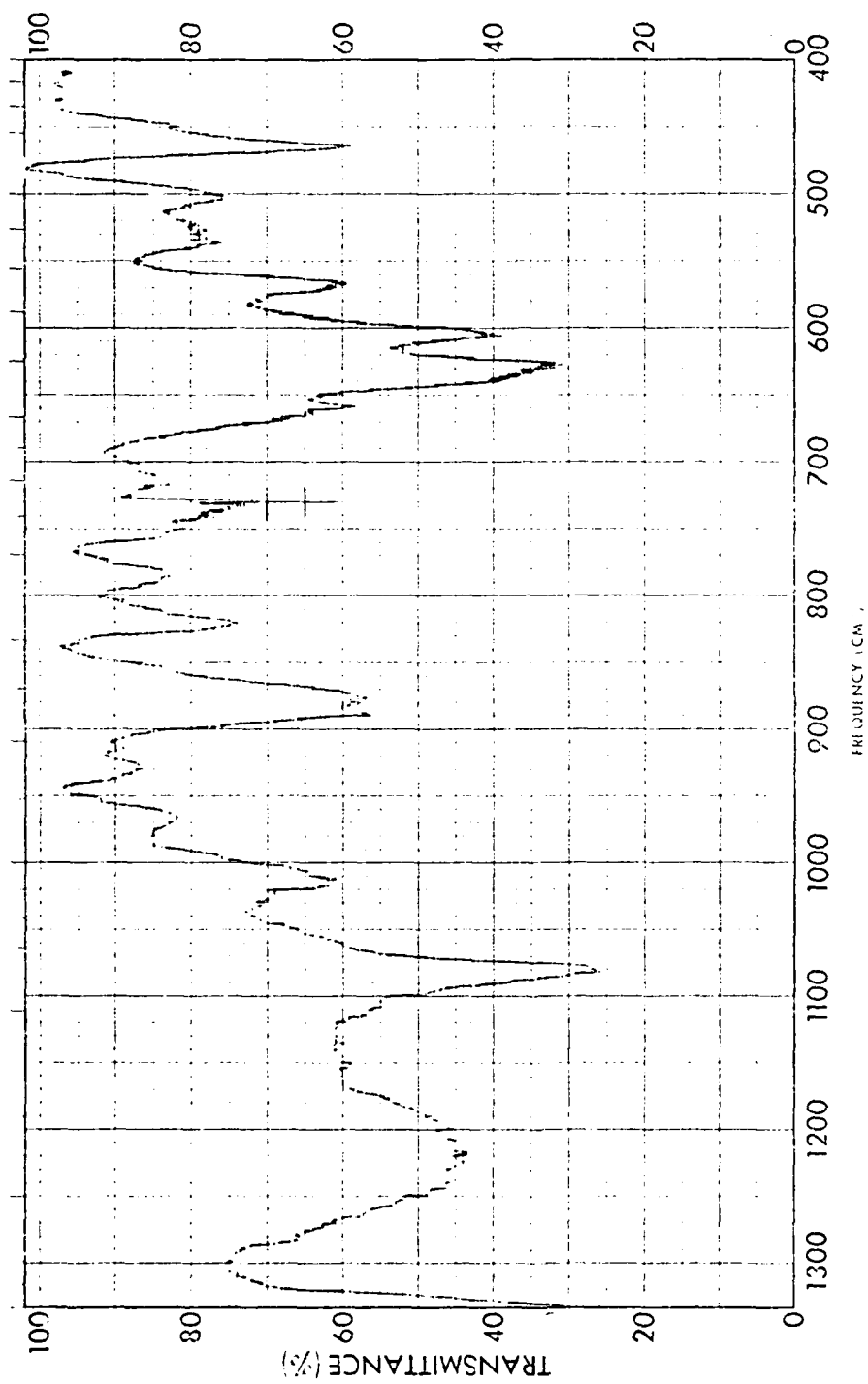


Fig. 3.9 IR spectrum of NF_3 , BF_3 and ClF mixture at 77K after photolysis.

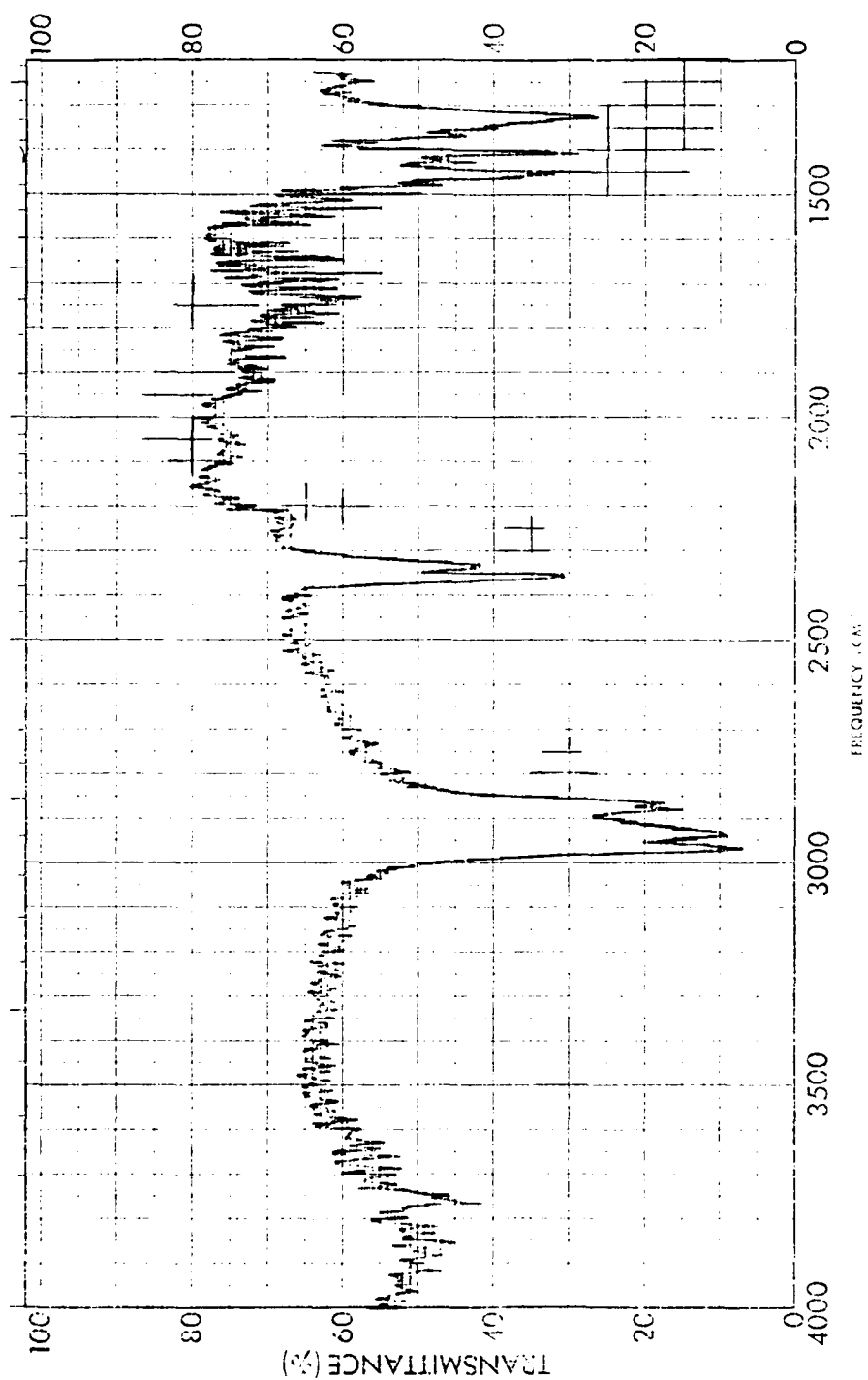


Fig. 3.10 IR spectrum of photolysed NF_3 , BF_3 and ClF mixture after warming to room temperature.

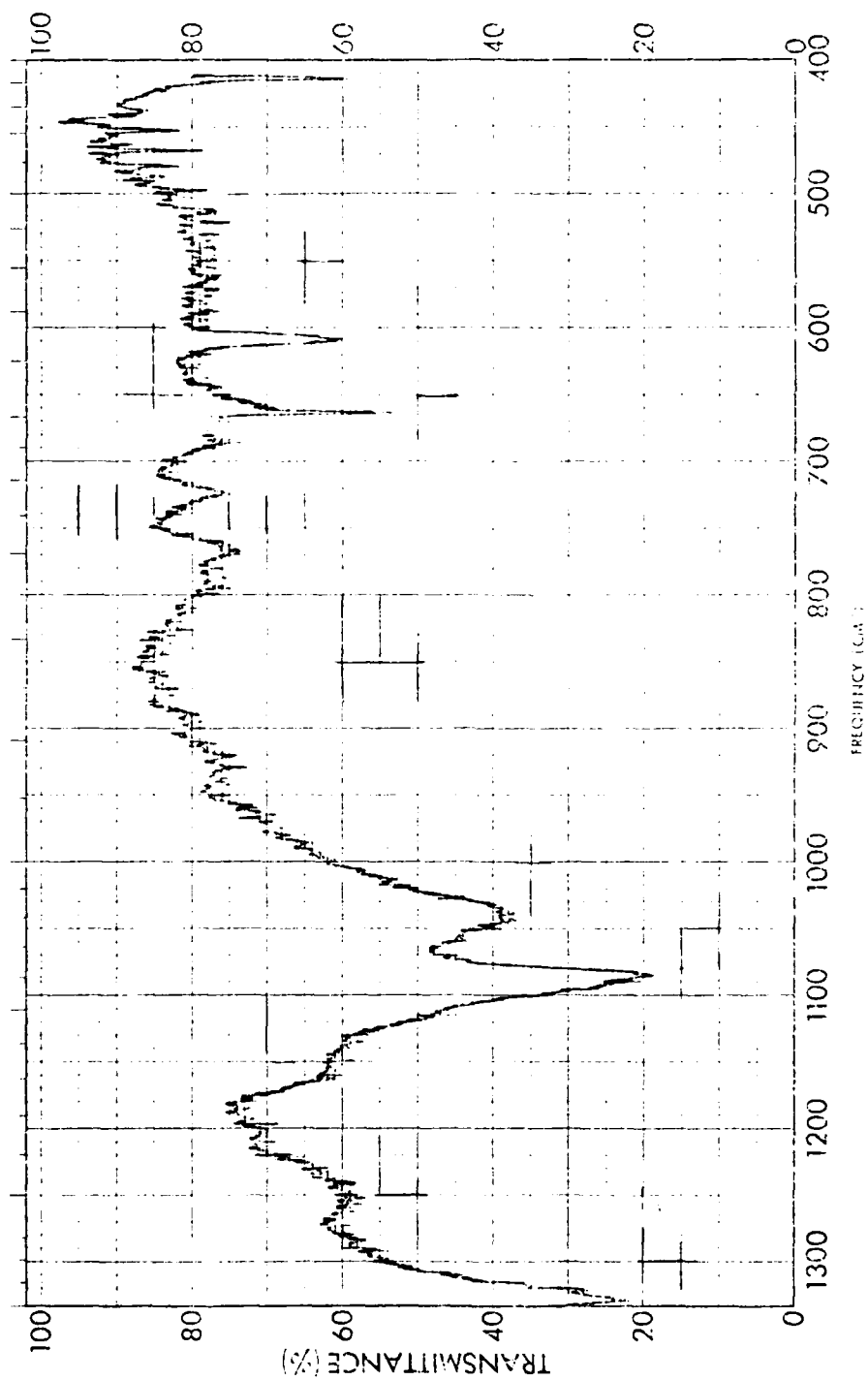


Fig. 3.11 IR spectrum of photolysed NF_3 , BF_3 and ClF mixture after warming to room temperature.

is a group of bands at around 2900 cm^{-1} arising from the oil used to lubricate the rotating seal. For comparison on a spectrum of this oil, recorded later as a thin film between CsI plates, is shown in Figs. 3.12-3.13, and it can be seen that some of the minor features in Figs. 3.9-3.10 are also due to this oil. Gradual wear of the o-rings in the seal during extended rotation permits leakage onto the drum and, on subsequent warm-up, onto the optical surface.

Neither the reasons for the failure of the matrix method nor the poor results from the rotating cryostat are immediately obvious. A common problem in matrix photolysis is the 'cage effect',¹⁴ in which photoproducts cannot escape from the immediate environment in which they were created, and they therefore suffer recombination. However, our work in section 1, as well as that of others, has demonstrated the migration of F^{\bullet} in matrices, and raising the matrix temperature should enable easy motion of F^{\bullet} . A possible rationalization is that, in this case, it is energetically more favorable for F-atom recombination to occur than for addition of F^{\bullet} to NF_3 . Even if NF_4^{\bullet} were formed, it is probable that in the matrix its nearest neighbour would be F^{\bullet} rather than BF_3 , and a facile back reaction is possible. Put alternatively, in a condensed phase, the reaction may require the close proximity of NF_3 , BF_3 and F_2 , a situation which is not realized even in matrices as concentrated as those used in this study. The concentration of such clusters may have been too low. The failure of the rotating cryostat studies may reflect a 'mixing' problem - i.e. despite depositing a homogeneous gas-phase mixture, separation may occur rapidly at 77K, and the intimate mixture necessary for the success of the reaction may not be present.

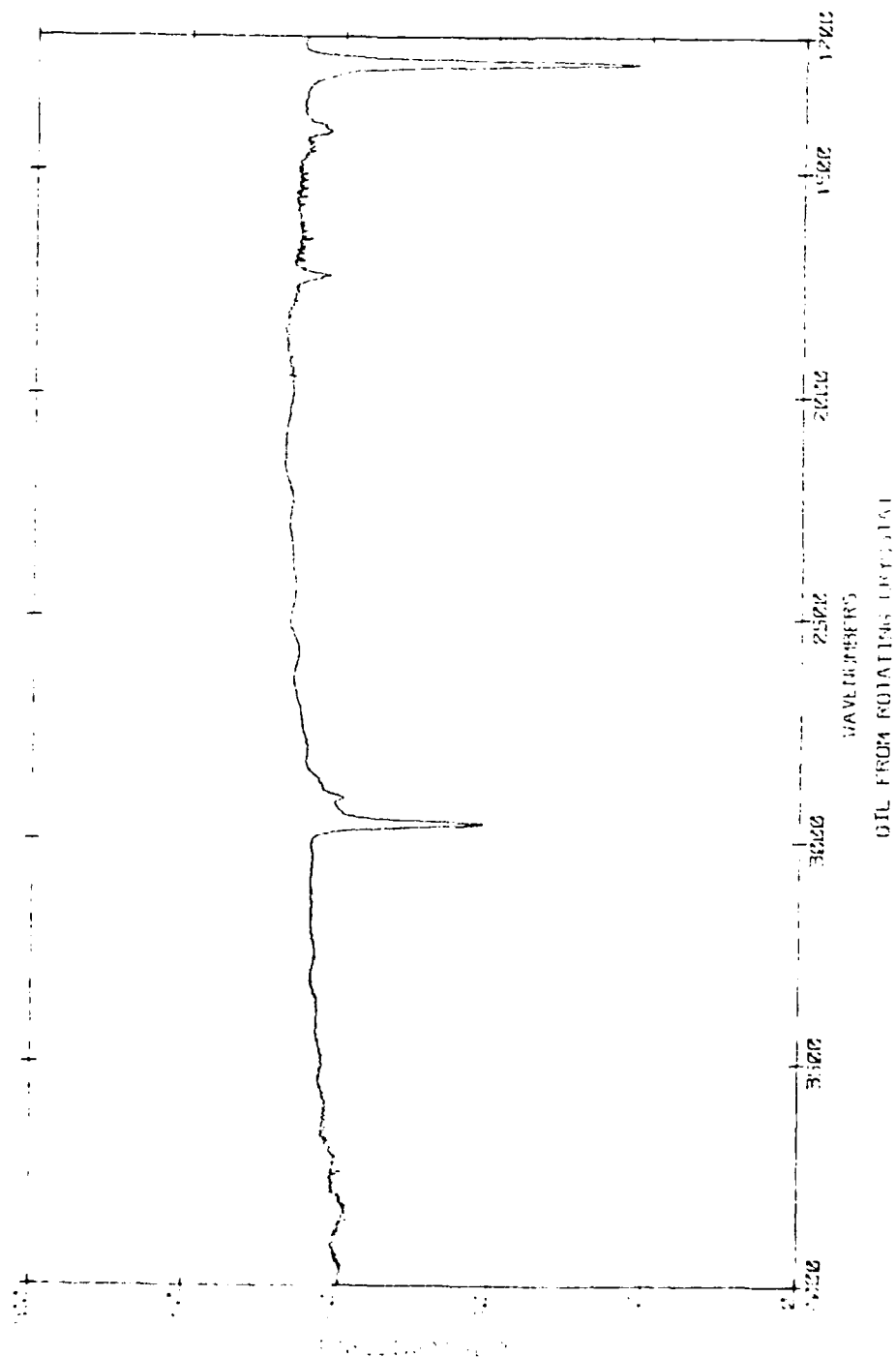


FIG. 3.12 FT-IR spectrum of lubricating oil.

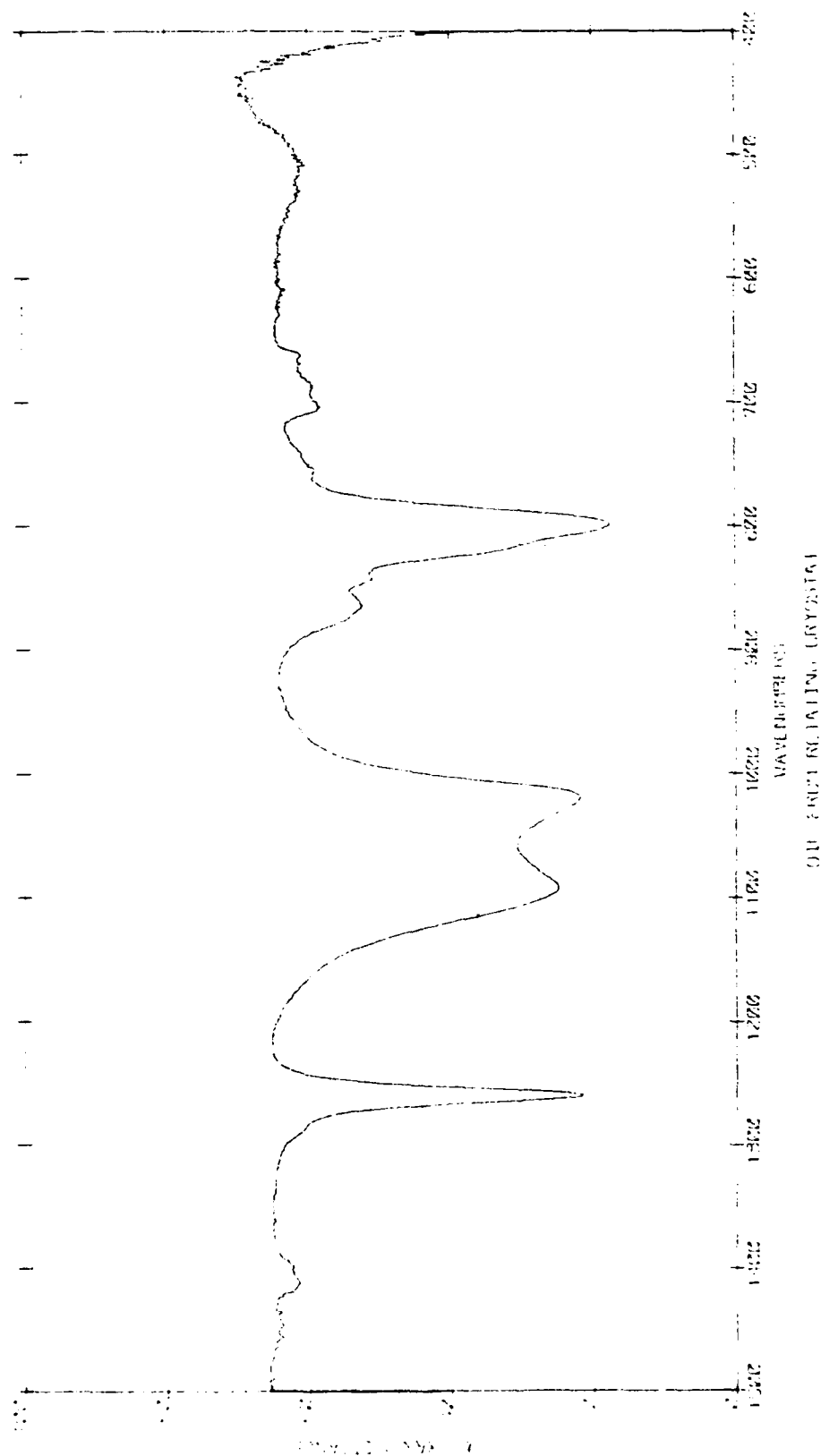


Fig. 3.13 FT-IR spectrum of lubricating oil.

(A) REFERENCES FOR SECTION 3.

1. W. E. Tolberg, R. T. Rewick, R. S. Stringham and M. E. Hill, Inorg. Nucl. Chem. Lett., 2, 79 (1966).
2. W. E. Tolberg, R. T. Rewick, R. S. Stringham and M. E. Hill, Inorg. Chem, 6, 1156 (1967).
3. C. T. Goetschel, V. A. Campanile, R. M. Curtis, K. R. Loos, C. D. Wagner and J. N. Wilson, Inorg. Chem., 11, 1696 (1972).
4. K. O. Christe, J. P. Guertin and A. E. Pavlath, Inorg. Nucl. Chem. Lett., 2, 83 (1966).
5. J. P. Guertin, K. O. Christe and A. E. Pavlath, Inorg. Chem., 5, 1921 (1966).
6. S. P. Mishra, M. C. R. Symons, K. O. Christe, R. D. Wilson and R. I. Wagner, Inorg. Chem., 14, 1103 (1975).
7. K. O. Christe, W. W. Wilson and C. J. Schack, J. Fluorine Chem., 11, 71 (1978).
8. K. O. Christe, R. D. Wilson and A. E. Axworthy, Inorg. Chem., 12, 2478 (1973).
9. K. O. Christe, C. J. Schack and R. D. Wilson, Inorg. Chem., 15, 1275 (1976).
10. K. O. Christe and I. B. Goldberg, Inorg. Chem., 17, 759 (1978).
11. I. B. Goldberg, H. R. Crowe and K. O. Christe, Inorg. Chem., 17, 3189 (1978).
12. K. O. Christe, R. D. Wilson and I. B. Goldberg, Inorg. Chem., 18, 2572 (1979).
13. S. M. Sinel'nikov and V. Ya. Rosolvskii, Dokl. Akad. Nauk. SSSR 194, 1341 (1970).
14. See e.g. A. J. Downs and S. C. Peake, Molecular Spectroscopy, Vol. 1, The Chemical Society, London, 1973.

4. TIME RESOLVED SPECTROSCOPY

The major methods for the study of radical species have been matrix isolation spectroscopy¹, gas-phase UV-visible spectroscopy², and, recently, laser-magnetic resonance³ and laser-electric resonance spectroscopy⁴. The latter two techniques are capable of providing detailed information but are only operative in small spectral ranges. Thus in cases where there is a little information from UV-visible spectroscopy it is necessary to rely upon matrix isolation frequencies, which are frequently subject to large shifts from those found in the gas phase¹. It would therefore be of great value to develop an infrared method for detecting radical and transient species in the gas phase, which covers a large frequency range. Infrared gas phase methods have not been popular largely owing to the weakness of infrared emission and absorption, the poor performance of IR detectors and the lack of a multiplex IR detector equivalent to a photographic plate, or array detector. The development of fast, sensitive IR detectors and IR multiplex methods have partially solved these problems.

A time resolved technique based on interferometric methods has great potential, since it will benefit from the 'advantages' of the method⁵. It should therefore be possible to obtain a high resolution spectrum of a transient over a wide range, which should enable unequivocal assignments to be made in systems not previously studied. A method for time resolved IR spectroscopy was developed in the early seventies using a step scan interferometer⁶⁻⁸. The principles of this technique have been adapted to rapid scanning interferometers^{9,10} and Digilab Inc. now markets a commercial device for use with its FTS series interferometric spectrometer¹¹. Details of the operation of this time resolved unit are given in Appendix 4, but here it can be noted that spectra can easily be obtained at 200, 400, 800, and 1200 μ s intervals, and with suitable equipment it may be possible at 25 μ s intervals.

Mantz^{9,10} claimed observation of the HCO radical and ketene ($\text{CH}_2=\text{CO}$), produced by the flash photolysis of acetaldehyde and acetone, respectively, using this method. A Digilab 'TRS' unit was acquired for use with this laboratory's FTS 20 and Digilab kindly loaned this group some of the ancillary equipment used by Mantz. The initial plan was to repeat the work of Mantz on HCO¹⁰ to confirm the viability of the technique, and then investigate the mechanism of certain photolytically induced halogen reactions, with special emphasis upon the formation of NF_4BF_4 in the gas phase. However detailed studies showed that the original work of Mantz was in error, and that he had not observed any transient species, but had produced spurious spectra

in the course of his experiments. A paper describing the mechanism by which this error occurred and outlining the experimental constraints in TRS is attached as Appendix 4. (Appl. Spectrosc., 34, 399 (1980)).

One of the major problems in the work of Mantz was the choice of compounds, (acetaldehyde and acetone), that are not greatly photosensitive so that, using the flashlamp available, only a very small quantity of products result - too small to be detected by infrared spectroscopy. In attempts to overcome this, several compounds were considered, and preliminary experiments performed. These were CF_3COCF_3 , known to give CF_3^\bullet ; CF_3NO , an exceptionally photosensitive compound known to produce CF_3^\bullet , $(\text{CF}_3)_2\text{NO}^\bullet$ and finally $(\text{CF}_3)_2\text{NONO}$; and a mixture of $\text{Cl}_2 + \text{O}_2$. The photolysis source available could not, in any of these cases, generate sufficient products for the experiment to succeed, but the latter two systems appear to offer the best prospects. A quantitative evaluation of these systems was not possible because Digilab requested the return of the photolysis source and insufficient funds were available for the purchase of a suitable replacement unit.

The requirements for a flashlamp unit are stringent; an ideal system should be able to produce at least 100J per flash at a rate of not less than 50Hz. However the TRS experiment can be employed in the study of other processes apart from flash photolysis, and any source that can reproducibly form a sufficient quantity of radical or excited species at about 50Hz is applicable. Attractive sources include high energy pulsed lasers (e.g. TEA CO_2 or Eximer lasers). Unfortunately the maximum rate of the Lumonics 103-2 CO_2 laser is only 2Hz. At low rates the experiments become unwieldy in both time and data manipulation senses (and may fail entirely due to the particular parameters of the Digilab unit), so that this mode of excitation was not attempted.

(A) REFERENCES FOR SECTION 4.

1. See e.g. A. J. Downs and S. C. Peake, Molecular Spectroscopy, Vol. 1 The Chemical Society, London, 1973.
2. See e.g. G. Herzberg, 'The Spectra and Structures of Simple Free Radicals', Cornell, Ithaca, 1971.
3. J. M. Brown, J. Buttenshaw, A. Carrington and C. R. Parent, Mol. Phys., 33, 589 (1977).
4. B. M. Landsberg, A. J. Merer and T. Oka, J. Mol. Spectrosc., 67, 459 (1977).
5. See e.g. P. R. Griffiths, 'Chemical Infrared Fourier Transform Spectroscopy', John Wiley, New York, 1975.
6. R. E. Murphy and H. Sakai, in 'Proceedings of Aspen International Conference on Fourier Spectroscopy', G. A. Vanasse, A. T. Stair and D. Baker, eds., Air Force Geophysics Laboratory, Cambridge, Mass., 1971, p. 301.
7. R. E. Murphy, F. Cook and H. Sakai, J. Opt. Soc. Am., 65, 600 (1975).
8. H. Sakai and R. E. Murphy, Appl. Optics, 17, 1342 (1978).
9. A. W. Mantz, Appl. Spectrosc., 30, 459 (1976).
10. A. W. Mantz, Appl. Optics, 17, 1347 (1978).
11. Digilab Inc., 237 Putnam Ave., Cambridge, Mass., 02139.

[Reprinted from *Inorganic Chemistry*, 17, 970 (1978.)]
 Copyright © 1978 by the American Chemical Society and reprinted by permission of the copyright owner.

Contribution from the Departments of Chemistry, University of Virginia, Charlottesville, Virginia 22901, and University of Tennessee, Knoxville, Tennessee 37916

Matrix Reactions of Fluorine with Chlorine, Bromine, and Iodine. Infrared Detection of the XF_2 , X_2F_2 , and X_3F_2 Species

ELEANOR S. PROCHASKA,^{1,2} LESTER ANDREWS,^{1,2} NORMAN R. SMYRL,^{1b} and GLEB MAMANTOV^{1b}

Received May 6, 1977

Infrared and laser-Raman matrix isolation studies have been done on the $\text{X}_2 + \text{F}_2$ systems, where $\text{X} = \text{Cl}, \text{Br}, \text{or I}$. Mercury arc photolysis produced the new species XF_2 , X_2F_2 , and X_3F_2 , as well as some of the normally unfavored members of the series XF_n ($n = 1, 3, 5$). The symmetric, T-shaped XXF_2 species is the dominant product in all three infrared studies. Other species were identified based on photolysis, concentration, and temperature cycling behavior of new infrared absorptions.

Introduction

The usual reaction between molecular fluorine and another halogen molecule X_2 follows the stoichiometry shown in reaction 1, where products with $n = 1$ or 3 are favored with Cl_2 , $\text{X}_2 + n\text{F}_2 \rightarrow 2\text{XF}_n$ (1)

$n = 3$ or 5 with Br_2 , and $n = 5$ with I_2 . Matrix isolation is a method by which intermediates in this reaction may be trapped for spectroscopic observation. Also, photolysis induced reaction products from X_2 , F_2 , and XF_n may be observed in a matrix. Of particular interest are unfavored XF_n species, as well as the new species XF_2 , X_2F_2 , and X_3F_2 .

Mamantov and co-workers² have studied the ClF_2 species, produced by photolysis of isolated ClF_3 or of codeposited $\text{ClF} + \text{F}_2$. Recently, Prochaska and Andrews,³ reexamined the ClF_2 radical, for which the most favorable synthetic route was photolysis of ClF and F_2 in a nitrogen matrix. Mamantov and co-workers⁴ have also reported spectra of chlorine-fluorine mixed species produced by photolysis of isolated chlorine and fluorine and have proposed assignments to vibrations of Cl_2F_2 , Cl_2F_3 , and Cl_2F_4 . The migration of photolytically produced fluorine atoms in matrices was established as a crucial step in the formation of these new mixed halogen species.

This paper reports a study of the reaction of fluorine with each of the molecular halogens, chlorine, bromine, and iodine, upon photolysis in solid matrices. Some experiments using BrF_3 as precursor are also reported, as well as some using equilibrium mixtures of Br_2 , F_2 , BrF , and BrF_3 .

Experimental Section

The closed cycle refrigerators and vacuum systems for infrared^{5a} and Raman^{5b} experiments at Virginia have been described previously. The stainless steel vacuum apparatus was thoroughly passivated with fluorine prior to sample preparation. Infrared samples were deposited on a CsI cold window, and spectra were recorded on a Beckman IR-12 spectrophotometer from 200 to 800 cm^{-1} . Photolysis was done using a General Electric BH-6 high-pressure mercury arc, focused by a quartz lens system mounted on a 10-cm water filter cell (220–1000 nm) plus a Pyrex plate (290–1000 nm). Raman samples were deposited on an OFHC tilted block, and laser-Raman spectra were recorded on a Spex Ramalog instrument (500 μ slits), using the 488.0- and 514.5-nm lines of a Coherent Radiation Model 52 argon ion laser. Laser lines were used with a dielectric spike filter for recording spectra and were unfiltered for photolysis of Raman samples.

Chlorine (Matheson) samples were purified by freeze-pump-thaw cycles at liquid nitrogen temperature. $^{37}\text{Cl}_2$ was prepared by oxidizing Rb^{37}Cl in concentrated HNO_3 and purified by condensing with Drierite. Bromine (Mallinckrodt) vapor over liquid was purified by freeze-pump-thaw cycles in a glass finger at liquid nitrogen temperature. Iodine (Mallinckrodt) crystals were outgassed by pumping while being held at liquid nitrogen temperature in the finger of a glass bulb. Iodine samples were prepared by putting the appropriate amount of argon over the solid in the bulb at room temperature (vapor pressure = 0.25 Torr). Fluorine (Matheson) was expanded through a "U" tube immersed in liquid N_2 before sample preparation to remove condensable impurities. Argon (Air Products, 99.998%) was used directly as the matrix gas.

Because of the variation in reactivity between fluorine and the three heavy halogens, different methods of sample deposition were used. Some samples were prepared with both halogens premixed in the same sample can. This was satisfactory for $\text{Cl}_2 + \text{F}_2$ samples, as only a moderate amount of ClF was formed by gas-phase reaction. However, for bromine and fluorine samples, an equilibrium mixture of BrF , BrF_2 , and BrF_3 with the halogens was actually deposited from a single can and with iodine and fluorine a thorough conversion to IF_5 occurred with premixing. This type of experiment will later be referred to as a "premixed" experiment. To avoid prior reaction, bromine or iodine samples were prepared in separate cans from the fluorine, and the halogen and fluorine were mixed in the sample deposition line, about 10 cm above the cold window. These experiments will later be referred to as "separate can" experiments. In addition, some samples were prepared in completely separate vacuum manifolds and deposited through separate tubes. These will later be referred to as "separate manifold" experiments.

Matrix-isolation experiments at Tennessee utilized a Cryodyne Model 350 closed cycle helium refrigerator and experimental techniques previously described.^{2,4} Temperatures were monitored and controlled to within ± 1 K utilizing a Cryogenic Technology Inc. digital electronic temperature controller in conjunction with a gold-chromel thermocouple and resistance heater. Matrix mixtures were prepared in a stainless steel vacuum line well-passivated with chlorine trifluoride (Matheson, 98.0%). Research grade argon (Matheson, 99.9995%) was utilized as the matrix gas. Purified fluorine (99.99%), obtained from W. N. Hubbard, Argonne National Laboratory, was used without further purification. Reagent grade bromine (Fisher) was purified by passing the vapors over the liquid through a tube containing molecular sieve utilizing vacuum transfer techniques. Bromine trifluoride (Matheson, 98.0%) was purified by transfer from a lecture bottle under vacuum by pumping into a trap held at $\sim -20^\circ\text{C}$. Matrix samples were photolyzed by BH-6 mercury arc, with an 11-cm water-filled quartz cell (220–1000 nm), with the addition of a Corning CS-7-54 glass filter (280–420 nm) for more limited photolysis. Microwave discharge experiments at Tennessee used a Raytheon Microtherm Model CMD-10 microwave generator to supply a maximum of 125 W at 2450 MHz. The microwave energy was directed through an Evenson type cavity to generate discharge in a 0.5-in. o.d. Lucalox tube using a gas flow rate of about 1.0 cm^3/min . Infrared spectra were recorded under low resolution on a Perkin-Elmer Model 337 infrared spectrophotometer and at high resolution using a Digilab Model LTS-20 Fourier transform infrared spectrometer.

Results

Infrared. $\text{Cl}_2 + \text{F}_2$. All experiments with chlorine and fluorine were done with premixed samples, and ClF was the major gas-phase reaction product observed in the spectrum of the condensed samples. In the first experiment, an $\text{Ar}/\text{F}_2/\text{Cl}_2 = 100:1:1$ sample was deposited for 22 h and photolyzed for 10 min with 220–1000 nm light; a very strong band system appeared at 636 cm^{-1} (completely absorbing), a sharp doublet was observed at 559.0, 551.0 cm^{-1} (absorbance = 4 = 0.29 and 0.09), a partially resolved triplet was found at 464, 462, 459 cm^{-1} (4 = 0.10, 0.07, 0.01), and a new band appeared at 270 cm^{-1} (4 = 0.06). Additional photolysis for 25 min reduced these bands to approximately half of their first observed intensities.

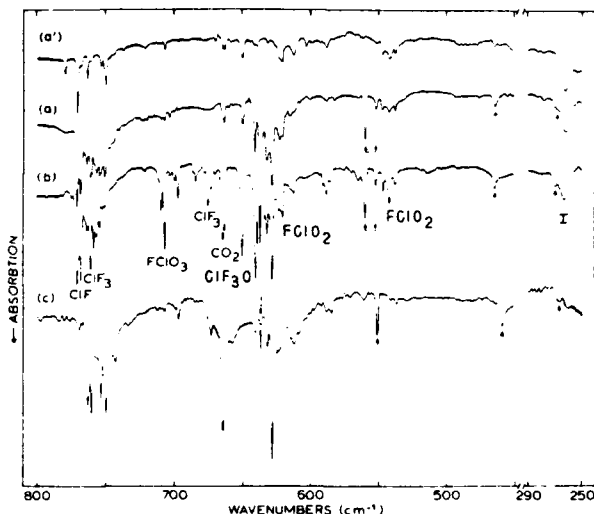


Figure 1. Infrared spectra of premixed chlorine and fluorine samples: (a') $Ar/F_2/Cl_2 = 400/1/4$, 61 mmol deposited, before photolysis; (a) previous sample after 55 min of Hg arc photolysis with the water and Pyrex plate filters; (b) $Ar/F_2/Cl_2 = 400/4/1$, 60 mmol deposited, after 51 min of Hg arc photolysis, same filters; (c) $Ar/F_2/^{37}Cl_2 = 250/2.5/1$, 46 mmol of deposited, after 21 min of Hg arc photolysis, same filters.

Two additional experiments were performed using samples with one reagent concentration reduced a factor of 4 relative to the above higher yield study. The spectrum of an $Ar/F_2/Cl_2 = 400/1/4$ sample after deposition is shown in Figure 1a'. Following 55 min of photolysis with 290–1000 nm light, a strong new doublet was observed at 636 cm^{-1} ($A = 0.54$), 627 cm^{-1} ($A = 0.16$) with weaker site splittings at 640 and 631 cm^{-1} , another doublet was observed at 559 cm^{-1} ($A = 0.10$), 551 cm^{-1} ($A = 0.03$), and weaker bands were produced at 464 cm^{-1} ($A = 0.03$) and 270 cm^{-1} which are shown in Figure 1a.

The next sample, $Ar/F_2/Cl_2 = 400/4/1$, with excess fluorine, gave the spectrum in Figure 1b after photolysis; the $636, 627\text{ cm}^{-1}$ doublet ($A = 0.72, 0.22$) was increased while the other three absorptions, 559 cm^{-1} ($A = 0.10$), 464 cm^{-1} ($A = 0.03$), and 270 cm^{-1} remained the same as in the above excess chlorine sample, and in addition, ClF and ClF_3 were produced by photolysis. The $FCIO_3$ and $FCIO_2$ impurities,⁸ present throughout this study, were more intense in Figure 1b. Also, another chlorine-isotopic doublet at $649, 640\text{ cm}^{-1}$ present before photolysis in all experiments, and enhanced in the excess fluorine run, is due to ClF_3O .⁸ The broad 260-cm^{-1} band is due to an impurity often observed in fluorine experiments.

Thermal cycles of these samples into the 32–38 K range decreased the above new bands by approximately half and weak new bands appeared at 454 and 305 cm^{-1} .

The chlorine-37 sample, $Ar/F_2/^{37}Cl_2 = 400/2.5/1$, gave the lower multiplet components at 627 ($A = 0.90$), 551 ($A = 0.11$), and 459 cm^{-1} ($A = 0.05$) which indicates that these absorptions are due to chlorine-37 vibrations. A weak shoulder was observed at 268 cm^{-1} . A thermal cycle decreased these bands while a sharp feature at 571 cm^{-1} due to $^{37}ClF_2$,^{2,3} and weak 450- and 300-cm^{-1} bands appeared.

Two further experiments were done on the chlorine fluorine system using different fluorine atom sources. A study with $Ar/ClF/Cl_2 = 200/1/1$ produced only ClF_3 , $FCIO_2$, and $FCIO_3$ upon photolysis. Another experiment with a sample of $Ar/OF_2/Cl_2 = 200/1/1$ yielded only small amounts of ClF , ClF_3 , and again $FCIO_2$ and $FCIO_3$.⁸

$Br_2 + F_2$. Experiments were run using BrF_3 in argon, equilibrium mixtures of BrF , BrF_3 , and Br_2 in argon, alone and codeposited with F_2 in argon, and Br_2 in argon and F_2 in

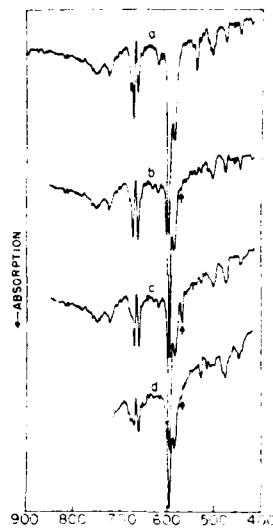


Figure 2. Infrared spectra of a BrF_3 sample: (a) $Ar/BrF_3 = 2000/1$, 17 mmol deposited; (b) after 25 min of Hg arc photolysis with the quartz-water and Corning CS-7-54 glass filters; (c) after a thermal cycle to 25 K; (d) after a thermal cycle to 33 K.

argon deposited from separate manifolds. Microwave discharge experiments were done with samples of Ar/Br_2 and Ar/F_2 mixed before and during discharge. Bands assignable to BrF and BrF_3 monomers and BrF_3 dimer were observed, and several BrF_5 absorptions were seen as well.^{7,9} New bands that appeared on photolysis and warmup and during microwave discharge will be described in more detail.

Several experiments with Ar/BrF_3 ($M/R = 2000$ and 1000) samples were done at Tennessee to optimize the yield of a new doublet at $567, 569\text{ cm}^{-1}$. This feature was observed after 10 min of photolysis with the quartz-water filter and enhanced by a thermal cycle to 25 K. The yield was maximized by subsequent photolysis for 25 min using the quartz-water plus Corning filters, followed by a thermal cycle to 25 K, as shown in Figure 2. Subsequent thermal cycling to 36 K destroyed the band completely. A small band was observed at 527 cm^{-1} in these experiments, that was enhanced by photolysis and thermal cycling. This band was not destroyed even by warming to 36 K. A similar experiment was done by co-condensing an equilibrium mixture of Br_2 , BrF , and BrF_3 in argon at $M/R = 50$ with F_2 in argon at $M/R = 170$ using 8.5 mmol of each mixture. After 40 min of photolysis with the quartz-water plus Corning filter combination, new doublets at $554, 556$ and $561, 563\text{ cm}^{-1}$ were observed, plus a very small feature at $567, 569\text{ cm}^{-1}$ on the side of the large BrF_3 monomer and dimer bands. Thermal cycling to 25 K caused the 555-cm^{-1} doublet to increase significantly, while the 562-cm^{-1} doublet decreased with loss of resolution. The 569-cm^{-1} feature had increased slightly. The 527-cm^{-1} band was observed on deposition and was unaffected by photolysis but grew considerably on warmup.

Similar experiments were done at Virginia on two chemical systems. Two experiments were done in which bromine and fluorine were premixed and allowed to react such that a mixture of Br_2 , BrF , BrF_3 , and some F_2 was actually deposited. With excess F_2 ($Ar/Br_2/F_2 = 200/1/2$, 58 mmol deposited), large amounts of BrF at $660.0, 661.5\text{ cm}^{-1}$, BrF_3 monomer and dimer, and some BrF_5 were observed. Ten minutes of photolysis with the quartz-water and Pyrex filters resulted in good yields of new bands at $554.1, 556.1\text{ cm}^{-1}$, with a smaller pair at $562.0, 564.0\text{ cm}^{-1}$. A thermal cycle to 26 K caused a small decrease in both these bands, and a new doublet at $568.0, 570.2\text{ cm}^{-1}$ appeared. Thirty minutes more photolysis and a thermal

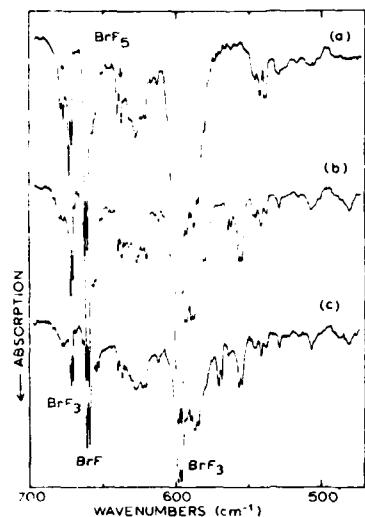


Figure 3. Infrared spectra of a premixed bromine and fluorine experiment: (a) $\text{Ar}/\text{F}_2/\text{Br}_2 = 200/1/1$, 53 mmol deposited; (b) after 40 min of Hg arc photolysis with the quartz-water and Pyrex plate filters; (c) after a thermal cycle to 28 K.

cycle regenerated the 555-cm^{-1} band, but both the higher frequency bands lost intensity and resolution. A band at 529 cm^{-1} grew slightly on warmups. A similar experiment with equal initial bromine and fluorine ($\text{Ar}/\text{F}_2/\text{Br}_2 = 200/1/1$, 53 mmol deposited) gave a reduced yield of the mixed halogen species, which is illustrated in Figure 3. Ten minutes of photolysis with the quartz-water and Pyrex filter produced both the 554.1- , 556.1-cm^{-1} and 562.0- , 564.0-cm^{-1} doublets. The less dominant BrF_3 bands show clearly that none of the 569-cm^{-1} feature is present after photolysis. A thermal cycle to 28 K causes a decrease in both bands, with loss of resolution on the higher doublet. The 568.0- , 570.2-cm^{-1} feature grows in clearly with good yield (absorbance = 0.13). A band at about 538 cm^{-1} was decreased considerably by photolysis, but no photolysis or temperature effect was observed for a small band at 529 cm^{-1} .

Two further experiments simultaneously codeposited Ar/Br_2 and Ar/F_2 samples from separate vacuum lines. With excess F_2 ($\text{Ar}/\text{F}_2 = 50/1$, 46 mmol; $\text{Ar}/\text{Br}_2 = 200/1$, 46 mmol), no bands are observed on initial deposition. Ten minutes of photolysis with the quartz-water and Pyrex combination produced numerous bands assignable to BrF_3 dimer, plus small amounts of BrF_3 and BrF_4 monomers. In addition, a full scale band was observed centered at 555 cm^{-1} , and a smaller feature at 560.0 cm^{-1} was seen, with a shoulder at about 562 cm^{-1} . A band at 507 cm^{-1} was considerably sharper than the BrF_3 dimer feature observed in the premixed experiments and is relatively larger than other BrF_3 dimer bands in this experiment. A very weak band was observed at 529 cm^{-1} . Thirty minutes more photolysis produced growth in the 507- , 529- , and 555-cm^{-1} features, as well as the BrF_3 dimer bands. The 560-cm^{-1} feature lost intensity and resolution, and a very small feature appeared at 570 cm^{-1} . A subsequent thermal cycle to 26 K resulted in a slight increase in the 507-cm^{-1} band, little change in the 529- and 560-cm^{-1} features, and a decrease in both the 555-cm^{-1} and in the tiny 570-cm^{-1} feature. A similar experiment with equal bromine and fluorine concentrations ($\text{Ar}/\text{Br}_2 = 100/1$, 34 mmol; $\text{Ar}/\text{F}_2 = 100/1$, 43 mmol) gave analogous results and is shown in Figure 4. Nothing was observed on initial deposition, but 40 min of photolysis with the quartz-water plus Pyrex assembly produced the 507-cm^{-1} feature, a strong 555.0- , 557.0-cm^{-1} doublet with a 561-cm^{-1} shoulder and very small BrF_3 dimer bands. A thermal cycle to 27 K caused all features to lose intensity, and the 555-cm^{-1}

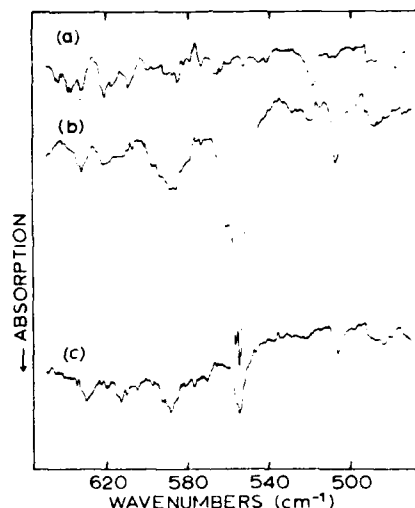


Figure 4. Infrared spectra of a separate manifold bromine and fluorine experiment: (a) $\text{Ar}/\text{Br}_2 = 100/1$, 34 mmol, and $\text{Ar}/\text{F}_2 = 100/1$, 43 mmol deposited; (b) after 40 min of Hg arc photolysis with the quartz-water and Pyrex plate filters; (c) after a thermal cycle to 27 K.

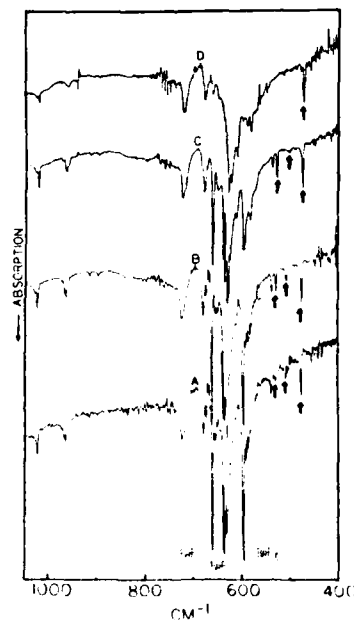


Figure 5. Infrared spectra of a premixed bromine and fluorine discharge experiment: (A) $\text{Ar}/\text{F}_2/\text{Br}_2 = 425/2.5/1$ deposited during microwave discharge; (B) after a thermal cycle to 25 K; (C) after a thermal cycle to 30 K; (D) after a thermal cycle to 40 K.

feature lost resolution and most of the shoulder, as is shown in Figure 4.

Further experiments were done at Tennessee with bromine and fluorine samples passed through a microwave discharge. A blank experiment with 10 mmol of $\text{Ar}/\text{F}_2/\text{Br}_2 = 425/2.5/1$ deposited without discharge produced only features assignable to BrF_3 and BrF_4 . Discharge of a similar premixed sample resulted in the appearance of bands assignable to BrF_3 monomer, as well as BrF_3 and BrF_4 . New features observed at 475- , 507- , and 527-cm^{-1} are shown in Figure 5. A thermal cycle to 25 K caused an increase in the 507- and 527-cm^{-1} bands, while the 475-cm^{-1} band remains unchanged. Further cycling to 30 K resulted in a further increase in the 527-cm^{-1} band, and the loss of the 507-cm^{-1} band. Warming to 40 K

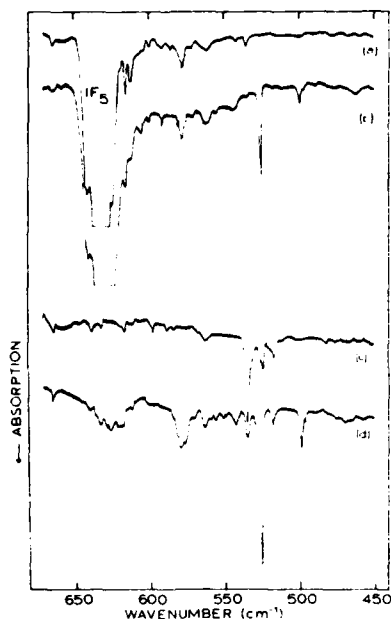


Figure 6. Infrared spectra of separate can and separate manifold iodine and fluorine experiments: (a) $Ar/F_2 = 100$, 11.6 mmol, and $Ar/I_2 = 200$, 7.5 mmol deposited from separate cans; (b) after 30 min of Hg arc photolysis with the quartz-water and Pyrex plate filters, plus 15 min with the quartz-water filter only; (c) $Ar/F_2 = 100$, 10.4 mmol, and $Ar/I_2 = 200$, 7.9 mmol deposited from separate manifolds; (d) after 15 min of Hg arc photolysis with the quartz-water and Pyrex plate filters, plus 20 min with the quartz-water filter only.

caused the loss of the 527- cm^{-1} band as well, but the 475- cm^{-1} feature remained virtually unchanged even on warming to 50 K.

In a similar experiment, Br_2 and F_2 samples were mixed just prior to discharge ($Ar/Br_2 = 160/1$, 26 mmol; $Ar/F_2 = 80/1$, 13 mmol). The 507- and 527- cm^{-1} bands were observed in good yield. The 527- cm^{-1} band is stable on thermal cycling as high as 30 K, while the 507- cm^{-1} band is decreased by warming to 25 K and further on warming to 30 K.

Another experiment was run, mixing the two reactants within the discharge ($Ar/Br_2 = 170/1$, 8 mmol; $Ar/F_2 = 85/1$, 8 mmol). The 527- cm^{-1} band was observed, but was quite small, and was stable on warming to as high as 30 K, but was gone after warming to 35 K. A band at 570 cm^{-1} appeared on warming to 25 K, increased on warming to 30 K, and was gone after a cycle to 35 K. A similar experiment with more dilute samples produced the 570- cm^{-1} band following a thermal cycle.

$I_2 + F_2$. Iodine and fluorine react very readily in the gas phase and spectra from premixed experiments showed strong bands at 704, 634, 370, and 317 cm^{-1} due to IF_5 .¹⁰ No new bands were produced by photolysis. Spectra from separate can experiments, which allow a short reaction time in the deposition line before the sample reaches the cold surface, also showed a good yield of IF_5 and weak bands at 578 and 535 cm^{-1} , which are shown in Figure 6a. Trace (b) illustrates the spectrum after photolysis with the quartz-water and Pyrex filters which produced new bands at 499 and 526 cm^{-1} , while the weak band at 535 cm^{-1} was destroyed. A subsequent photolysis with the quartz-water filter had little effect. A thermal cycle to ~ 35 K caused both bands to grow a small amount, but no other new bands appeared.

Two experiments were done using completely separate deposition lines allowing almost no gas-phase reaction. An experiment with excess fluorine, $Ar/F_2 = 100/1$ and $Ar/I_2 = 200/1$, is shown in scans (c) and (d) of Figure 6 before and

after photolysis with quartz-water and Pyrex filters. Before photolysis, weak bands at 516 and 524 cm^{-1} and a strong band at 535 cm^{-1} (absorbance = $A = 0.22$) were observed. After photolysis, a new band appeared at 499 cm^{-1} ($A = 0.048$), a strong band grew in at 526 cm^{-1} ($A = 0.98$), and the 535- cm^{-1} band lost intensity. Broad bands centered at 577 and 624 cm^{-1} grew in as well. Further photolysis with the quartz-water filter only produced some growth in the 499- cm^{-1} band, further reduction of the 535- cm^{-1} band, and slight reduction of the 526- cm^{-1} band. A thermal cycle had little effect on this sample.

Another separate manifold experiment, with equal iodine and fluorine concentrations ($Ar/I_2 = 200/1$, 813 mmol; $Ar/F_2 = 200/1$, 17 mmol) showed virtually the same spectrum as Figure 6c before photolysis. Pyrex-water filtered photolysis produced the 499- and 526- cm^{-1} bands, but this time, with lower fluorine concentration, the 535- cm^{-1} band grew slightly, rather than decreasing, as it did with excess fluorine. Further quartz-water filtered photolysis again produced growth of the 499- cm^{-1} band, slight growth of the 526- cm^{-1} band, and reduction of the 535- cm^{-1} band.

$Cl_2 + Br_2$. Two separate can experiments were done with chlorine and bromine, since these elements react to give $BrCl$ in the gas phase. The first, using 1% samples, produced a weak, broad band at 427 cm^{-1} after Pyrex- and water-filtered photolysis. The second experiment with $Ar/Cl_2 = Ar/Br_2 = 50/1$ samples produced a stronger 427- cm^{-1} absorption ($A = 0.08$) after water-filtered photolysis.

Raman. Raman experiments were done for the three fluorine-halogen systems. Premixed and separate manifold experiments were run with chlorine and fluorine, with total M/R for each halogen of 50 and 100. Initial scans showed signals corresponding to Cl_2 , ClF , and F_2 at 562, 760, and 892 cm^{-1} shifted from the laser line.⁹ Laser photolysis produced a weak signal at 528 cm^{-1} due to ClF_3 ¹¹ on the low-frequency side of the Cl_2 band and a weaker band approximately coinciding with the ClF band near 760 cm^{-1} . Otherwise, no new features were observed.

Bromine and fluorine experiments did produce new scattered light signals on laser photolysis. A typical experiment is illustrated in Figure 7 using $Ar/F_2 = 25/1$ and $Ar/Br_2 = 25/1$ samples. The first scan (a) shows a strong signal at 296 cm^{-1} ¹² and a weak F_2 signal and a broad feature which is actually two weak signals at about 603 and 638 cm^{-1} . Twenty-five minutes of 488.0-nm laser photolysis, scan (b), caused definite growth in the 603- cm^{-1} band, and a new band grew in at 675 cm^{-1} , while the 638- cm^{-1} band was lost. A thermal cycle to about 29 K, scan (c), caused further growth in the 675- cm^{-1} band but a reduction in the 603- cm^{-1} band. Further laser photolysis for 15 min, scan (d), regenerated the 603- cm^{-1} band, with little further effect on the 675- cm^{-1} band. Similar behavior was observed for a premixed experiment ($Ar/F_2/Br_2 = 100/2/1$), except that the 675- cm^{-1} band was favored slightly with the excess F_2 . Another premixed experiment ($Ar/F_2/Br_2 = 50/1/1$) again showed the 603- cm^{-1} band in better yield. Interestingly, the two photolysis-product bands showed up in the initial scan in the experiment where 514.5-nm laser light was used. Further separate manifold experiments using $Ar/F_2/Br_2 = 50/1/1$ samples produced only very weak bands in the 600–700- cm^{-1} region.

Laser Raman experiments with iodine and fluorine produced no new signals. Initial spectra showed a weak F_2 band, and strong resonance Raman spectra of isolated I_2 .¹² Prolonged photolysis only decreased these signals while resonance Raman bands due to aggregated I_2 appeared. All experiments were done with separate manifolds, using Ar/F_2 and Ar/I_2 as low as 25/1.

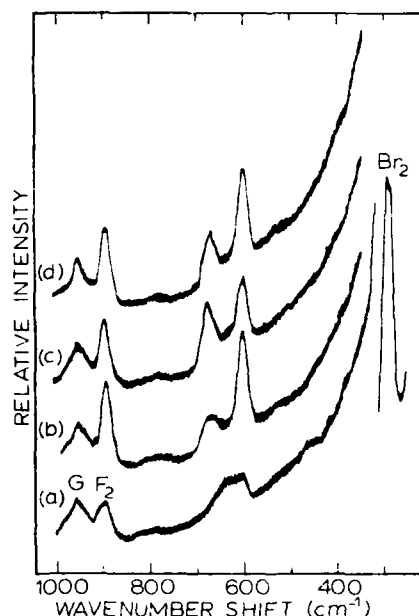


Figure 7. Raman spectra of a separate manifold bromine and fluorine experiment: (a) $\text{Ar}/\text{F}_2 = 25/1$, 13.7 mmol, and $\text{Ar}/\text{Br}_2 = 25/1$, 13.5 mmol deposited; (b) after 25 min of unfiltered 488.0-nm laser photolysis 470 mW at sample; (c) after a thermal cycle to 29 K; (d) after 15 min more unfiltered laser photolysis. Scans were taken at $50 \text{ cm}^{-1}/\text{min}$, $500\text{-}\mu$ slits, range = 1×10^{-9} A, dielectric spike filter (Br_2 peak, range = 3×10^{-9} A); G = grating ghost.

Discussion

Absorptions assigned to new photolysis product species for each chemical system will be discussed in turn.

Chlorine and Fluorine. The four infrared absorptions in these chlorine-fluorine experiments were observed and assigned previously by Mamantov et al.⁴ The present reexamination done at Virginia suggests an alternate assignment for three of these bands.

The 627-, 636- cm^{-1} Doublet. The 627-, 636- cm^{-1} absorptions were the most intense new product feature. The 3/1 relative intensities of these two bands clearly indicate that they are the ^{35}Cl , ^{37}Cl isotopic components of a single chlorine atom vibration. The isotope splitting of 9 cm^{-1} is larger than that of isolated ClF , 7 cm^{-1} . Such a large, distinct isotope splitting is characteristic of a nearly linear $\text{F}-\text{Cl}-\text{F}$ antisymmetric vibration containing a single chlorine atom, as proposed earlier.⁴ This band was also favored by an abundance of molecular fluorine, indicating that it probably involves more than one fluorine atom. The evidence supports assignment of this feature to the antisymmetric stretch of the $\text{F}-\text{Cl}-\text{F}$ unit in a symmetric, T-shaped ClClF_2 species. The location of this absorption slightly below the corresponding vibration of matrix-isolated ClF_2 at 683 cm^{-1} in argon⁷ is consistent with this assignment, which is in agreement with the previous work.⁴

The 559-, 464-, and 270- cm^{-1} Absorptions. The 464- and 270- cm^{-1} features were previously observed in very concentrated samples ($\text{Ar}/\text{F}_2/\text{Cl}_2 = 400/10/1$) and assigned⁴ to another stretch and a bend of the Cl_2F molecule, and the 559- cm^{-1} band was attributed to Cl_2F_2 . The 559- cm^{-1} absorption was observed when the 636- cm^{-1} feature was intense, and it exhibited a large Cl isotope splitting, 559 to 551 cm^{-1} , so assignment to a derivative of the Cl_2F_2 molecule was proposed.⁴ There is, however, an alternate assignment that can be made for these three bands which is consistent with the earlier information and with these more recent observations.

Table I. Observed and Calculated Isotopic Frequencies (cm^{-1}), Vibrational Potential Function, and Potential Energy Distribution for Cl_2F

Isotope	Assignment	Obsd	Calcd ^a
35-35-19	ν_1	559.0	560.1
	ν_2	464.0	465.4
	ν_3	270.0	271.2
37-37-37	ν_1	551.0	549.9
	ν_2	459.0	457.6
	ν_3	268.0	266.7

Potential function	Potential energy distribution ^b		
	ν_1	ν_2	ν_3
$F_{\text{Cl}-\text{F}} = 2.12 \text{ mdyne/A}$	71.9 ^c	30.3	1.3
$F_{\text{Cl}-\text{Cl}} = 2.77 \text{ mdyne/A}$	50.1	51.0	2.4
$F_{\text{Cl}-\text{Cl}-\text{F}} = 0.95 (\text{mdyne A})/\text{rad}^2$	0.0	4.3	95.7
$F_{\text{Cl}-\text{Cl}, \text{Cl}-\text{F}} = 0.44 \text{ mdyne/A}$	-22.0	14.4	0.6

^a Average difference between calculated and observed frequencies is 1.2 cm^{-1} . ^b For 35-35-19 isotope. ^c Interpretation: ν_1 is 71.9% Cl-F bond stretching in character.

One important point must be made with respect to the dependence of the 559- cm^{-1} band on fluorine concentration. The previous work showed that this feature was favored by an abundance of fluorine atoms, based on relative growth after photolysis with wavelengths that favor F_2 dissociation. The recent data indicate, however, that these bands are favored relative to the 627-, 636- cm^{-1} features in experiments with lower total fluorine concentration. The earlier experiments used a many (10-20)-fold excess of F_2 , while the recent ones employed only a fourfold F_2 excess and also a fourfold Cl_2 excess. This latter observation does not support assignment of these absorptions to a fluorine addition product of Cl_2F_2 . A species that would be favored by both efficient fluorine atom production and low total fluorine concentration is one containing a single fluorine atom, specifically Cl_2F .

The 464- and 270- cm^{-1} absorptions appear to be associated with the 559- cm^{-1} absorption on changing the F_2/Cl_2 ratio in the sample. It is reasonable to consider these lower two bands for assignment to the Cl-Cl stretching mode and the bending mode of $\text{Cl}-\text{Cl}-\text{F}$, respectively. In the most productive experiment, the 464- cm^{-1} feature contained partially resolved components at 462 and 459 cm^{-1} with the appropriate relative intensities for a vibration of two chlorine atoms. The 559- cm^{-1} band is assigned to the Cl-F stretching mode of Cl_2F ; the chlorine isotopic intensities show that one chlorine atom participates in this vibration.

Force constant calculations were done for the $\text{Cl}-\text{Cl}-\text{F}$ radical with these assignments using the Schachtneider program FAD1 and the assumed bent structure (150°) with Cl-Cl and Cl-F distances of 2.2 and 1.8 Å, respectively. Bond lengths for the diatomic molecules are 1.99 and 1.63 Å, respectively.⁹ A satisfactory agreement was obtained between calculated and observed frequencies (average difference = 1.2 cm^{-1}); a substantial Cl-Cl, Cl-F stretch-stretch interaction force constant was required to fit the isotopic data which are listed in Table I along with the force constants. It can be seen from the potential energy distribution that the two bond stretching modes are extensively mixed; however, the 559- cm^{-1} band is more Cl-F stretch and the 464- cm^{-1} band is predominantly Cl-Cl stretch in character. This vibrational analysis is supportive of the Cl_2F assignment, but it cannot be considered to confirm the observation of Cl_2F .

If this identification of the Cl_2F free radical is correct, another interesting 21-electron species is available for bonding considerations. The two stretching fundamentals of Cl_2F , 559 and 464 cm^{-1} , are near the stretching modes¹ of ClF_2 at 578 and 500 cm^{-1} . Comparison between the two modes for Cl_2F with the Cl-Cl and Cl-F fundamentals at 549 and 770 cm^{-1} in solid argon,¹⁰ and the force constants in Table I with values

for ClF ($4.29 \text{ mdyne}/\text{\AA}$)⁶ and Cl_2 ($3.10 \text{ mdyne}/\text{\AA}$)¹³ suggests that Cl_2F contains a weak $Cl-F$ bond and a Cl_2 bond only slightly weaker than diatomic Cl_2 . This is reminiscent of the $F\cdots ClO$ and $Cl\cdots ClO$ molecules and the bonding in $F\cdots ClCl$ can be rationalized by the simple $p-\pi^*$ bonding model used for these species.^{6,14} However, in the $F\cdots ClCl$ case, a three-electron $F(2p)-Cl_2(\pi^*)$ bond is involved which affects the $Cl-Cl$ bond by increasing antibonding electron density, opposite to the case in $F\cdots ClO$. Finally, a simple molecular orbital model for X_3 systems using valence s and p orbitals gives three more bonding than antibonding electrons which also predicts one "single" bond and one "half" bond for $F\cdots ClCl$.

The failure to produce $ClClF_2$ and $ClClF$ with the alternate but less prolific fluorine atom sources, ClF and OF_2 , may shed some light on a possible mechanism by which these species are formed. This observation suggests that the mechanism is not only simple addition of fluorine atoms to molecular chlorine but that chlorine molecule-fluorine molecule van der Waals dimers may play an important role. $ClClF_2$ could be formed directly upon photolysis of $Cl_2\cdots F_2$ van der Waals dimers and Cl_2F could result when one fluorine escapes this cage. Of course, direct fluorine addition to Cl_2 can form Cl_2F as well.

Bromine and Fluorine. The infrared experiments on the $Br_2 + F_2$ system were the most interesting and fruitful in terms of new species observed. The moderate gas-phase reactivity of the reagents made the contrast between premixed and separate experiments particularly illuminating and informative.

The 554-, 556-cm⁻¹ Doublet. The 554-, 556-cm⁻¹ doublet exhibited a distinct bromine isotope splitting characteristic of a vibration involving a single Br atom. The bromine isotopic splitting for BrF is 1.5 cm^{-1} for the 661-cm^{-1} fundamental in solid argon, whereas the splitting on the 554-556-cm⁻¹ doublet is 2.0 cm^{-1} , a good bit larger. This suggests an antisymmetric stretch of an approximately linear $F-Br-F$ unit. The fact that this band is strongly favored in experiments where Br_2 is the bromine source leads to the conclusion that the species contains two Br atoms. Finally, the increased yield with excess F_2 suggests that the molecule probably contains more than one F atom. These observations lead to the assignment of this band to the symmetric T-shaped $BrBrF_2$ molecule. The 555-cm⁻¹ band was the major product species in these studies, as was the analogous Cl_2F_2 molecule in chlorine-fluorine experiments. This species is probably produced largely from the photoreaction of Br_2-F_2 van der Waals dimers trapped in the matrix, although the reaction of two successive fluorine atoms with Br_2 is also expected. It is noteworthy that the antisymmetric $F-Br-F$ mode in $Br-BrF_2$, 555 cm^{-1} , is slightly reduced from that of $F-BrF_2$, 597 cm^{-1} .

The 568-, 570-cm⁻¹ Doublet. The 568-, 570-cm⁻¹ band exhibits the same distinct splitting characteristic of a nearly linear $F-Br-F$ antisymmetric vibration. The fact that this feature grows dramatically on warming shows that it is produced by the diffusion and reaction of F atoms. The species may be formed during photolysis as well but destroyed at roughly the same rate. This behavior was observed less dramatically with the ClF_2 radical.²³ The 569-cm^{-1} band is only observed in experiments where precursor molecules with a single Br atom are present, BrF and BrF_2 , indicating that it probably contains only one Br atom. Further, it is not especially favored in experiments where excess fluorine is present in which case the single Br species BrF_2 would be the preferred product. This evidence leads to the assignment of this feature to the BrF_2 radical.

Although the formation and behavior of this species are comparable to that of ClF_2 , it is noteworthy that a comparison of the ClF and BrF frequencies, and the ClF_2 and BrF_2 ra-

modes, predicts BrF_2 in the low 500-cm^{-1} region, where bands are observed at 507 and 527 cm^{-1} . Still, the parallel photolytic behavior and the bromine isotopic splitting point to assignment of the 569-cm^{-1} band to ν_3 of BrF_2 .

The isotopic fundamentals 570.2 and 568.0 cm^{-1} , respectively, for $^{79}BrF_2$ and $^{81}BrF_2$ can be used to calculate a lower limit to the $F-Br-F$ valence angle. This value, $152 \pm 8^\circ$, is in good agreement with the $136 \pm 4^\circ$ lower limit³ for ClF_2 and it strongly suggests that the 21-electron BrF_2 free radical is obtusely bent.

The 507-cm⁻¹ Band. The band at 507 cm^{-1} falls in a region with a broad unstructured BrF_3 dimer band⁷ that is observed in experiments where this compound is present. However, the band is much sharper in experiments where bromine and fluorine are deposited separately, and its intensity is large relative to other BrF_3 dimer bands in these experiments. This leads to the conclusion that a new, photolysis-product species is responsible for this sharp feature. The fact that this feature is most prominent in experiments with Br_2 parent indicates again a species containing two Br atoms. Further, it is favored over BrF_3 dimer in an experiment with low F_2 concentration, indicating that it contains fewer F atoms. These observations justify the tentative assignment of this feature to the asymmetric $Br-F$ species formed by reaction of one F atom with Br_2 . Unfortunately, no bromine isotopic splitting was resolved on this absorption; however, the splitting is only 1.0 cm^{-1} for a simple $Br-F$ mode in this region, which would be difficult to resolve for a weak absorption.

The observation of the 507-cm^{-1} band in discharge experiments is consistent with the Br_2F assignment. It is not expected in the blank experiment, since only the known reaction products BrF_n ($n = 1, 3, 5$) would be formed without any photolysis after deposition, and the premixed sample would be expected to react such that little Br_2 would be available anyway. The good yield obtained with reactants mixed just prior to discharge is consistent with the deposition of intact bromine molecules and fluorine atoms.

The 527-cm⁻¹ Band. The band at 527 cm^{-1} is of interest as it was observed in both photolysis and discharge experiments. It is present in scans of premixed samples *prior to photolysis* but was not observed in the blank discharge experiment, although no BrF_3 was observed either. It seems to be favored by excess fluorine and by thermal cycling but is lost on thermal cycling above 35 K . The 527-cm^{-1} absorption observed before photolysis is most likely due to $(BrF_3)_2$, as assigned previously.⁷ This species could be formed by warming a sample containing Br_2 and excess fluorine atoms since the Br_2 unit need not separate in the dimer. However, its disappearance on warming above 35 K in discharge experiments suggests that a more reactive species might contribute to the 527-cm^{-1} absorption. A possibility is BrF_4 which is expected to increase on diffusion and reaction of F atoms to a point. BrF_4 should be more stable than ClF_4 (which has been detected by ESR¹⁵ and studied via computer experiments¹⁶) as shown by the comparison of ClF_4 and BrF_4 .

Others. The small band at 538 cm^{-1} is noticeable by virtue of its photolysis behavior. This feature has been observed in other work with mixed $Br-F$ compounds, where it was attributed to an impurity, obviously photosensitive. This assignment is acceptable, insofar as its behavior is not particularly compatible with any of the other assigned new bands. The 475-cm^{-1} band observed in discharge experiments may possibly be due to higher polymers of BrF_3 , based in particular on its stability to relatively high thermal cycling to 50 K .

The doublet observed at $561, 563 \text{ cm}^{-1}$ has not been assigned to a new species; it is probably due to a site splitting of the $554-, 556\text{-cm}^{-1}$ BrF_2 feature. The intensity of the smaller band decreases slightly more than the $554-, 556\text{-cm}^{-1}$ feature

on warming, and the resolution of the doublet is lost. This is reasonable behavior for a less stable matrix site.

Iodine and Fluorine. Premixed iodine and fluorine samples revealed a good yield of IF_3 on decomposition, and no new products were formed on photolysis. Even separate can experiments, which provide a short reaction time in the spray on line, produced a large amount of IF_3 , indicating that this is the strongly favored product. The matrix isolation experiments, that allow a brief reaction time even just at the matrix surface, provide a situation in which IF or IF_2 could be observed as intermediates in the formation of IF_3 .

The 535- cm^{-1} Band. The 535- cm^{-1} band was present before photolysis in both separate can and separate manifold experiments, with larger yields in the latter case. The band was observed to decrease significantly on photolysis when an initial twofold excess of fluorine over iodine was present. However, with a lower fluorine concentration, the band increased on initial quartz, water, and Pyrex photolysis, though further photolysis did decrease it. The species, then, is favored by a lower fluorine concentration and can be both formed and destroyed by photolysis. A species that could form and be trapped during deposition is IF_3 , and the observed photolysis behavior can be readily rationalized for this assignment. In solid IF_3 the corresponding band occurs¹⁷ at 480 cm^{-1} . We have, however, observed¹⁸ a frequency shift of similar magnitude for the ν_4 band of solid ClF_3 .

Photolysis of a sample containing an excess of fluorine would result in conversion of IF_3 to IF_2 , by addition of fluorine atoms. Indeed, a broad band in the region of IF_2 absorption is seen to grow in on photolysis in the separate manifold experiments (Figure 6d). Growth of IF_3 on photolysis with less F_2 could arise from fluorine reaction with IF or I atoms liberated in the initial fluorine-iodine reaction during sample condensation. Finally, assignment of the 535- cm^{-1} band to IF_3 is in reasonable correlation with ClF_3 at 683 cm^{-1} and BrF_3 at 597 cm^{-1} in argon matrices.⁷

The 526- cm^{-1} Band. The 526- cm^{-1} band is by far the dominant absorption produced by photolysis in the iodine-fluorine experiments. This new species is expected to contain two iodine atoms, as it is probably formed from isolated I_2 in the matrix. It probably contains more than one fluorine atom, since the best yields are obtained in excess-fluorine experiments. The straightforward assignment for this band is to the symmetric IF_2I_2 species. This assignment is in good agreement with those for Cl_2F_2 at 636 cm^{-1} and Br_2F_2 at 555 cm^{-1} , which were the major products in their respective experiments.

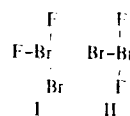
The 499- cm^{-1} Band. This species is present in considerably lower yields in all experiments, as might be expected for a species with either fewer or more fluorine atoms than the dominant species. The position of this band makes reasonable a tentative assignment to I_2F , following Cl_2F at 559 cm^{-1} and Br_2F at 507 cm^{-1} . However, the continued growth of this band on successive photolyses, and the fact that it is favored relative to the 526- cm^{-1} band in the excess-fluorine separate manifold experiment, means that assignment to a higher fluorine species such as I_2F_3 or I_2F_4 cannot be ruled out. Higher fluorine species are expected to be more stable in experiments with iodine, as compared to chlorine or bromine.

Others. The broad, weak feature centered at about 624 cm^{-1} is slightly lower than the strong IF_2 absorption, and it is reasonably assigned to this molecule. The small feature at 578 cm^{-1} is present both before and after photolysis in separate can experiments and only after photolysis in separate manifold experiments. This feature and a weak band at 518 cm^{-1} present throughout the separate manifold experiments are probably due to more stable species which cannot be identified without additional information.

Bromine and Chlorine. The only new infrared absorption produced by photolysis of $\text{Br}_2\text{-Cl}_2$ samples appeared at 427 cm^{-1} . This feature was not observed in a previous study involving discharged mixtures of Br_2 and Cl_2 which suggested the Br-BrCl_2 identification for a band near 325 cm^{-1} .¹⁹ The BrCl fundamental has been observed at $430 \pm 2 \text{ cm}^{-1}$ in Raman studies;¹³ this suggests that the present 427- cm^{-1} band is due to bromine monochloride monomer and perhaps the dimer, $(\text{BrCl})_2$. The earlier Br-BrCl_2 assignment appears reasonable relative to BrCl at 430 cm^{-1} considering the present XXF_2 species as compared to the XF diatomics. It is interesting to note that the failure to form BrBrCl_2 by photolysis indicates its instability relative to 2BrCl or $(\text{BrCl})_2$; however, the XXF_2 species are produced by photolysis which shows that the symmetric XXF_2 molecule is more stable than the $(\text{XF})_2$ dimer species.

Raman Spectra. Most of the assignments made from the infrared work to single modes of polyatomic species are based on relative band intensity and concentration behavior. Supporting evidence could, in principle, be obtained from Raman spectra, but, unfortunately, the Raman observations were not helpful in this regard. Bromine and fluorine experiments were the only ones that showed new photolysis product signals, which came at 603 and 675 cm^{-1} . Neither of these bands correspond to signals observed in the infrared, which is not surprising, since Raman and infrared intensities often vary indirectly.

The 603- cm^{-1} Raman signal is below the equatorial Br-F stretching mode⁷ of BrF_3 at 672 cm^{-1} and the 603- cm^{-1} band could be due to the equatorial mode of an asymmetric species (I). Infrared data were obtained for the symmetric species



(II) and not the asymmetric species; however, the symmetric isomer is probably the stronger infrared absorber. It is also possible for ultraviolet photolysis to favor the production of one isomer and visible laser photolysis to favor the other. Isomerization could also occur by a dimer exchange mechanism.⁷ The Raman observation suggests that an asymmetric Br_2F_2 species is also formed, but it does not provide a definitive identification.

Although the 675- cm^{-1} band is markedly similar to the equatorial Br-F mode of BrF_3 , absence of the stronger axial Br-F mode for BrF_3 at 547 cm^{-1} rules out BrF_3 monomer for the present Raman band. However, this band increased on sample warming which suggests a dimer that presumably contains two Br_2F_2 species, but this is not a definitive identification.

Conclusions

Matrix samples containing fluorine and chlorine, bromine, or iodine were photolyzed and infrared absorptions were produced for new interhalogen species. The major absorption in each study was assigned to the symmetric XXF_2 molecule, analogous to XeF_2 . Three infrared bands have been attributed to each of the ^{35}Cl and ^{37}Cl isotopic species. A sharp 568.0-, 570.2- cm^{-1} doublet was assigned to the Br-F -free radical. A new band produced by the matrix cocondensation reaction of I_2 and F_2 was assigned to IF_2 , which was converted to IF_3 by photolysis in samples with excess fluorine. A summary of vibrational modes for interhalogen molecules in solid argon is given in Table II. The production of these species on photolysis is indicative of mechanisms involving fluorine atom migration through the matrix and the photoreaction of van der Waals dimers. The matrix allows new

Table II. Vibrational Modes (cm^{-1}) for Interhalogen Molecules in Solid Argon

Mode	Cl-F species	Br-F species	I-F species
X-F str	Cl-F 770	Br-F 661	I-F 603 ^a
Antisym X-F	ClF_2 578 ^b	BrF_2 569	
Eq X-F	ClF_3 754 ^c	BrF_3 672 ^c	
Ax, antisym X-F	ClF_3 683	BrF_3 597	IF_3 535
Ax, antisym X-F	Cl_2F_2 636	Br_2F_2 555	I_2F_2 526
X-F' str	ClF_4 722 ^d	BrF_4 681	IF_4 704
Antisym X-F	ClF_5 726	BrF_5 636	IF_5 634
X-F str	Cl_2F 559	(Br_2F 507)	(I_2F 499)
X-X str	Cl_2F 464		
X-X-F bend	Cl_2F 270		

^a Deduced from electronic spectra. ^b References 2 and 3.^c Reference 7. ^d G. M. Begun, W. H. Fletcher, and D. F. Smith, *J. Chem. Phys.*, **42**, 2236 (1965).

intermediate interhalogen species to be produced and trapped for spectroscopic study.

Acknowledgment. The Virginia study was supported by a grant from the National Science Foundation. The work done at Tennessee was supported by the Army Research Office and by the Air Force Office of Scientific Research. G.M. would like to thank W. N. Hubbard of the Argonne National Laboratory for a sample of purified fluorine.

Registry No. ClF, 7790-89-8; ClF_2 , 7790-91-2; Cl_2F_2 , 37621-12-8; ClF_3 , 13637-63-3; Cl_2F , 65516-29-2; BrF, 13863-59-7; BrF_2 , 64973-51-9; BrF_3 , 7787-71-5; Br_2F_2 , 65414-56-4; BrF_4 , 7789-30-2; Br_2F , 64973-52-0; IF_3 , 22520-96-3; I_2F_2 , 65414-57-5; IF_5 , 7783-66-6;

I_2F , 58751-33-0; F_2 , 7782-41-4; Cl_2 , 7782-50-5; Br_2 , 7726-95-6; I_2 , 7553-56-2.

References and Notes

- (1) (a) University of Virginia. (b) University of Tennessee.
- (2) G. Mamantov, E. J. Vasini, M. C. Moulton, D. G. Vickroy, and T. Mackawa, *J. Chem. Phys.*, **54**, 3419 (1971).
- (3) E. S. Prochaska and L. Andrews, *Inorg. Chem.*, **16**, 339 (1977).
- (4) M. R. Clarke, W. H. Fletcher, G. Mamantov, E. J. Vasini, and D. G. Vickroy, *Inorg. Nucl. Chem. Lett.*, **8**, 611 (1972).
- (5) (a) L. Andrews, *J. Chem. Phys.*, **48**, 972 (1968); **54**, 4933 (1977); (b) *ibid.*, **51**, 57 (1972).
- (6) L. Andrews, F. K. Chi, and A. Arkell, *J. Am. Chem. Soc.*, **96**, 1997 (1974).
- (7) R. A. Frey, R. L. Redington, and A. L. K. Aljibury, *J. Chem. Phys.*, **54**, 344 (1971).
- (8) (a) D. R. Lide and D. E. Mann, *J. Chem. Phys.*, **25**, 1128 (1956); (b) D. F. Smith, G. M. Begun, and W. H. Fletcher, *Spectrochim. Acta*, **20**, 1763 (1964); (c) K. O. Christe and E. C. Curtis, *Inorg. Chem.*, **11**, 2196 (1972).
- (9) B. Rosen, Ed., "Spectroscopic Data Relative to Diatomic Molecules", Pergamon Press, Oxford, 1970.
- (10) G. M. Begun, W. H. Fletcher, and D. F. Smith, *J. Chem. Phys.*, **42**, 2236 (1965).
- (11) H. Selig, H. H. Claassen, and J. H. Holloway, *J. Chem. Phys.*, **52**, 3517 (1970).
- (12) W. F. Howard, Jr., and L. Andrews, *J. Raman Spectrosc.*, **2**, 447 (1974).
- (13) C. A. Wight, B. S. Ault, and L. Andrews, *J. Mol. Spectrosc.*, **56**, 239 (1975).
- (14) M. M. Rochkind and G. C. Pimentel, *J. Chem. Phys.*, **46**, 4481 (1967).
- (15) J. R. Morton and K. F. Preston, *J. Chem. Phys.*, **58**, 3112 (1973); L. Nishikida, F. Williams, G. Mamantov, and N. R. Smryl, *J. Am. Chem. Soc.*, **97**, 3526 (1975).
- (16) S. R. Ungemach and H. F. Schaefer, III, *J. Am. Chem. Soc.*, **98**, 1658 (1976).
- (17) M. Schmeisser, D. Naumann, and E. Lehmann, *J. Fluorine Chem.*, **3**, 441 (1973).
- (18) D. G. Vickroy and G. Mamantov, unpublished work.
- (19) L. Y. Nelson and G. C. Pimentel, *Inorg. Chem.*, **7**, 1695 (1968).

6. APPENDIX 2: DIATOMIC INTERHALOGENS(A) INTRODUCTION

Many of the physical parameters of chlorine monofluoride have not been well determined. The gas phase infrared spectrum was analyzed in 1951¹, but the resolution was insufficient for precise evaluation of the rotational constants, and the data were treated with reference to parameters calculated from earlier microwave² and optical spectra^{3,4}. The microwave spectrum was remeasured in 1955⁵, but in both microwave studies some high order constants were neglected so that the reported B_e and α_e are in fact $B_e + 3/4\gamma_e$ and $\alpha_e + 2\gamma_e$. The data from these studies were recalculated in 1974⁶ but the same truncation was used. The optical spectrum was remeasured in 1968⁷, and the optical, infrared and microwave data was reassessed in 1975⁸ in the context of the dissociation energy of ClF and other halogen fluorides. The photoelectron spectrum has been reported⁹. There has been a discussion of the sign of the dipole moment of ClF which has been resolved in favor of the intuitive direction i.e. $\text{Cl}^+\text{F}^{-10}$.

In this work the infrared spectra of the 1-0, 2-0 and 3-0 bands of ³⁵ClF and ³⁷ClF were recorded and analyzed. The constants ω_e , $\omega_e x_e$ and D_e were precisely determined for the first time, while B_e and α_e agree with the (corrected) values from the earlier microwave data.

(B) CHLORINE MONOFLUORIDE SPECTRA

The 1-0 (fundamental), 2-0 (first overtone) and 3-0 (second overtone) bands were recorded and are shown in Figures 6.1 - 6.3. In addition in Fig. 6.1 a few 2-1 transitions (hot bands) can also be seen. The quality of the spectrum obtained for 3-0 bands was poor. The only suitable inert cell had a pathlength of 10 cm, so that in order to observe this band a pressure of 1000 torr had to be used at which substantial pressure broadening occurs, reducing the effective resolution to about $0.2\text{-}0.3\text{ cm}^{-1}$. However the gross features of the band may be seen including the R-branch heads for both ³⁵ClF and ³⁷ClF. At the resolution used not all the lines in the 1-0 and 2-0 manifolds are resolved; some of the ³⁵ClF and ³⁷ClF features are blended. Nevertheless the position of lines up to $J=50$ for 1-0 and $J=40$ for 2-0 were measured with a precision of about $1/20$ of the resolution, i.e. about 0.005 cm^{-1} .

(C) SPECTRAL INTERPRETATION

The symbols used in analysis of the data are defined in the equations;

$$E/hc = E_e/hc + G(v) + F(J)$$

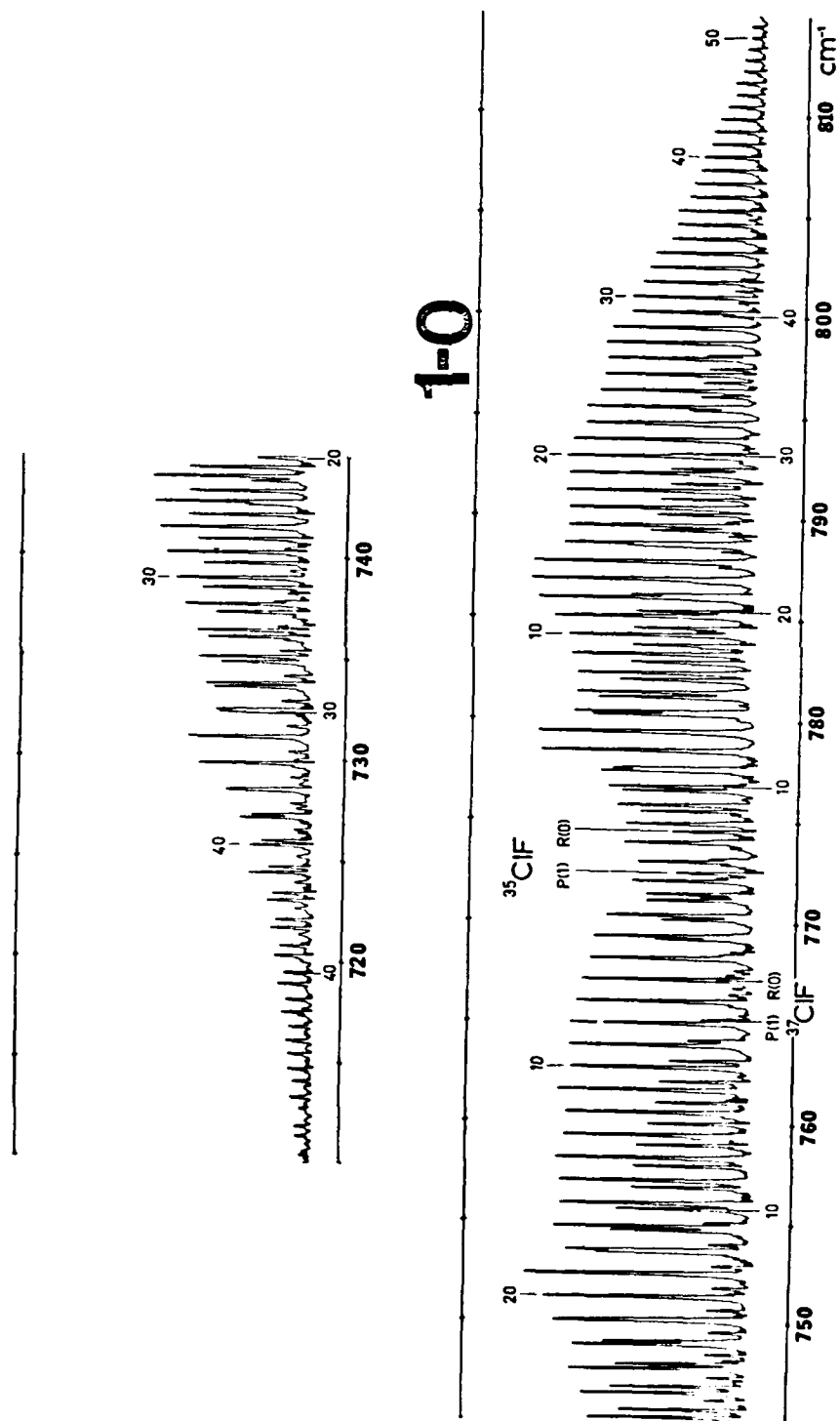


Fig. 6.1 FT-IR spectrum of the 1-0 band of ClF.

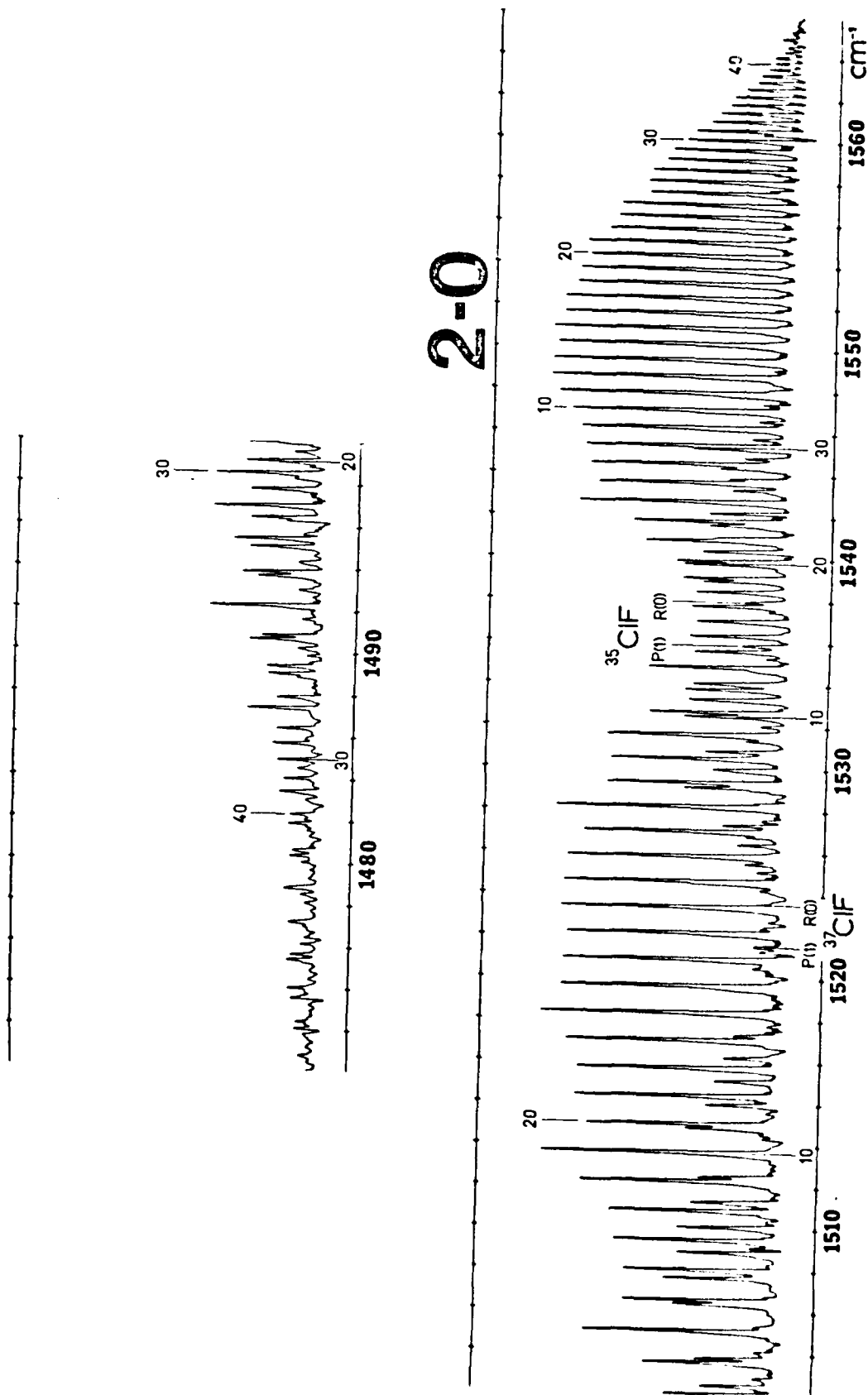


Fig. 6.2 FT-IR spectrum of the 2-0 band of ClF.

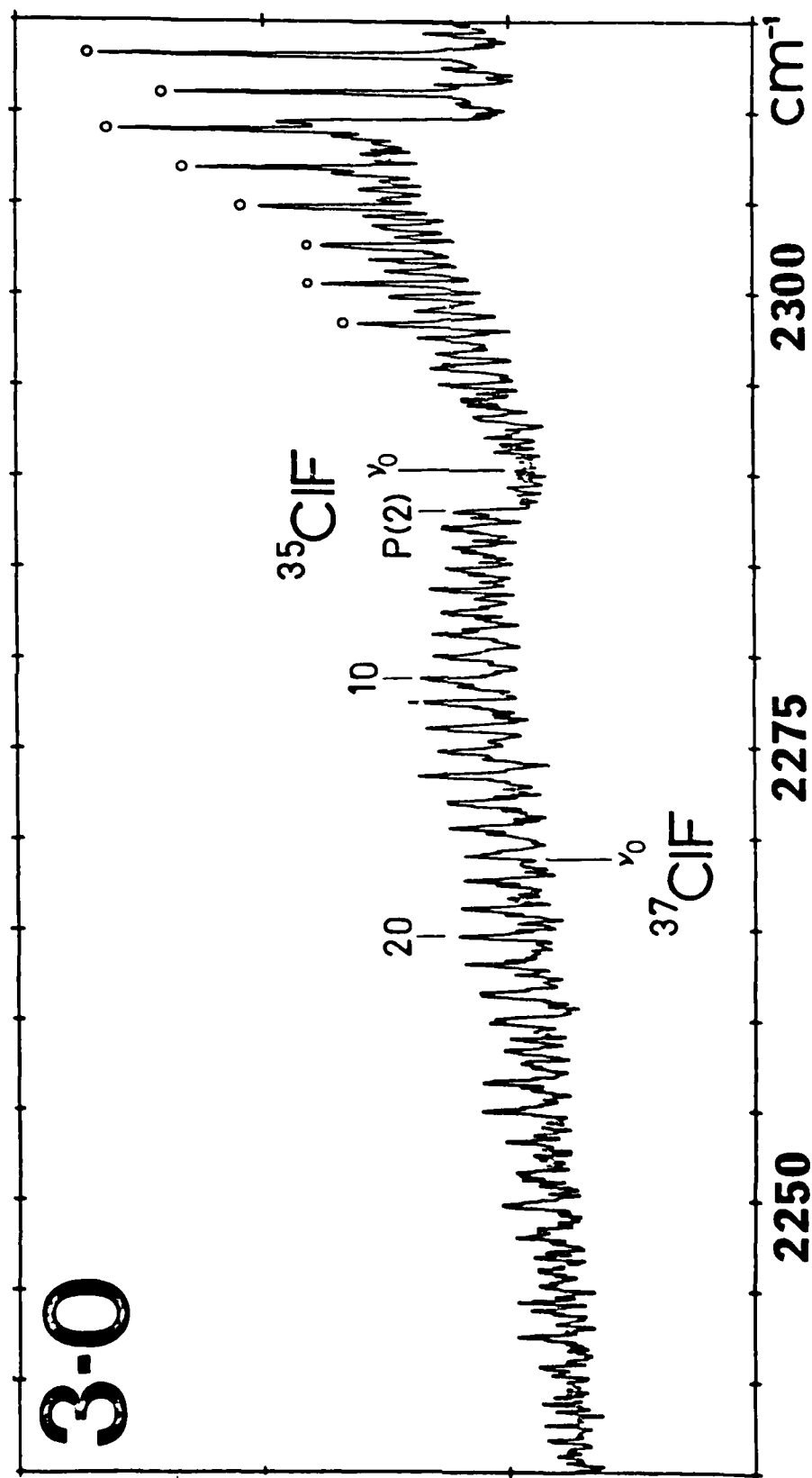


Fig. 6.3 FT-IR spectrum of the 3-0 band of ClF.

$$G_v = \omega_e(v + 1/2) - \omega_e x_e(v + 1/2)^2 + y_e \omega_e(v + 1/2)^3 \dots$$

$$F_v(J) = B_v J(J + 1) - D_v J^2(J + 1)^2 + H_v J^3(J + 1)^3 \dots$$

$$B_v = B_e - \alpha_e(v + 1/2) - \gamma_e(v + 1/2)^2 \dots$$

$$D_v = D_e - \beta_e(v + 1/2) \dots$$

$$\text{Hence } B_o = B_e - 1/2\alpha_e - 1/2\alpha_e - 1/4\gamma_e \dots$$

$$\text{and } D_o = D_e - 1/2\beta_e \dots$$

The first step in the analysis consisted of the standard graphical plots¹, allowing for checks of measurement errors and the initial assignments. The ground state combination differences and upper state combination differences are shown in Figure 6.4 while the combination sums plots are shown in Figure 6.5. A drawback with this approach is that it requires specific pairs of lines, which, owing to the blending problem alluded to above, may not be available in all cases. An approach which does not suffer this constraint is generalized transition frequency analysis. Here all the measured frequencies, in this case 197, are fitted simultaneously using the number of variables appropriate. In this particular case the maximum number of variables to be determined is seven, so that the problem is greatly over-determined. Therefore a procedure is used that employs variable statistical weighting for individual data points. After several refinement cycles some points may receive zero weighting (typically a blended line whose apparent peak center may be considerably displaced from the 'true' position). 186 of the original 197 lines were fitted with a standard deviation of 0.0062 cm^{-1} , which compares well to the accuracy to which the lines could be measured.

Because only poor data was available for the 0-3 band, some of the higher order parameters could not be determined independently, so that in this fit the values of B_e and α_e were constrained enabling a realistic value of γ_e to be calculated. Also in the fit the value of β_e was constrained to a figure calculated from a theoretical relationship between other parameters. The data in the Table represent the best values calculated so far, but are being refined further and some small changes are anticipated.

(D) EXPERIMENTAL

Chlorine monofluoride, with natural abundance ^{35}Cl and ^{37}Cl , was obtained from Ozark-Mahoning (Tulsa, Oklahoma). It was handled exclusively in a well-passivated metal vacuum line, and distilled from a -126°C trap before use. Samples at pressures ranging from 20 to 1000 torr were contained in a 10 cm long stain-

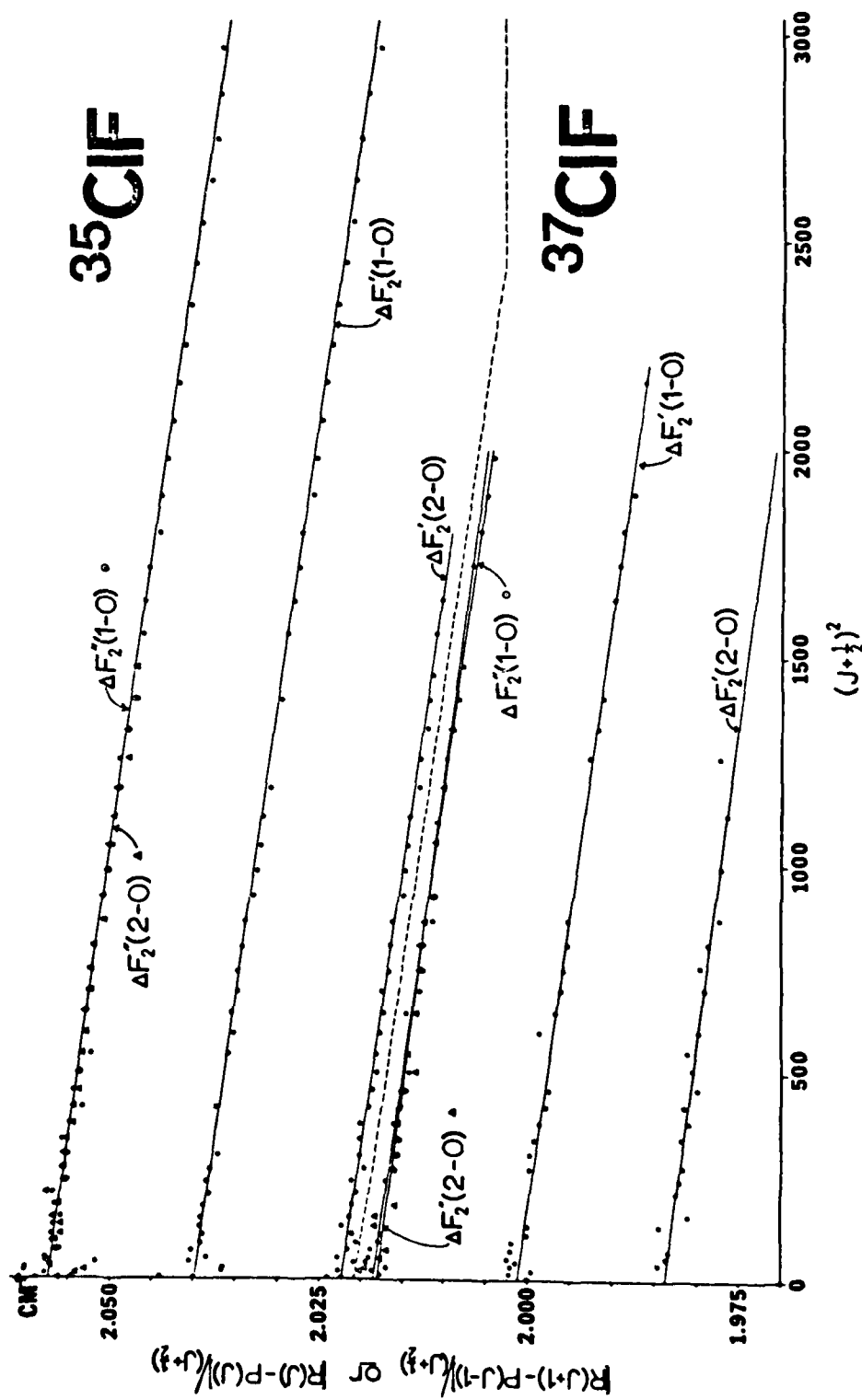


Fig. 6.4 Ground and upper state combination differences for ClF.

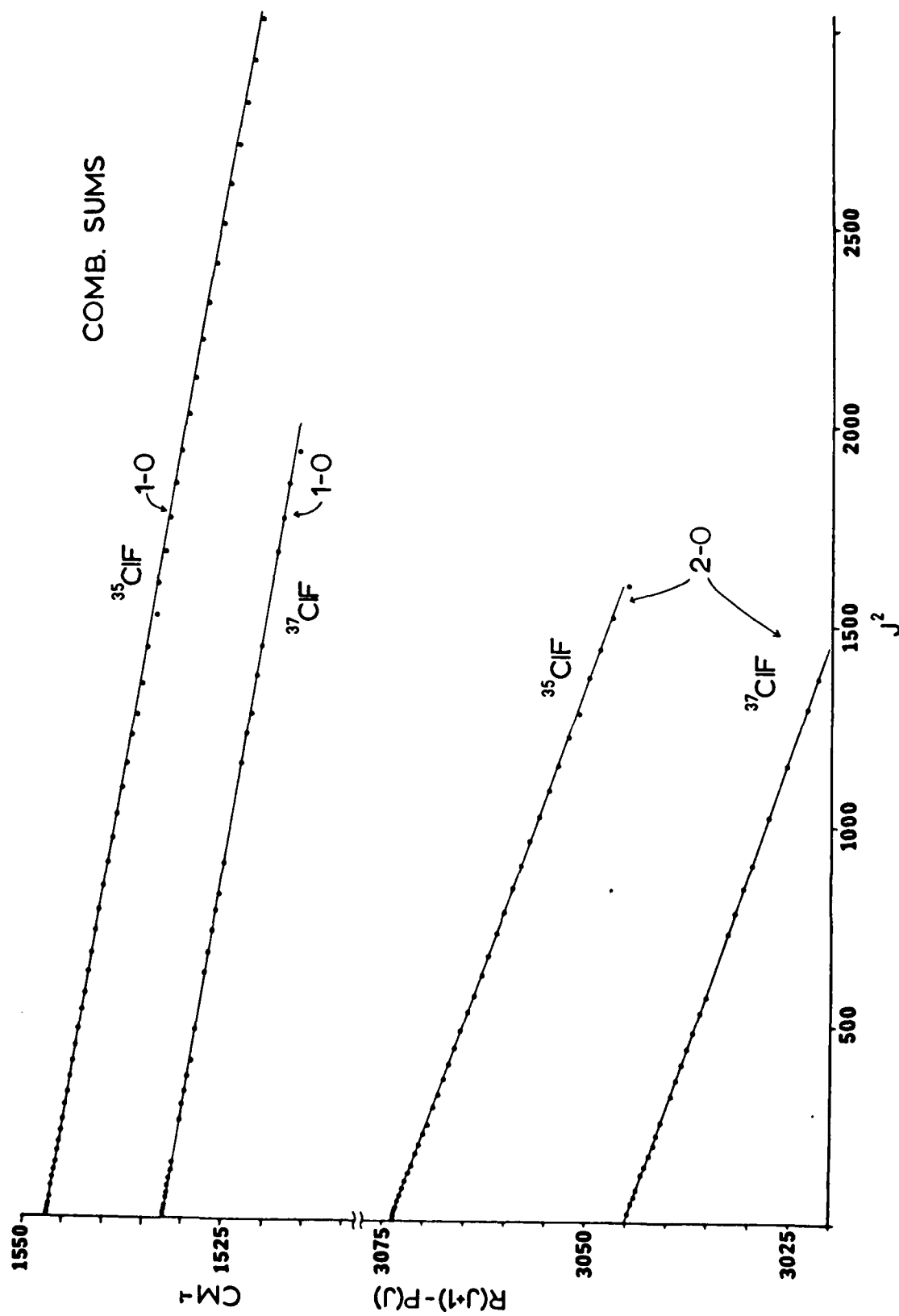


Fig. 6.5 Combination sums for ClF.

COMPARISON OF PRESENT WORK WITH PREVIOUS RESULTS FOR $^{35}\text{ClF(a)}$

PARAMETER	MW ^(b)	IR ^(e)	ELECTRONIC		PRESENT WORK	CALC.
			(f)	(g)		
$B_e + \frac{3}{4}v_e$	0.5164788(13)				0.516480 (h)	
$a_e + 2v_e$	4.3578(17) $\times 10^{-3}$				4.3602(13) $\times 10^{-3}$ (i)	
D_e	8.77(17) $\times 10^{-7}$ (c)				9.02(9) $\times 10^{-7}$ (j)	8.976 $\times 10^{-7}$ (0)
B_e	0.5164638		0.518(1)	0.5167(2)	0.516465 (i)	
a_e	4.3158 $\times 10^{-3}$		6(2) $\times 10^{-3}$	4.5(4) $\times 10^{-3}$	4.3090 $\times 10^{-3}$ (i)	4.332 $\times 10^{-3}$ (n)
ω_e		786.34	793.2	784.1(1.0)	738.512(24) (j)	
$\omega_e x_e$		6.23	9.9	5.3(5)	5.014(9) (j)	
$\tilde{\nu}_e$					4.189 $\times 10^{-9}$ (k)	4.189 $\times 10^{-9}$ (k)
γ_e					21 $\times 10^{-6}$ (h)	
H_e						-2.08 $\times 10^{-13}$ (p)
B_0	0.5142999(22) (d)				0.514306(41) (1)	
B_1	0.5099421(39) (d)				0.509954(30) (1)	
B_2	0.5055843(56) (d)				0.505561(35) (1)	
D_0					9.07(8) $\times 10^{-7}$ (1)	9.00 $\times 10^{-7}$ (d)
D_1					9.12(7) $\times 10^{-7}$ (1)	9.04 $\times 10^{-7}$ (d)
D_2					9.17(15) $\times 10^{-7}$ (1)	9.08 $\times 10^{-7}$ (d)
$\nu_0(1-0)$		773.88			773.485(6) (m)	
$\nu_0(2-0)$		1535.30			1536.943(5) (m)	

- (a) All values in cm^{-1} .
- (b) Microwave studies: summarized by Lovas and Tiersmann, J. Phy. Chem. Ref. Data 3, 663 (1974). Conversion to cm^{-1} using $c = 2.997924562 \times 10^{10}$ cm/sec.
- (c) Calculated from $D_e = 48 \frac{3}{\omega_e^2}$ using earlier value of $\omega_e = 793.2 \text{ cm}^{-1}$ [Wahrhaftig, J. Chem. Phys. 10, 248 (1942)].
- (d) Assuming $B_v = B_e - \alpha_e(v + 1/2)$ or $D_v = D_e + \beta_e(v + 1/2)$.
- (e) Nielsen and Jones, J. Chem. Phys. 19, 1117 (1951).
- (f) Wahrhaftig. see (c).
- (g) Stricker and Krauss, Z. Naturforsch. 23A, 1116 (1968).
- (h) From analysis of B_0 , B_1 and B_2 values from comb. diff. to determine B_e , α_e and γ_e .
- (i) From comb. sum analysis of 1-0 band.
- (j) From a restricted least square molecular parameter fitting. Listed values derived from $v_0(1-0) + v_0(2-0)$ assuming $\omega_e \gamma_e = 0$.
- (k) Calculated from $B_e = D_e \left[\frac{8\omega_e \alpha_e}{\omega_e^2} - \frac{5\alpha_e}{B_e} - \frac{\alpha_e \omega_e}{24B_e^3} \right]$
- (l) From combination different analysis.
- (m) From combination sum analyses.
- (n) Calculated from $\alpha_e = \frac{6\sqrt{\omega_e B_e^3}}{\omega_e} - \frac{6B_e^2}{\omega_e^2}$
- (o) Calculated from $D_e = \frac{4B_e}{\omega_e^2}$.
- (p) Calculated from $H_e = \frac{2D_e}{3\omega_e} (12B_e^2 - \alpha_e \omega_e)$.

less steel cell equipped with silver chloride windows, sealed via Viton o-rings with a light film of Kel-F grease. Spectra were obtained using a Digilab FTS 20/C/V interferometer at 0.125 cm⁻¹ resolution with appropriate (4mm-12mm diameter) apertures, and typically 1000 to 2000 scans were co-averaged. The beamsplitter was a Ge film supported on a KBr substrate and a TGS detector was used. Interferograms were transformed using 'boxcar' apodization and the resulting single-beam spectra were interpolated using an 11-degree polynomial to allow accurate measurement of band positions. The spectrometer was evacuated during data collection, but small absorptions due to residual carbon dioxide and water vapor were nonetheless detected. The spectra were calibrated using standard tables and referenced using the internal He-Ne interferometer.

(E) BROMINE MONOCHLORIDE SPECTRA

BrCl is another interhalogen for which only low resolution spectra are available. The problem is complicated since BrCl is in equilibrium with Br₂ and Cl₂ at room temperature; the equilibrium constant for the reaction $\text{Br}_2 + \text{Cl}_2 \rightleftharpoons 2 \text{BrCl}$ is 0.15¹¹. There have been two reports^{11,12} of the low resolution infrared spectrum of the gas, both more than 25 years old, which agree in placing the band center at $439.5 \pm 0.5 \text{ cm}^{-1}$. There have been several studies of the Raman spectrum of the vapor and liquid^{13,15}, the microwave spectrum has been measured^{6,16}, and in recent years work has been done on the UV-visible^{17,18} and laser induced fluorescent spectra¹⁹. BrCl has been observed in matrices²⁰ and the pure solid has been prepared at low temperatures²¹. It therefore seemed appropriate to reinvestigate the infrared spectrum of the gas at high resolution.

The 1-0 band is shown in Fig. 6.6. This spectrum is a complex overlay of four isotopic molecules - ⁷⁹Br³⁵Cl, ⁷⁹Br³⁷Cl, ⁸¹Br³⁵Cl and ⁸¹Br³⁷Cl - and since the rotational constant 'B' is of the order of 1 cm⁻¹ and the isotope splitting is small all these bands overlap severely. The spectra have not yet been analysed in detail.

(F) EXPERIMENTAL

The spectroscopic, chemical and physical properties of BrCl posed several problems. In order to cover the range of the fundamental band (approx. 400-500 cm⁻¹) with reasonable signal to noise ratios, a germanium beamsplitter supported upon a CsI substrate was used giving a spectral range of 2800-250 cm⁻¹. The usual window materials used for corrosive halogen compounds (e.g. AgCl, CaF₂, NaCl etc.) do not transmit in the 400-500 cm⁻¹ region, and polyethylene, a frequently used for - IR window material, does not transmit greatly above 650 cm⁻¹, thus making simulta-

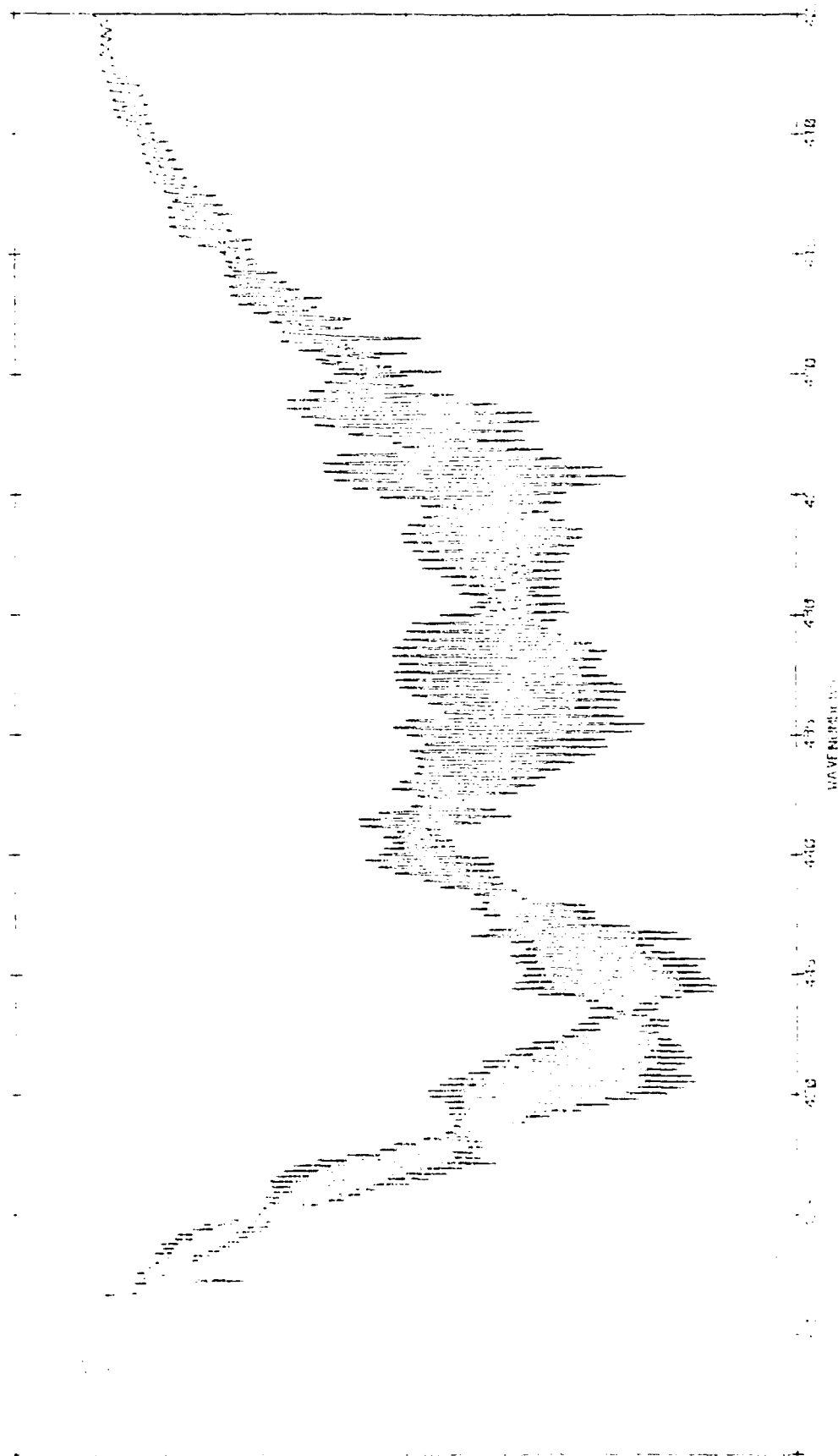


Fig. 6.6 FT-IR transmittance spectrum of the 1-0 band of BrCl.

neous measurement of the 1-0 and 2-0 bands impossible. The solution chosen was to use CsI windows. These are attacked by Br_2 to give a thin layer of CsBr and I_2 on the window but further attack is slow and the transmittance is not seriously diminished. BrCl was formed by mixing Br_2 (Eastman, CP grade, dried over activated alumina, degassed and distilled in vacuo before use) and Cl_2 (Matheson, research grade, used as received) in the cells used. To obtain the 1-0 band the 10cm cell described previously was used. The pressure of gas in the cell was limited by the vapor pressures of Br_2 and BrCl. In this case 150 mm of Br_2 followed by 150 mm Cl_2 were admitted to the cell. Only an exceedingly weak 0-2 band was detected and therefore a longer cell was constructed. The long cell had a glass body and the windows were held in place with aluminum end pieces and Viton o-rings. The pathlength was 90 cm and so the cell had to be mounted exterior to the spectrometer, between the beamsplitter and an external carbon rod source. The aluminum end pieces were slightly attacked by the halogens.

(G) REFERENCES FOR APPENDIX 2.

1. A. H. Nielsen and E. A. Jones, J. Chem. Phys., 19, 1117 (1951).
2. D. A. Gilbert, A. Roberts and P. A. Griswold, Phys. Rev., 76, 1723 (1949).
3. A. L. Wahrhaftig, J. Chem. Phys., 10, 248 (1942).
4. H. Schmitz and H. J. Schumacher, Z. Naturforsch., 2A, 359 (1947).
5. R. L. White, Rev. Mod. Phys., 27, 276 (1955).
6. F. J. Lovas and E. Tiemann, J. Phys. Chem. Ref. Data, 3, 609 (1974).
7. W. Stricker and L. Krauss, Z. Naturforsch., 23A, 1116 (1968).
8. J. A. Coxon, Chem. Phys. Lett., 33, 136 (1975).
9. C. P. Anderson, G. Mamantov, W. E. Bull, F. A. Grimm, J. C. Carver, and T. A. Carlson, Chem. Phys. Lett., 12, 137 (1971).
10. B. Fabricant and J. S. Muentner, J. Chem. Phys., 66, 5274 (1977).
11. H. C. Mattraw, C. F. Pachucki and N. J. Hawkins, J. Chem. Phys., 22, 1117 (1954).
12. W. V. F. Brooks and B. Crawford, J. Chem. Phys., 23, 363 (1955).
13. H. Stammreich, R. Fournieris and Y. Tavares, Spectrochim. Acta, 17, 1173 (1961).
14. W. Holzer, W. F. Murphy and H. J. Bernstein, J. Chem. Phys., 52, 399 (1970).
15. F. Wallart, Can. J. Spectros., 17, 128 (1972).
16. D. F. Smith, M. Tidwell and D. V. P. Williams, Phys. Rev., 79, 1007 (1950).
17. J. A. Coxon, J. Mol. Spectrosc., 50, 142 (1974).
18. S. G. Hadley, M. J. Bina and G. D. Brabson, J. Phys. Chem., 78, 1883 (1974).
19. C. A. Wright, B. S. Ault and L. Andrews, J. Mol. Spectrosc., 56, 239 (1975).
20. See e.g. Appendix 1.
21. M. Schmeisser and K. H. Tytko, Z. Anorg. Chem., 403, 231 (1974).

7. APPENDIX 3

[Reprinted from the *Journal of the American Chemical Society*, 100, 6526 (1978).]
Copyright © 1978 by the American Chemical Society and reprinted by permission of the copyright owner

Infrared Laser Photochemistry of Matrix-Isolated Molecules

Sir:

Two groups have reported studies of infrared laser induced photochemistry of matrix-isolated species. Turner et al.¹ have examined rearrangements of isotopically labeled carbonyl fragments induced by radiation from a carbon monoxide laser in the 1900-cm⁻¹ region. These authors have concluded^{1b} that "a single molecule requires absorption of only one photon to undergo isomerization". Ambartzumian et al.² claim to have observed selective dissociation of ¹²SiF₄ in argon matrices using a carbon dioxide laser operating in the 940-cm⁻¹ region. They estimate that each molecule absorbs energy corresponding to about 150 quanta of CO₂ laser radiation.^{2b} Some aspects of their reported conclusions appeared unusual to us and we attempted to reproduce their results and extend work in this field.

We were surprised that no dissociated products were detected using infrared spectroscopy,^{2b} since for the species that may be produced (SF₄, S₂F₁₀, and SF₆) vibrational data are available.³⁻⁵ A reported decrease in absorption due to ¹²SiF₄ from ~95 to ~55%^{2b} would be expected to yield photoproducts having substantial absorbances.

We have carried out a series of experiments involving CO₂ laser irradiation of various matrix-isolated molecules and have not observed any evidence for dissociation or reaction in this medium. Table I shows some of the species studied, the vi-

brational modes excited, and the laser wavenumbers employed. Matrix ratios were in the range 100:1 to 40 000:1, and slow spray-on techniques were used. Our observations of the effects of irradiation are that no spectroscopic or visual effects were observed (a) for irradiation of pure argon matrices or (b) when the exciting frequency was more than 10 cm⁻¹ away from an absorption band. Irradiation of the matrix at a guest absorption frequency (or at up to 5 cm⁻¹ to lower wavenumber) with low energy density (0.4 J cm⁻²) causes "fogging" of the previously glassy matrices, and at higher densities (40 J cm⁻²) causes matrix destruction with complete evaporation. Prolonged photolyses have led to fracturing of the cesium iodide substrate. We are led to the conclusion that the spectra presented by Ambartzumian et al. show no conclusive evidence of dissociative photochemistry but may simply be interpreted in terms of differential evaporation of ¹²SiF₄ from the matrices.

After submitting this paper, we have learned that Davies et al.⁶ have also observed *apparent* isotopic enrichment when SiF₄, isolated in solid CO or Ar, is irradiated with a pulsed CO₂ laser. The authors attribute this result to a spectroscopic artefact caused by the ablation of the matrix.⁶

The vacuum, cryogenic and spectroscopic equipment has been described previously.⁷ A Lumonics TEA 103-2 CO₂ laser was operated in the 10.6-μ region with an energy of 1-2 J per pulse. Output modes were monitored using an Optical Engineering Model 10R spectrum analyzer.

Acknowledgment. This work has been supported by the AI Office of Scientific Research, Grant No. 77-3165.

References and Notes

- (1) (a) A. McNeish, M. Poliakoff, K. P. Smith, and J. J. Turner, *J. Chem. Soc., Chem. Commun.*, 859 (1976). (b) B. Davies, A. McNeish, M. Poliakoff, and J. J. Turner, *J. Am. Chem. Soc.*, **99**, 7573 (1977). (c) B. Davies, A. McNeish, M. Poliakoff, M. Tranquille, and J. J. Turner, *Chem. Phys. Lett.*, **52**, 477 (1977). (d) B. Davies, A. McNeish, M. Poliakoff, M. Tranquille, and J. J. Turner, *J. Chem. Soc., Chem. Commun.*, 36 (1978).
- (2) (a) R. V. Ambartzumian, Yu. A. Gorokhov, G. N. Makarov, A. A. Runetzky, and N. P. Fuznikov, *JETP Lett.*, **24**, 287 (1976). (b) R. V. Ambartzumian, Yu. A. Gorokhov, G. N. Makarov, A. A. Runetzky, and N. P. Fuznikov in *Laser Spectroscopy*, Vol. III, J. C. Hall and J. L. Carlsten, Ed., Springer-Verlag, New York, 1977, p. 439.
- (3) K. O. Christe, E. C. Curtis, C. J. Schack, S. J. Cyvin, J. Brunvoll, and W. Sawodny, *Spectrochim. Acta, Sect. A*, **32**, 1141 (1976).
- (4) R. R. Smardzewski, R. E. Noffle, and W. B. Fox, *J. Mol. Spectrosc.*, **62**, 449 (1976).
- (5) R. R. Smardzewski and W. B. Fox, *J. Chem. Phys.*, **67**, 2309 (1977).
- (6) B. Davies, M. Poliakoff, K. P. Smith, and J. J. Turner, *Chem. Phys. Lett.*, in press. We are grateful to Dr. Poliakoff for a preprint of this paper.
- (7) E. S. Prochaska, I. Andrews, N. R. Smyrl, and G. Mamantov, *Inorg. Chem.*, **17**, 970 (1978).

R. A. Crocombe, N. R. Smyrl, G. Mamantov*

Department of Chemistry, University of Tennessee
Knoxville, Tennessee 37916

Received June 15, 1978

Table I

compd ^a	laser line	frequency	mode	reported IR gas phase photolysis
SiF ₄ ^b	P(20) 001 100	944.2	<i>ν</i> ₃	<i>c</i>
	P(26)	938.7		
N ₂ F ₄ ^d	P(20) 001 100	944.2	<i>ν</i> _g ^e	<i>f</i>
NF ₃ ^e	P(38) 001 020	1029.4	<i>ν</i> ₁	
COS ^h	P(20) 001 020	1046.8	2 <i>ν</i> ₂	
O ₃ ⁱ	P(30) 001 020	1037.4	<i>ν</i> ₁	

^a Matrix materials used were Ar, 99.9998% (Matheson); N₂, 99.997% (Linde); and NO, 99.0% (Matheson). ^b Matheson, 99.8%. ^c R. V. Ambartzumian, Yu. A. Gorokhov, V. S. Tetokhov, and G. N. Makarov, *JETP Lett.*, **21**, 171 (1975); J. L. Lyman, R. J. Jensen, J. P. Rink, C. P. Robinson, and S. D. Rockwood, *Appl. Phys. Lett.*, **27**, 87 (1975). ^d Air Products, 98%. ^e Gauche isomer, J. R. Durig, B. H. Gimarc, and J. D. Odom in "Vibrational Spectra and Structure", Vol. 2, J. R. Durig, Ed., Marcel Dekker, New York, 1975, p. 35. ^f J. L. Lyman and R. J. Jensen, *Chem. Phys. Lett.*, **13**, 421 (1972). ^g Air Products, 98%. ^h Matheson, 97.5%. ⁱ Prepared in situ using microwave discharge. See I. Brewer and J. L. Wang, *J. Chem. Phys.*, **56**, 759 (1972).

8. APPENDIX 4

Practical Aspects of Rapid Scanning Fourier Transform Time-resolved Infrared Spectroscopy*†

ARLENE A. GARRISON, R. A. CROCOMBE, GLEB MAMANTOV,‡ and JAMES A. de HASETH

University of Tennessee, Department of Chemistry, Knoxville, Tennessee 37916 (A.A.G., R.A.C., G.M.) and University of Alabama, Department of Chemistry, University, Alabama 35486 (J.A.deH.)

The results of experiments designed to study the infrared spectra of transient species produced by ultraviolet photolysis of acetaldehyde are reported and analyzed. Spectra obtained in similar work [A. W. Mantz, *Appl. Opt.* 17, 1347 (1978)] are critically reinterpreted. The evidence presented demonstrates that insufficient attention has been given to the necessary stringent control of experimental conditions. The consequences of poor control are described and a qualitative explanation is offered. This paper discusses, in particular, the production of spectral artifacts consisting of displaced (not folded) bands and their previous erroneous assignments. Other practical aspects of time resolved Fourier transform spectroscopy with a rapid

scanning Michelson interferometer are outlined.

Index Headings: Infrared; Interferometry; Time-resolved spectroscopy.

INTRODUCTION

Studies of dynamic systems and the characterization of reaction intermediates by infrared spectroscopy are of considerable current interest.¹ Of particular interest to this work is the utilization of Fourier transform infrared methods (FT-IR) in time resolved spectroscopy. This technique was originally developed for step scan interferometry^{2,4} and was later adapted to rapid scan methods by Mantz.^{5,6} In general, the rapid scan interferometric technique has a temporal resolution of a few hundred microseconds or less. Recently, a technique of infrared spectral photography, which involves the upconversion

Received 27 December 1979.

* This work was performed at the University of Tennessee

† Presented in part at the 31st Pittsburgh Conference on Analytical Chemistry and Applied Spectroscopy, Atlantic City, NJ, March, 1980

‡ Author to whom correspondence should be addressed

filter gave a usable spectral range of 3800 to 600 cm^{-1} . Between 50 and 200 scans were co-added for each interferogram. A triglycine sulfate (TGS) pyroelectric bolometer detector was used.

B. Sorting Tests. Two types of tests were performed on the sort routine. First, one interferogram was duplicated n times, and this set was sorted and transformed into n spectra. Second, interferograms obtained from gas phase samples at both the same and different pressures were sorted and transformed. In a typical test, interferograms were collected from samples of carbon monoxide at pressures of 50, 60, and 70 Torr in a conventional 10 cm cell using the spectrometer in its normal configuration. The parameters (e.g., 1 cm^{-1} resolution, LP filter, UDR of 4, etc.) used to collect the test interferograms and the time-resolved data were similar. These interferograms were duplicated to form a set and then sorted and transformed as if they arose from a single KS experiment. A large number of such tests was done varying the sample (e.g., CO, CO_2 , H_2O), pressure, number of interferograms, resolution, undersampling ratio, etc. Initially the software for TR and TK modes did not function correctly, and therefore no experiments were performed using these modes.

C. Reagents. Acetaldehyde (Eastman, reagent grade) was degassed by vacuum freeze-thawing before use. Carbon monoxide (Air Products 99.3%), helium (Air Products 99.995%), argon (Linde 99.998%), and carbon dioxide (Air Products 99.8%) were used as received.

II. RESULTS AND DISCUSSION

Mantz^{1,6} reported the observation of a well-resolved emission band centered at about 3195 cm^{-1} , which he assigned to the HCO radical, during the flash photolysis of acetaldehyde in the presence of carbon monoxide and helium with gas pressures of about 7, 20, and 50 Torr, respectively. It was commented that the addition of carbon monoxide enhanced the production of HCO at the expense of CH_3 . The flashlamp was operated in the range of 75 to 150 pps, and, using the TR mode, a spectrum was recorded at the peak of the flash. The time scale of such an experiment is on the order of an hour, and because the sample was static in this particular run,²³ the concentration of the products (mainly CO and CH_3) increased during data collection.

In experiments at Tennessee using essentially the same equipment, but in "kinetic studies" mode, neither "emission" bands nor other evidence for any transients was observed when acetaldehyde-carbon monoxide-helium mixtures were allowed to flow through the cell under carefully controlled conditions at pressures comparable to those described by Mantz.^{1,6} The flow rates and pressures were maintained such that spectral absorbances did not vary by more than 2% throughout data collection. A typical flow rate resulted in about one change of the cell contents per single scan (i.e., about 30 changes/min), but this was deliberately varied by a factor of 0.2 to 5 from experiment to experiment.

In several experiments the flow rates and pressures varied during data collection. In these cases a weak absorption band with PR structure centered at 2460 cm^{-1} was detected in some spectra. The individual features of

the band were only poorly resolved but appeared to have a spacing of about 3.5 cm^{-1} . This frequency is reasonably close to that reported for ν_1 of HCO in its electronic ground state.¹¹ However, there was no evidence for ν_3 of HCO, which has been shown to be a stronger band.⁹ An intense acetaldehyde band²⁴ would overlap ν_2 . It soon became evident that the greater the variation of carbon monoxide pressure in the cell during data collection, the greater was the intensity of this band, implying that it did not arise from an HCO vibration.

Accordingly, a series of pseudo-time-resolved experiments (sorting tests) was performed to investigate this phenomenon. When interferograms obtained from carbon monoxide samples at various pressures under conventional conditions (i.e., no photolysis) was subjected to the KS sorting process, the transformed spectra generally showed many displaced carbon monoxide type bands. Fig. 1 shows a typical spectrum resulting from sorting 25 interferograms under conditions resembling our acetaldehyde experiments. The fundamental CO band is shown at 2143 cm^{-1} , and displaced bands can be seen centered at approximately 1510, 1830, 2460, 2780, 2920, and 3080 cm^{-1} . These bands occur in "emission" or "absorption" mode, or in transition between these states. The bands at 3080 and 2920 cm^{-1} are typical of "absorption", those at 1510 and 2780 cm^{-1} typical of "emission" while those at 1830 and 2460 cm^{-1} display intermediate behavior. In the set of 25 spectra, individual bands independently changed between these states but maintained their frequencies. The components of these bands possessed the relative intensity and spacing of the carbon monoxide fundamental with a feature matching the P branch appearing at a lower frequency to that matching the R branch. This is not the behavior observed when aliasing^{17, 18} or double-passing²⁵ occurs, as these phenomena result in folded (i.e., spectrally reversed) features. The displaced bands appear at both higher and lower frequencies than the fundamental and therefore this is not caused by a Nyquist sampling problem.^{17, 18} The strongest of these bands is centered at 2460 cm^{-1} , and in our actual

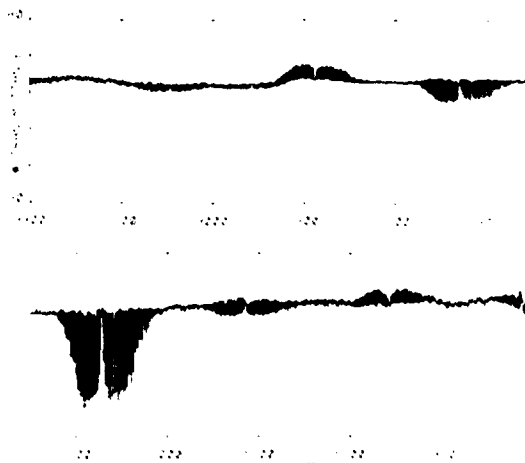


Fig. 1. FT-IR transmittance spectrum from a pseudo-time resolved experiment using carbon monoxide samples. This figure shows the CO fundamental at 2143 cm^{-1} and displaced bands at higher and lower frequencies exhibiting "emission," "absorption," and intermediate behavior.

of infrared frequencies to the visible region and photographic recording of the signal, has been developed; it has a temporal resolution of 5 ns.⁷ Although this upconversion technique permits better temporal resolution than the FT method, the latter is capable of studying a wider bandwidth and is commercially available.⁸ It has been noted that stringent control of experimental conditions is necessary for the successful application of the FT technique.^{1,6} Evidence produced in this laboratory demonstrates that insufficient attention has been given to this control, leading to the production of spectral artifacts and erroneous interpretation of experimental data. The report of the infrared emission spectrum of the HCO radical^{1,6} is not consistent with existing spectral evidence; in attempting to repeat and extend this work we encountered anomalous spectroscopic features.

The spectroscopic parameters of HCO in its electronic ground state are well established. The infrared matrix isolation work of Milligan and Jacox^{9,10} identified the fundamental vibrational frequencies in a carbon monoxide matrix as 2488, 1861, and 1090 cm⁻¹ and found that the intensity ratios of these bands were $I_{\nu_2} \approx 2I_{\nu_1} \approx 4I_{\nu_3}$. Ogilvie¹¹ confirmed these results and extended the earlier work of Herzberg and Ramsay¹² to derive the following:

Rotational constants (cm ⁻¹)	Fundamental frequencies (cm ⁻¹)
A_{rot} 22.37 ₄	ν_1 2482
B_{rot} 1.49 ₁	ν_2 1861
C_{rot} 1.400 ₆	ν_3 1083

These values have been refined using a variety of laser techniques.¹³⁻¹⁵ The time and wavelength dependence of the photolysis of acetaldehyde has also recently been reported.¹⁶

The assignment of the emission band at 3195 cm⁻¹ to HCO by Mantz^{1,6} appears questionable because:

1. The frequency does not match any fundamental, combination, or overtone band of the HCO radical in either its ground or first excited electronic state.^{11,12}
2. The spacing of the features in the band, estimated at 4 cm⁻¹ at the center from an enlargement of the published spectrum, does not match any combination of the rotational constants.¹¹
3. The band is simple, implying emission from a single excited vibrational state ($v = 1$).
4. No other expected bands (e.g., the fundamentals) are reported, and their absence or presence is not discussed.
5. The power developed by the flashlamp appears to be inadequate to generate a sufficient quantity of HCO radicals per flash (vide infra).

Based on experimental and theoretical work in this laboratory, this paper reinterprets the published spectra^{1,5,6} to show that infrared bands assigned to transient species are spectroscopic artifacts. The practical problems of time-resolved spectroscopy using a rapid scanning interferometer are discussed.

I. EXPERIMENTAL

A. Time-Resolved Spectroscopy. Spectra were obtained using a Digilab FTS 20C/V spectrometer. This system includes a rapid scanning interferometer¹⁷⁻¹⁹ with 0.125 cm⁻¹ maximum resolution, a Data General Nova 3/12 minicomputer with 32 768 words of memory and a

Data General five megaword disk. The time-resolved hardware and software were purchased from Digilab, Inc.⁶ The system operates in three modes: "kinetic studies" (KS), "time resolve" (TR), and "time kinetic" (TK).

1. Kinetic Studies. A key part of the spectrometer is the He-Ne laser reference interferometer which clocks 100 μ s intervals. In KS mode the flashlamp is triggered by this clock and data points can be taken at 100 μ s intervals; however, an undersampling ratio (UDR) is normally used thus collecting data on every n th clock pulse ($n = 4, 8$ etc.) and limiting the spectral range available (e.g., to 0 to 3950, 0 to 1975, or 1975 to 3950 cm⁻¹, etc.). In a typical case the lamp is triggered every 20 ms with a UDR of 4, and data points are collected every 400 μ s for a total of 50 data points between flashes. After the interferograms are sorted and transformed, 50 individual spectra result corresponding to times of 0 to 19.6 ms after the flashlamp trigger at 400 μ s intervals.

2. Time Resolve. In this mode only one spectrum results at time $\tau = n \mu$ s (where n is an integer) after the flashlamp trigger. This delay is controlled by a 1 MHz clock.

3. Time Kinetic. This is similar to TR mode except that three spectra result corresponding to $\tau = n, n + 25$, and $n + 50 \mu$ s after the flashlamp trigger.

The infrared cell, flashlamp, and power supply were those described by Mantz in his acetaldehyde experiment.^{1,6} This apparatus was supplied to this laboratory on a temporary basis by Digilab, Inc.⁶ The flashlamp power supply (Uvion Corporation) was specified to supply up to 5 kW raw dc power and to deliver a maximum of 20 J/pulse at a rate up to 60 pps into an EG&G FX-65B-6 flashtube.²⁰ The lamp output consisted of a band at 250 nm superimposed on a continuum.²¹ Although it was designed to have a 10 to 15 μ s wide current pulse, the light pulse was measured as 60 to 65 μ s wide at one-third peak height using a Xenon Corporation model H pulse monitor. The lamp was usually operated at 50 pps.

Infrared radiation from a carbon rod furnace,²² drawing 300 A at 8 V, was collimated by a spherical mirror into the interferometer. A 30 cm long, 50 mm diameter cylindrical quartz cell¹ equipped with potassium bromide windows was located exterior to the interferometer, between the source and the beamsplitter. The interferometer itself was evacuated while the flashlamp, cell, and external optics were surrounded by a lightproof box purged with dry nitrogen. Samples were pumped through the cell; both the individual inlet and the outlet flows were controlled with micrometering valves, and the pressure in the cell was monitored with a Robertshaw Bourdon gauge. Data collection was started only when several successive spectra taken with the flashlamp in operation showed that steady pressures had been attained. Unsorted interferograms were transformed during the experiment to check that these pressures had remained constant. Although the cell was equipped with an outer water jacket for cooling and filtering infrared radiation emitted by the flashlamp,¹ this was found to be unnecessary in our experiments and instead a dry nitrogen atmosphere was maintained in this jacket.

Spectra were usually collected at 1 cm⁻¹ resolution using a germanium beamsplitter on a potassium bromide substrate. A UDR of 4 combined with a long pass (LP)

filter gave a usable spectral range of 3800 to 600 cm^{-1} . Between 50 and 200 scans were co-added for each interferogram. A triglycine sulfate (TGS) pyroelectric bolometer detector was used.

B. Sorting Tests. Two types of tests were performed on the sort routine. First, one interferogram was duplicated n times, and this set was sorted and transformed into n spectra. Second, interferograms obtained from gas phase samples at both the same and different pressures were sorted and transformed. In a typical test, interferograms were collected from samples of carbon monoxide at pressures of 50, 60, and 70 Torr in a conventional 10 cm cell using the spectrometer in its normal configuration. The parameters (e.g., 1 cm^{-1} resolution, LP filter, UDR of 4, etc.) used to collect the test interferograms and the time-resolved data were similar. These interferograms were duplicated to form a set and then sorted and transformed as if they arose from a single KS experiment. A large number of such tests was done varying the sample (e.g., CO, CO_2 , H_2O), pressure, number of interferograms, resolution, undersampling ratio, etc. Initially the software for TR and TK modes did not function correctly, and therefore no experiments were performed using these modes.

C. Reagents. Acetaldehyde (Eastman, reagent grade) was degassed by vacuum freeze-thawing before use. Carbon monoxide (Air Products 99.3%), helium (Air Products 99.995%), argon (Linde 99.998%), and carbon dioxide (Air Products 99.8%) were used as received.

II. RESULTS AND DISCUSSION

Mantz^{1,6} reported the observation of a well-resolved emission band centered at about 3195 cm^{-1} , which he assigned to the HCO radical, during the flash photolysis of acetaldehyde in the presence of carbon monoxide and helium with gas pressures of about 7, 20, and 50 Torr, respectively. It was commented that the addition of carbon monoxide enhanced the production of HCO at the expense of CH_3 . The flashlamp was operated in the range of 75 to 150 pps, and, using the TR mode, a spectrum was recorded at the peak of the flash. The time scale of such an experiment is on the order of an hour, and because the sample was static in this particular run,²³ the concentration of the products (mainly CO and CH_3) increased during data collection.

In experiments at Tennessee using essentially the same equipment, but in "kinetic studies" mode, neither "emission" bands nor other evidence for any transients was observed when acetaldehyde-carbon monoxide-helium mixtures were allowed to flow through the cell under carefully controlled conditions at pressures comparable to those described by Mantz.^{1,6} The flow rates and pressures were maintained such that spectral absorbances did not vary by more than 2% throughout data collection. A typical flow rate resulted in about one change of the cell contents per single scan (i.e., about 30 changes/min), but this was deliberately varied by a factor of 0.2 to 5 from experiment to experiment.

In several experiments the flow rates and pressures varied during data collection. In these cases a weak absorption band with PR structure centered at 2460 cm^{-1} was detected in some spectra. The individual features of

the band were only poorly resolved but appeared to have a spacing of about 3.5 cm^{-1} . This frequency is reasonably close to that reported for ν_1 of HCO in its electronic ground state.¹¹ However, there was no evidence for ν_1 of HCO, which has been shown to be a stronger band.⁹ An intense acetaldehyde band²⁴ would overlap ν_2 . It soon became evident that the greater the variation of carbon monoxide pressure in the cell during data collection, the greater was the intensity of this band, implying that it did not arise from an HCO vibration.

Accordingly, a series of pseudo-time-resolved experiments (sorting tests) was performed to investigate this phenomenon. When interferograms obtained from carbon monoxide samples at various pressures under conventional conditions (i.e., no photolysis) was subjected to the KS sorting process, the transformed spectra generally showed many displaced carbon monoxide type bands. Fig. 1 shows a typical spectrum resulting from sorting 25 interferograms under conditions resembling our acetaldehyde experiments. The fundamental CO band is shown at 2143 cm^{-1} , and displaced bands can be seen centered at approximately 1510, 1830, 2460, 2780, 2920, and 3080 cm^{-1} . These bands occur in "emission" or "absorption" mode, or in transition between these states. The bands at 3080 and 2920 cm^{-1} are typical of "absorption", those at 1510 and 2780 cm^{-1} typical of "emission" while those at 1830 and 2460 cm^{-1} display intermediate behavior. In the set of 25 spectra, individual bands independently changed between these states but maintained their frequencies. The components of these bands possessed the relative intensity and spacing of the carbon monoxide fundamental with a feature matching the P branch appearing at a lower frequency to that matching the R branch. This is not the behavior observed when aliasing^{17,18} or double-passing²⁵ occurs, as these phenomena result in folded (i.e., spectrally reversed) features. The displaced bands appear at both higher and lower frequencies than the fundamental and therefore this is not caused by a Nyquist sampling problem.^{17,18} The strongest of these bands is centered at 2460 cm^{-1} , and in our actual

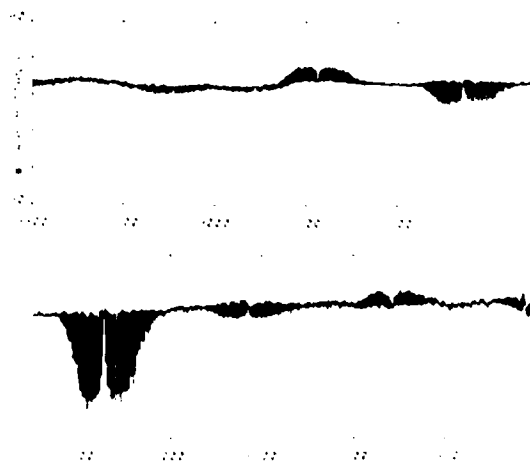


Fig. 1. FT-IR transmittance spectrum from a pseudo time resolved experiment using carbon monoxide samples. This figure shows the CO fundamental at 2143 cm^{-1} and displaced bands at higher and lower frequencies exhibiting "emission," "absorption," and intermediate behavior.

time-resolved experiments other artifacts were either too weak to be observed or obscured by acetaldehyde bands.

A second pseudo-time-resolved experiment was performed using carbon monoxide samples and parameters conforming as closely as possible to those of Mantz's acetaldehyde experiment.^{1,6} A displaced feature was observed, a well-resolved "emission" band centered at 3195 cm^{-1} . Fig. 2 shows the band obtained, and Fig. 3 demonstrates the close similarity of this displaced band to that observed by Mantz.^{1,6} In view of the static nature of his experiment,²³ the concentration of carbon monoxide (produced by acetaldehyde photolysis) increased during data collection. We attribute the appearance of the band to this increase and conclude that the band is not due to a transient species. It is significant that it was reproduced despite differences in experimental conditions (e.g., absence of acetaldehyde, use of a slower detector, etc.).

The phenomenon of displaced bands may be explained by examination of computer-generated interferograms. A

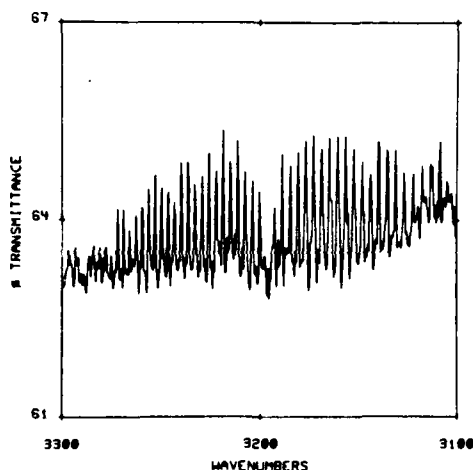


FIG. 2. Part of a FT-IR transmittance spectrum from a pseudo-time-resolved experiment using carbon monoxide samples. The displaced CO band is centered at 3195 cm^{-1} .

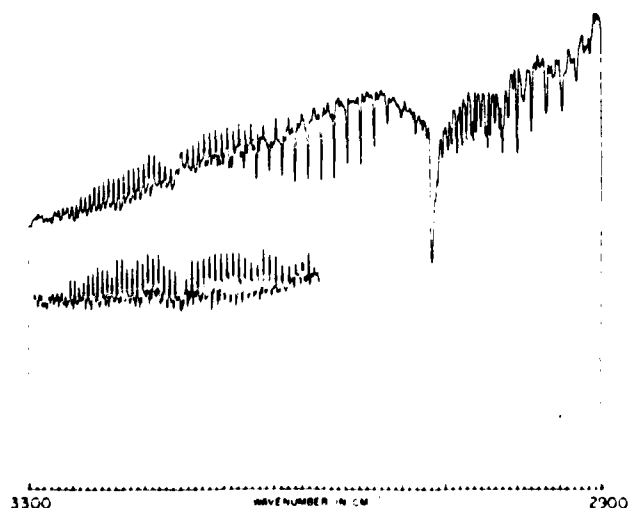
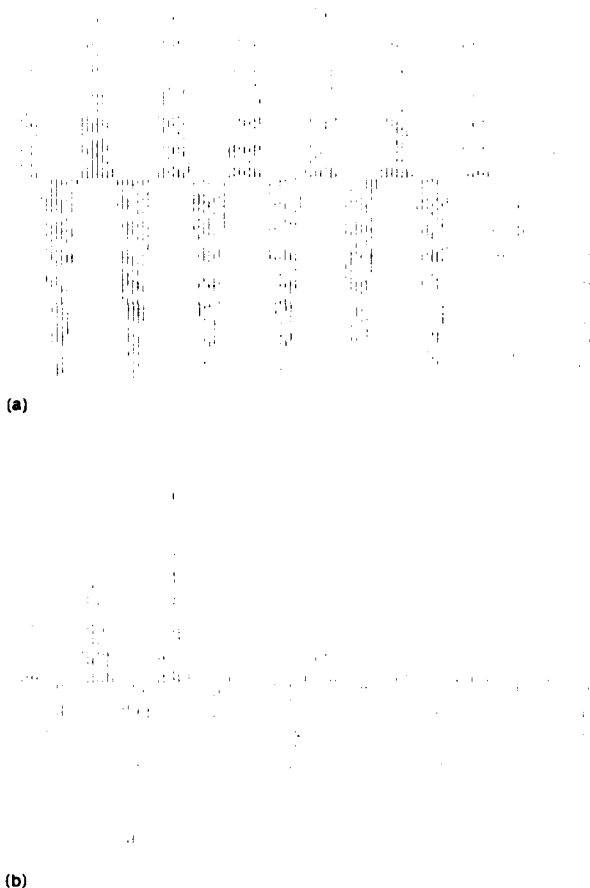


FIG. 3. Top: FT-IR spectrum claimed to show HCO radical in emission and ν_2 of methane in absorption (From Mantz). Bottom: Displaced carbon monoxide FT-IR transmittance spectrum from pseudo-time-resolved experiment.



(b)

FIG. 4. a. One of the set of cosine waves. b. An irregular waveform produced by the KS-type sort. (See text.)

simple model of the interferogram corresponding to a single narrow spectral line is a cosine wave.¹⁷⁻¹⁹ This is illustrated in Fig. 4a, where the cosine wave has been sampled at a frequency much greater than that of the signal itself. The amplitude of the cosine wave is determined by the intensity of the absorbance. The criterion for a faithful representation of this cosine wave in sorted interferograms is simple; its amplitude in each of the unsorted interferograms must be identical. This case was simulated in the laboratory when a single interferogram was duplicated n times, the resulting set sorted (as if the interferograms had been produced in a KS mode experiment) and transformed into n spectra. The resulting spectra displayed an increase in noise over a spectrum obtained from the original interferogram by less than 0.1%. On the other hand, if the absorbance of the single frequency considered in this simple case varies, then the cosine waves to be sorted will have differing amplitudes. The sorting of such a series results in an irregular pattern in place of the simple cosine wave. This was demonstrated as follows: 10 cosine waves, all having the frequency of the one in Fig. 4a but differing amplitudes, were computer sorted as if they were KS interferograms. Fig. 4b shows one of the sorted interferograms. This type of pattern will be transformed as a composite of two or more frequencies, which leads to the extraneous spectral

features. The introduced frequencies may constructively or destructively add to the genuine frequencies in the bandwidth leading to "emission" or "absorption" bands in the transformed spectra. In the more general case, the interferogram representing a spectral absorption band is actually a series of cosine waves. When an absorbance variation occurs in a time-resolved experiment, each member of the entire series of cosine waves is shifted in unison; hence, the band is not folded. The actual number of displaced bands and their relative positions depend upon the number of dissimilar interferograms sorted, the absorbance change, the rate of that change, and the undersampling ratio.

It has been observed that this displacement effect is most apparent when variations in the pressures of species that give rise to sharp bands are encountered and is more pronounced with increasing spectral resolution. Our studies indicate that, for a 50% absorbing band having observable rotational fine structure, fluctuations must be kept below $\pm 2\%$ absorbance when working at 1 cm^{-1} resolution. Finer control may be necessary in some instances and will be required at higher resolutions. For species that give broad, unresolved bands greater tolerance may be allowable, but undulating baselines in sorted spectra will result. We have obtained reasonable spectra using a compound that varied in absorbance by $\pm 25\%$ which has bands 50 cm^{-1} wide at half maximum.

The above conclusions apply not only to the pressures of reactants and products in a time-resolved spectroscopy experiment but also to the pressures of other absorbing species present—e.g., water vapor and carbon dioxide in a purged instrument. This was noted by Durana and Mantz (Ref. 1, p. 43), but the effects were not characterized nor the implications fully realized. The spectra obtained by Mantz in the study of acetone photolysis,⁵ in which the spectrometer and external optics were not purged, display a transient band at 3138 cm^{-1} . This was assigned to ketene,⁵ but a closer examination reveals the similarity between this band and ν_3 of carbon dioxide at 2348 cm^{-1} in the same spectra. On performing a pseudo-time-resolved experiment with a varying pressure of CO_2 , using the parameters of Ref. 5, this band is clearly reproduced (Fig. 5) along with a weaker band at 2750 cm^{-1} , also just discernable in the published spectra.⁵ The strange features observed by Mantz between 2500 and 2800 cm^{-1} (Fig. 3 of Ref. 5) which vary between "emission" and "absorption" can now be explained. These may be reproduced by varying the pressure of water vapor and correspond to the large, complex ν_2 band of water vapor centered at 1600 cm^{-1} .

In a more general case the large spectral range of water vapor absorption bands (4100 to 3400 , 2000 to 1200 , and 600 to 50 cm^{-1}), their intensity and superficial irregularity will produce, when displaced and overlapped, fine baseline fluctuations. Therefore, when purge conditions vary slightly during the experiment, this will result in a high apparent noise level in sorted spectra.

We have observed that lack of stability in other areas of the time resolved experiment can lead to a variety of spectroscopic problems. In particular, it has been found that a change in the location of the infrared centerburst with respect to the white-light trigger can produce band harmonics (Ref. 1, p. 55). This was particularly noticeable

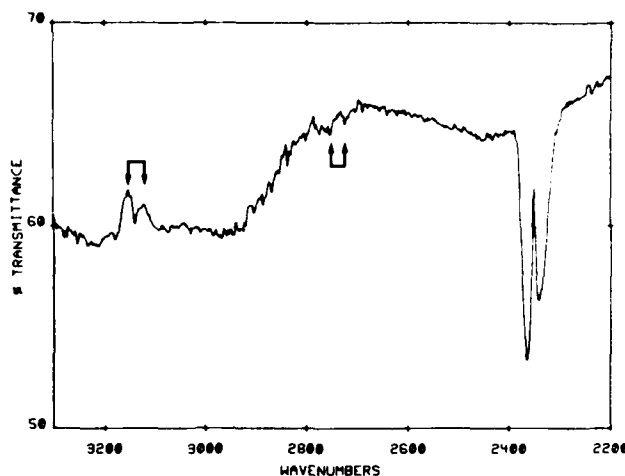


Fig. 5. FT-IR absorbance spectrum from a pseudo-time-resolved experiment using carbon dioxide samples. This figure shows ν_3 of CO_2 at 2348 cm^{-1} , and the displaced bands at 3138 and 2750 cm^{-1} are indicated.

when a germanium beamsplitter supported on a cesium iodide substrate was used. It appeared that the soft substrate gradually deformed even when maintained at a constant temperature in a vacuum.

III. PHOTOCHEMICAL CONSIDERATIONS

Although photochemical parameters will vary greatly from system to system, a few generalizations can be made. In order for a moderately strong IR absorber such as CO to be detected in the gas phase by FT-IR spectroscopy at 1 cm^{-1} resolution, a pressure of approximately 0.1 Torr in a 30 cm long single-pass cell will be required. At higher resolutions, or with the use of longer or multi-pass cells, this figure would be lower. The quantity of a transient species that can be produced by a single UV flash depends upon lamp characteristics (energy per pulse, spectral distribution, focusing efficiency, etc.), cell properties (transmission, reflection losses, pathlength, etc.), molecular parameters (absorption coefficient and its variation with wavelength, quantum yield for the production of the species of interest and lifetime of that species), and the pressure(s) of the precursor(s) in the cell. As the experiment detects transients in the presence of the starting materials, increasing the pressure of the precursor or use of long and multi-pass cells will not be an advantage if the transient species absorbs at similar frequencies to the precursor. It is therefore difficult to estimate the flashlamp power that is required in a particular experiment, but some observations can be made regarding the source used by Mantz.^{1,6}

As there was no vertical scale on the published spectrum in the acetaldehyde study, static experiments were performed to estimate the quantity of methane produced per flash. In one such experiment the 30 cm cell was filled with 5 Torr of acetaldehyde. This sample was subjected to $70,000$ flashes from the lamp, and the spectrum of the cell contents was then taken at 1 cm^{-1} resolution. This spectrum (Fig. 6) clearly shows the ν_3 band of methane, one of the stable products, and the height of its Q-branch at 3019 cm^{-1} was measured to be 0.32 absorbance unit. It can be seen that the methane

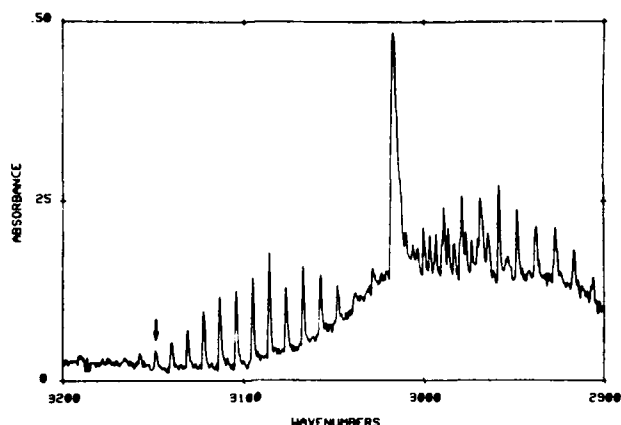


FIG. 6. FT-IR absorbance spectrum of photolyzed acetaldehyde sample showing ν_1 of methane. The arrow indicates the smallest clearly discernable feature, at 3157 cm^{-1} .

line at 3157 cm^{-1} is the weakest feature (0.025 a.u.) that can be clearly distinguished above the noise level (about 0.01 a.u.). Therefore, assuming a constant conversion per flash, it emerges that about 2000 flashes would be required to produce an observable quantity of methane, but for the time-resolved experiment to succeed this amount must be produced per flash. Thus, it is apparent that it is unrealistic to use this source for photolysis of acetaldehyde, with its low absorption coefficient ($\epsilon \approx 12\text{ liters/mol-cm}$ at 280 nm^{26}) and low quantum yield for the production of HCO ($\phi_1 = 0.4$ at 280 nm^{26}).

The flashlamp rate is determined by two factors. First, it is necessary for any photolytic reaction to be complete before the next flash is triggered; second, the maximum flash rate is dictated by the electrical characteristics of the power supply. For example, a 1 kW power supply can deliver 20 J/pulse up to, but not exceeding, 50 pps. The flashlamp rate, for a particular experiment, determines the total data collection time; that is, the lower the flash rate, the longer the acquisition time. This time is significant in many ways. Steady flow rates and pressures must be maintained over a period of several hours, resulting in the use of considerable quantities of the starting material (e.g., 0.1 to 1 mol). This consumption may imply a significant cost if isotopically modified or expensive compounds are used.

The time required for the sorting process is also a major consideration, particularly in KS mode, for which it has an approximate inverse quadratic relation to the flash rate. Using the Nova 3/12 computer system described, a sort of 50 interferograms, collected at 1 cm^{-1} resolution and a UDR of 4 (50 pps flash rate), required approximately 11 hours. When all other parameters remain the same, if the flash rate is lower, then the number of files produced is larger, and a shortage of computer space may result. This space may be reduced by using a higher UDR, which in turn results in a smaller available spectral range, limiting the usefulness of the experiment. A trade-off can be made by employing the more computer-storage-space conservative TR or TK modes; however, much kinetic information is lost. Furthermore, in TR and TK modes only partial interferograms are stored during data collection, and therefore changes in spectral

absorbances of reactants cannot be temporally monitored during the collection process.

IV. CONCLUSIONS

It has been demonstrated that the results of the time-resolved experiments previously published^{1,5,6} have been misinterpreted owing to the production of spectroscopic artifacts. The features in question were caused by pressure fluctuations during data acquisition and are not related to transient species. A large and varying number of artifacts can be produced in this manner in apparently random positions. The flashlamps used in the reported studies^{1,5,6} were not powerful enough to produce a sufficient quantity of products per flash to be detected by the FT-IR spectrometer used. It has been emphasized that key parts of the experiment are the fine control of precursor pressures, purge conditions, and maintenance of interferometer stability.

With these careful experimental controls this type of time-resolved spectroscopy should be a viable technique. Although examination of static systems in which irreversible products are formed will yield misleading data, study of rapidly reversible perturbations from equilibrium should be possible. A study of compounds with greater photochemical sensitivity than acetaldehyde and acetone with the use of a more powerful flashlamp is in progress.

ACKNOWLEDGMENTS

We would like to thank A. W. Mantz (Laser Analytics) for communicating details of his experiments, Digilab Inc. for the loan of the flash unit, S. J. Daut (Physics Department, University of Tennessee) for helpful discussions and loan of the infrared source, J. E. Caton (ORNL) for the loan of the LP filter, and R. S. Lowe (Herzberg Institute of Astrophysics) for communicating calculated spectra of HCO.

This work was supported by the Air Force Office of Scientific Research, Grant 77-3105.

1. J. F. Durana and A. W. Mantz, in *Fourier Transform Infrared Spectroscopy, Applications To Chemical Systems*, J. R. Ferraro and L. J. Basile, Eds (Academic Press, New York, 1979), vol. 2, chap. 1.
2. R. E. Murphy and H. Sakai, in *Proceedings of Aspen International Conference on Fourier Spectroscopy*, G. A. Vanasse, A. T. Stair and D. Baker, Eds. (Air Force Geophysics Laboratory, Cambridge, MA, 1971), p. 301.
3. R. E. Murphy, F. Cook, and H. Sakai, *J. Opt. Soc. Am.* **65**, 600 (1975).
4. H. Sakai and R. E. Murphy, *Appl. Opt.* **17**, 1342 (1978).
5. A. W. Mantz, *Appl. Spectrosc.* **30**, 459 (1976).
6. A. W. Mantz, *Appl. Opt.* **17**, 1347 (1978).
7. D. S. Bethune, J. R. Lankard, and P. P. Sorokin, *Opt. Lett.* **4**, 103 (1979).
8. Digilab Inc., 237 Putnam Ave., Cambridge, MA 02139.
9. D. E. Milligan and M. E. Jacox, *J. Chem. Phys.* **41**, 3032 (1964).
10. D. E. Milligan and M. E. Jacox, *J. Chem. Phys.* **51**, 277 (1969).
11. J. F. Ogilvie, *Spectrochim. Acta* **23A**, 737 (1967).
12. G. Herzberg and D. A. Ramsay, *Proc. Roy. Soc. London* **A233**, 34 (1956).
13. B. M. Landsberg, A. J. Merer, and T. Oka, *J. Mol. Spectrosc.* **67**, 459 (1977).
14. J. M. Brown, J. Buttenshaw, A. Carrington, and C. R. Parent, *Mol. Phys.* **33**, 589 (1977).
15. J. P. Reilly, J. H. Clark, C. B. Moore, and G. C. Pimentel, *J. Chem. Phys.* **69**, 4381 (1978).
16. R. J. Gill and G. H. Atkinson, *Chem. Phys. Lett.* **64**, 426 (1979).
17. R. J. Bell, *Introductory Fourier Transform Spectroscopy* (Academic Press, New York, 1972).
18. P. R. Griffiths, *Chemical Infrared Fourier Transform Spectroscopy* (John Wiley, New York, 1975).
19. P. R. Griffiths, Ed., *Transform Techniques in Chemistry* (Plenum, New York, 1978).
20. E. Blank, Union Corp., personal communication to J. A. de Haeth.
21. EG&G Electro Optics, 35 Congress St., Salem, MA 01970.
22. W. J. Boyd, Ph.D. Thesis, University of Tennessee, 1974.
23. A. W. Mantz, personal communication to J. A. de Haeth.
24. J. C. Evans and W. J. Bernstein, *Can. J. Chem.* **34**, 1063 (1956).
25. T. Hirschfeld, in *Fourier Transform Infrared Spectroscopy, Applications To Chemical Systems*, J. R. Ferraro and L. J. Basile, Eds. (Academic Press, New York, 1979), vol. 2, chap. 6.
26. See, e.g., J. G. Calvert and J. N. Pitts, *Photochemistry* (John Wiley, New York, 1966), pp. 868-871.